The Abdus Salam International Centre for Theoretical Physics
50th Anniversary 1964–2014

2572-16

Winter College on Optics: Fundamentals of Photonics - Theory, Devices and Applications

10 - 21 February 2014

Waveguide spectrometers and multiplexers

Pavel Cheben
National Research Council of Canada

Waveguide spectrometers and multiplexers

Pavel Cheben, National Research Council of Canada

A spectrometer

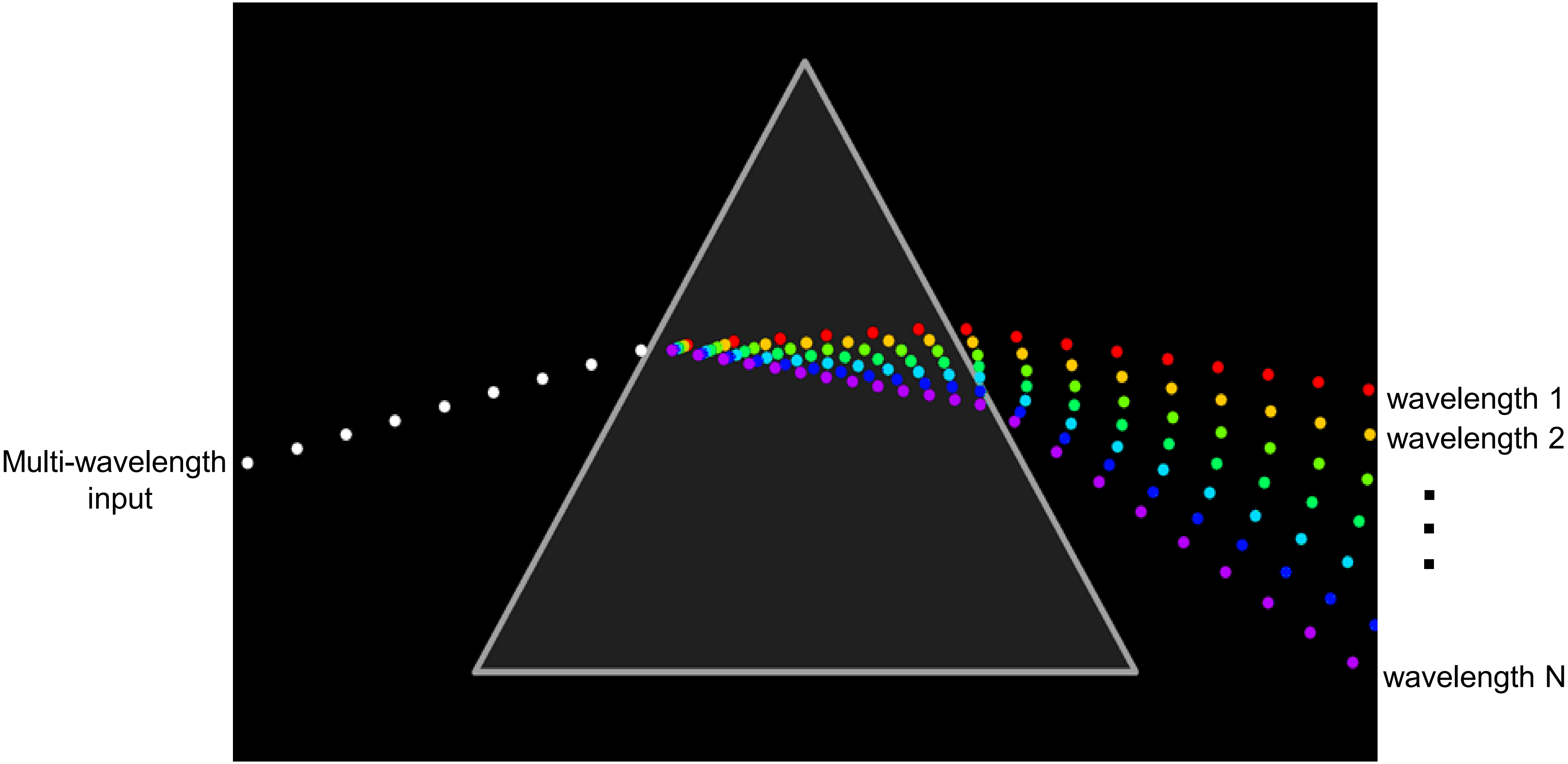

Isaac Newton

The first scientific paper of Newton, on light and colour,
the Philosophical Transactions of the Royal Society, 1672

Spectrometer miniaturization

Table top grating spectrometer

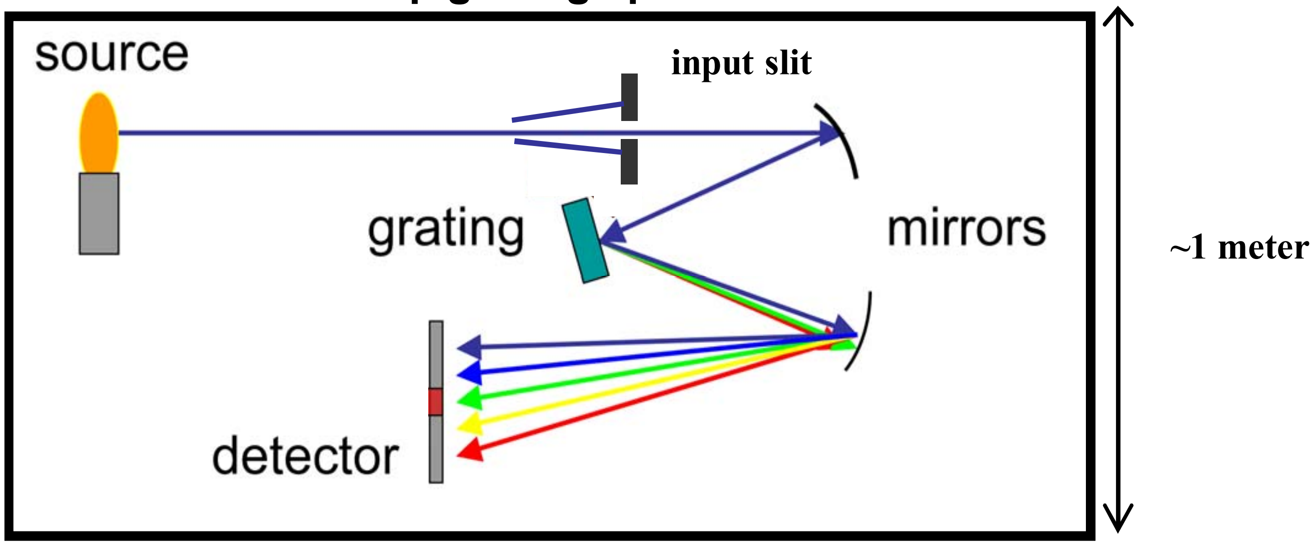

Waveguide grating microspectrometer

1 centimeter to 100 μm

1. Replace large table top instruments with semiconductor chips
2. Monolithic – no moving parts
3. Mass production at wafer level

Waveguide spectrometers

Image: NASA JPL
"The Tropospheric Emission Spectrometer, aboard NASA's Aura spacecraft"

- High spectral resolution integrated spectrometers are needed for a wide range of applications:
  - Optical communications
  - Medical diagnosis
  - Space instrumentation
- Specific features are desirable in these applications:
  - Small device size
  - Large light throughput (*étendue*)
  - Possibility to compensate fabrication imperfection and errors
  - No re-alignment of different optical component once in operational condition

Wavelength division multiplexing (WDM)

- A simple idea that revolutionized the way we communicate
- First conceived at Bell Telephone in 1960s
- Commercial WDM links deployed since early 1990s

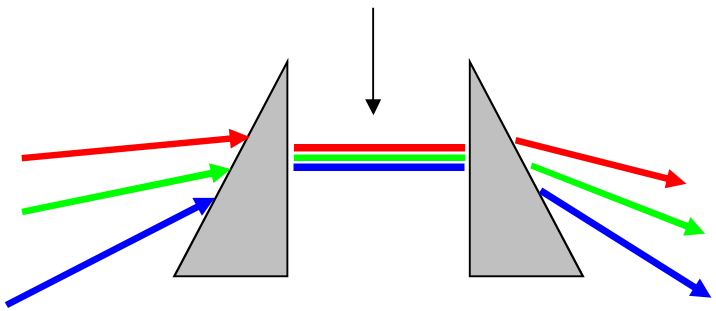

America Atlantic Europe

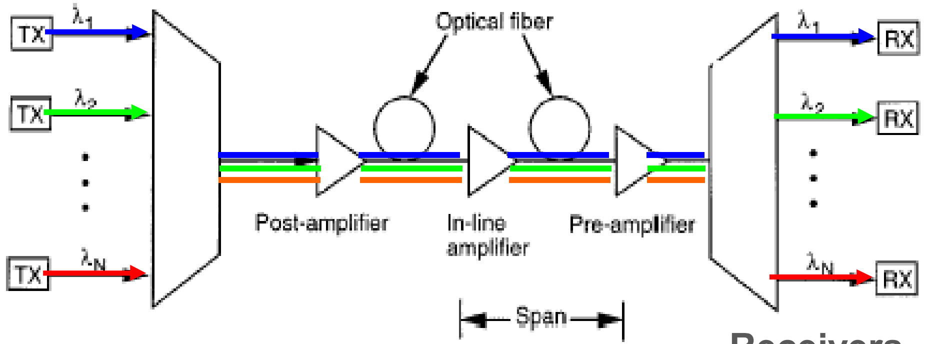

Receivers (photodetectors)

- 40 channels at 100 GHz (0.8 nm) spacing
- 80 channels with 50 GHz (0.4 nm) spacing
- Mux insertion loss (IL): < 3 dB (50%)
- Polarization dependent loss (PDL): < 0.3 dB (6.7 %)
- Crosstalk: < -30 to -40 dB
- Speed: 10 Gbit/s per wavelength channel
- Total capacity per cable: a few Tbit/s

South-East Asia - Middle East - Western Europe

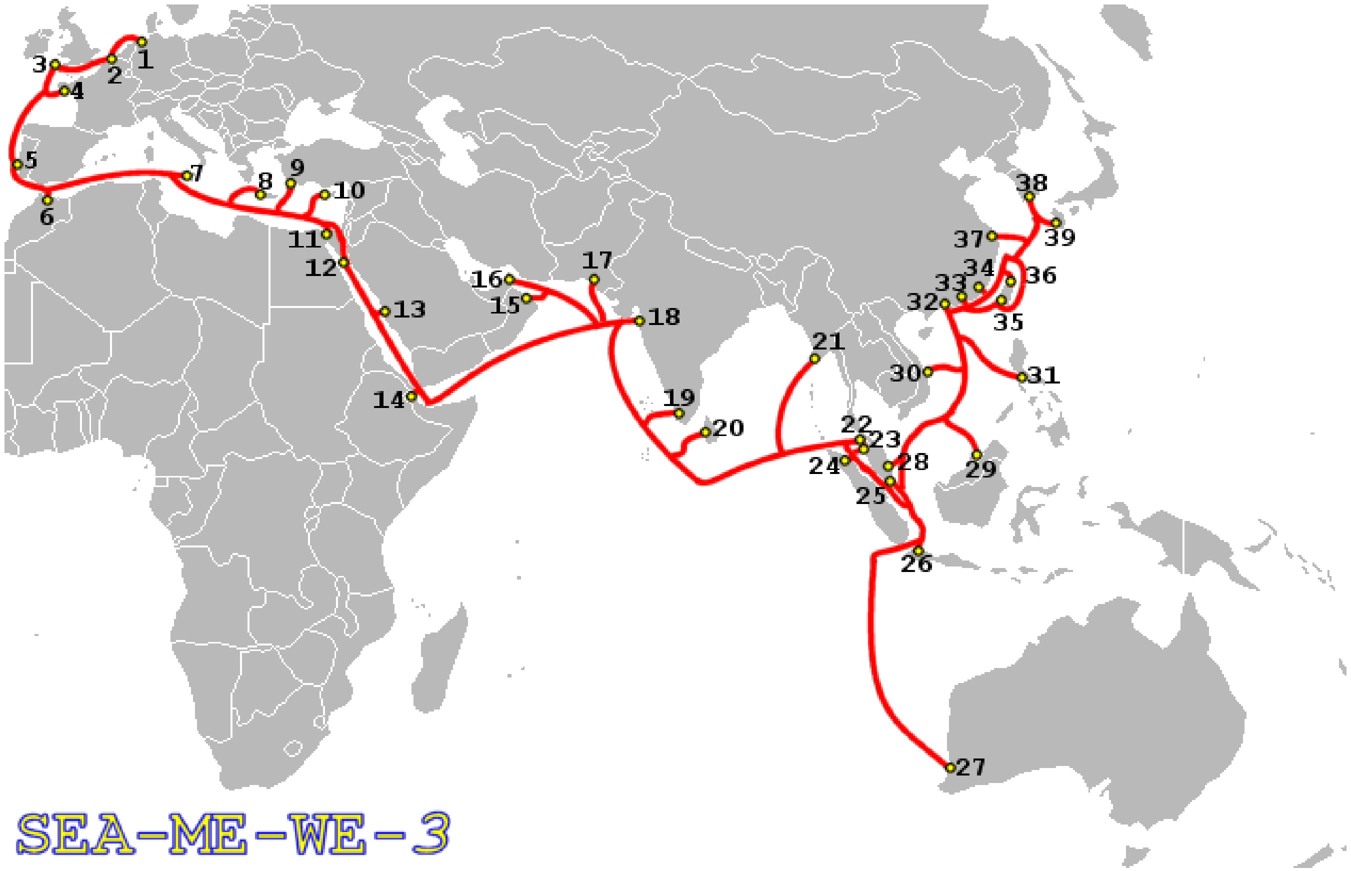

- SEA-ME-WE 3 or South-East Asia - Middle East - Western Europe 3. From North Germany to Australia and Japan. The longest in the world: 39,000 kilometres. 39 landing points. Completed in late 2000. Led by France Telecom and China Telecom, and is administered by SINGTEL, a consortium formed by 92 other investors from the telecom industry.
- Two fibre pairs, each carrying 48 wavelengths of 10 Gbit/s. One fibre in each pair is used for data carried in one direction and the other in the opposite direction.

Internet bandwidth capacity across the globe, 2011

Gigabytes per second (GBPS)

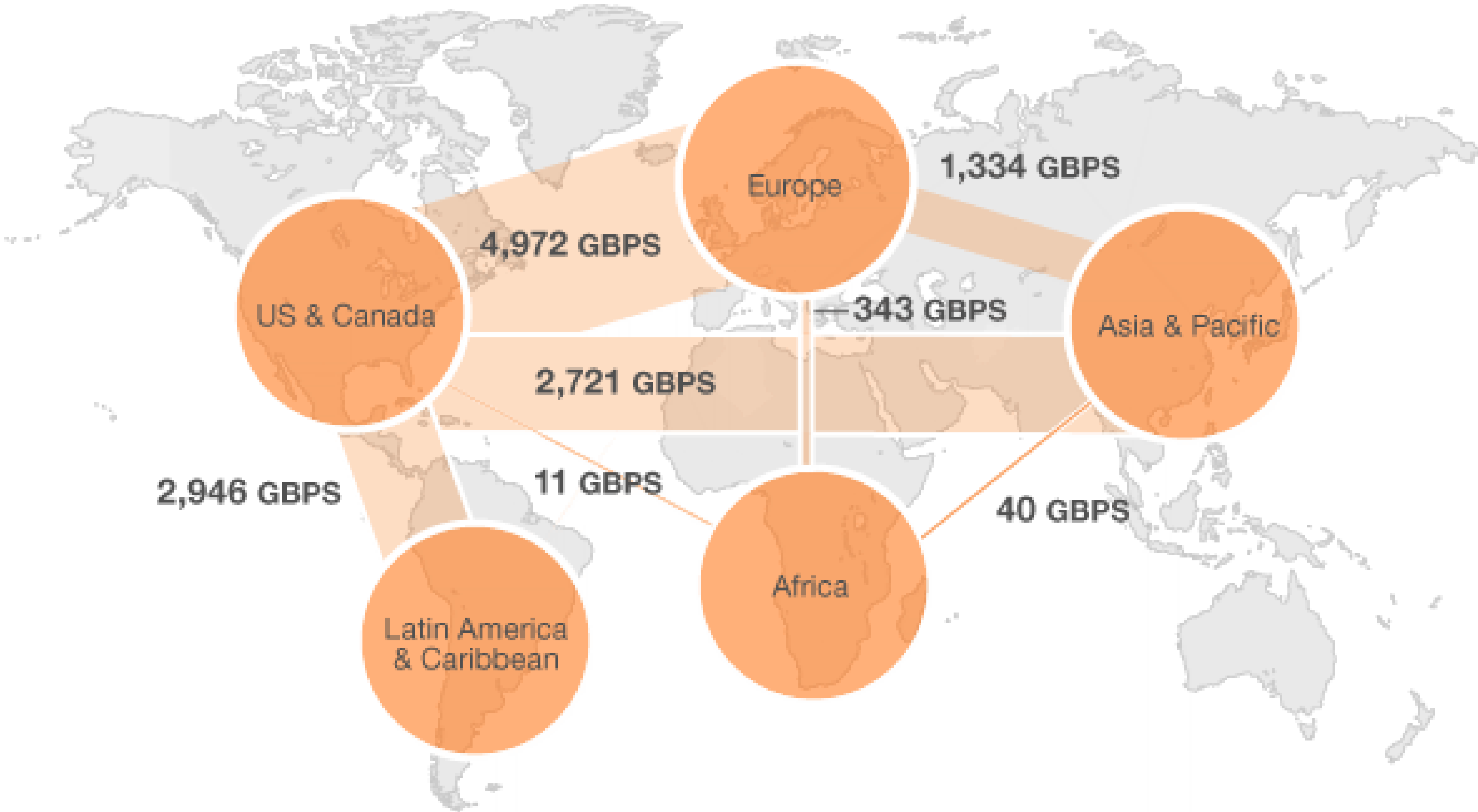

Source: TeleGeography

Total 12.4 Tbit/s

Data centers

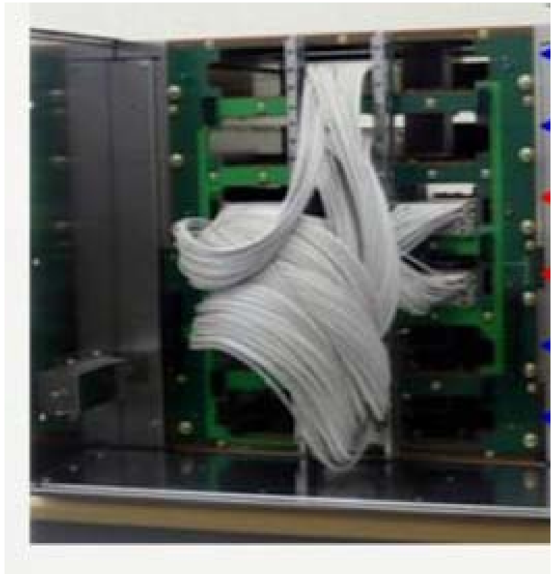

7.2 billion people, 2.4 billion using internet
Android: 900 million users
WDM interconnects are starting to be implemented in data centers

A bulk optics (de)multiplexer

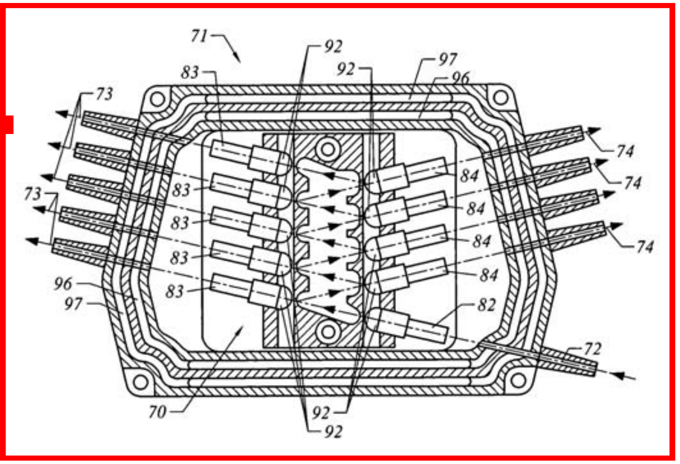

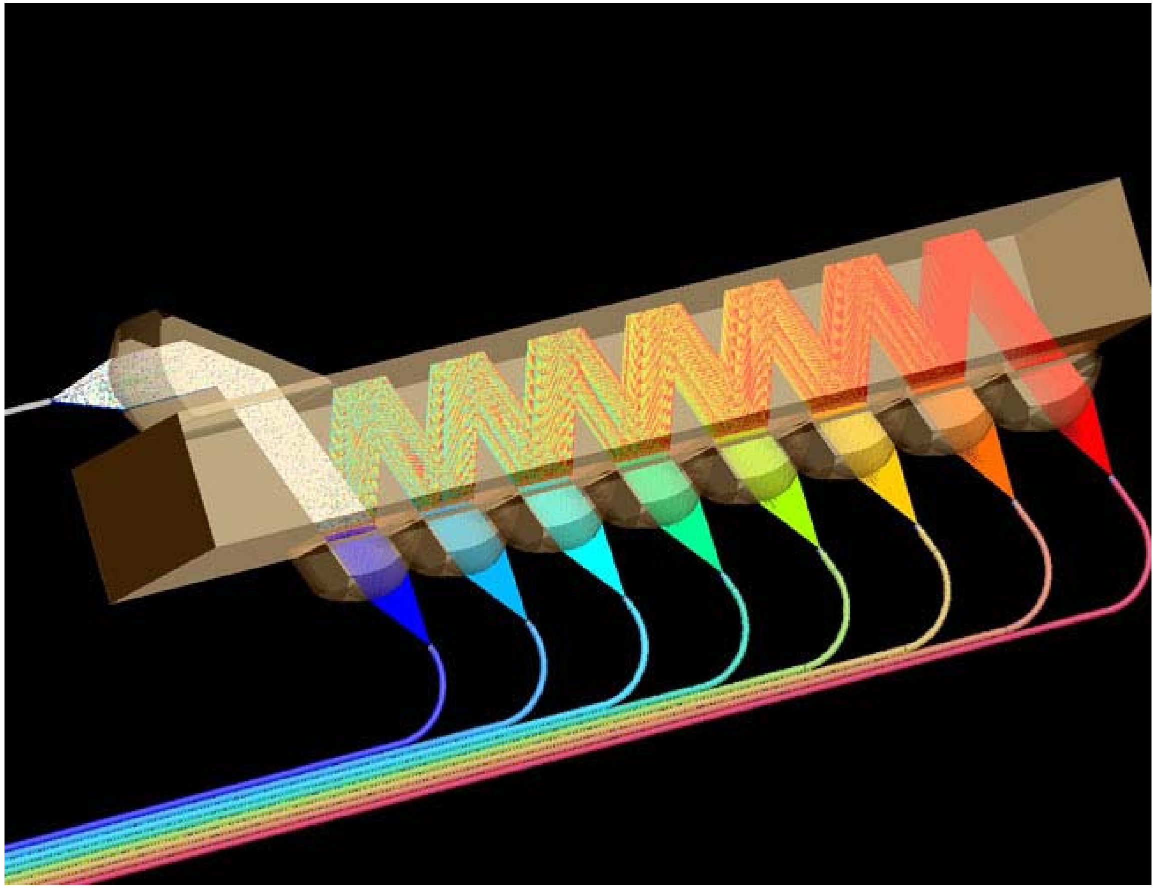

Miniature optical components (spectral filters and lenses) are assembled together

- Typically limited to 10 channels or less

- Requires precision optomechanical alignment

Diffraction grating (de)multiplexer

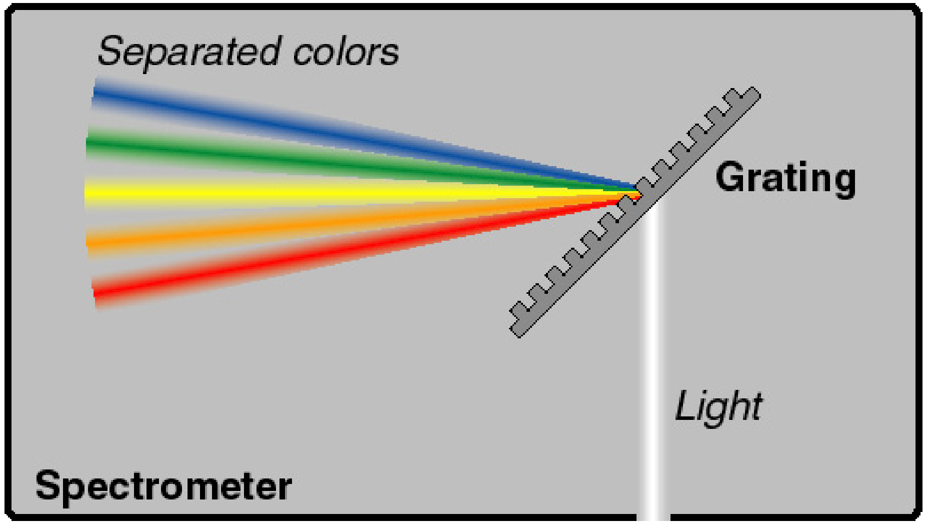

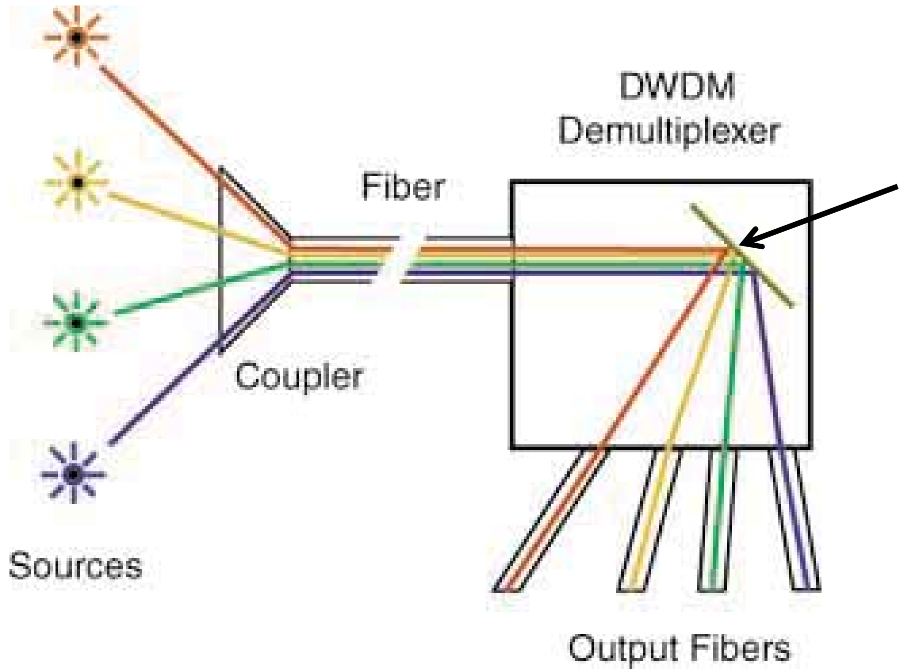

Difraction grating basics

- To separate or combine different wavelengths, a diffraction grating can be used as it is done in spectrometers, monochromators and other spectroscopic instruments.

- When a collimated beam is incident on the grating under an angle θ_i, a diffraction maximum is obtained in direction θ in which phase difference between the wavefronts originating from each grating facet is $2\pi m$, where m is an integer number called grating diffraction order.

- This is expressed by the scalar grating equation:

$$\sin\theta + \sin\theta_i = \frac{m\lambda}{n_{eff}\Lambda} \quad \Leftrightarrow \quad |\mathbf{BC}| + |\mathbf{BD}| = m\lambda/n_{eff} \;\; \textbf{or} \;\; \mathbf{OPD} = \Lambda n_{eff}(\sin\theta_i + \sin\theta)$$

- For a given incident angle, different wavelengths are diffracted in different angles $\theta(\lambda)$. This angular separation of different wavelength is the basic for (de)multiplexing.

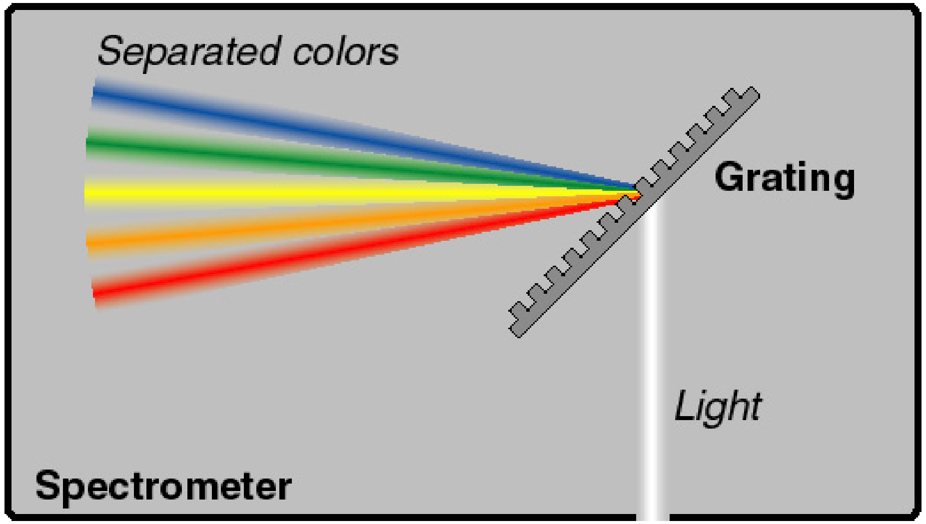

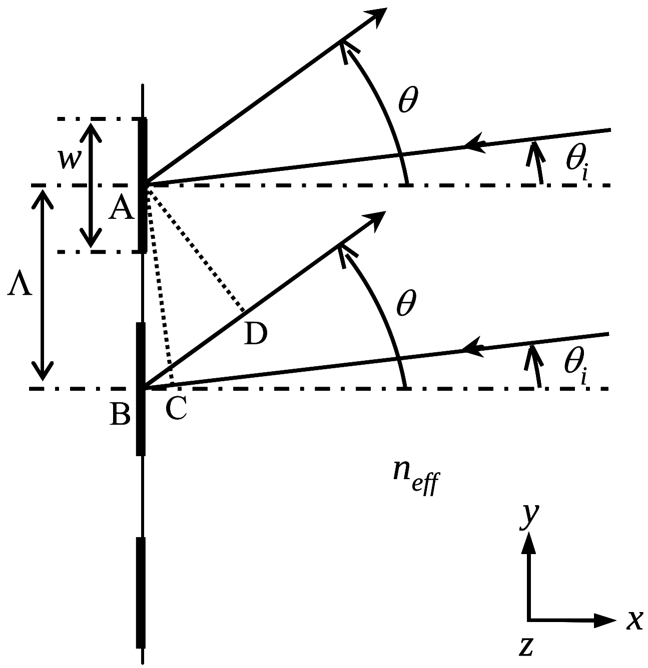

Arrayed Waveguide Grating

Arrayed waveguide grating

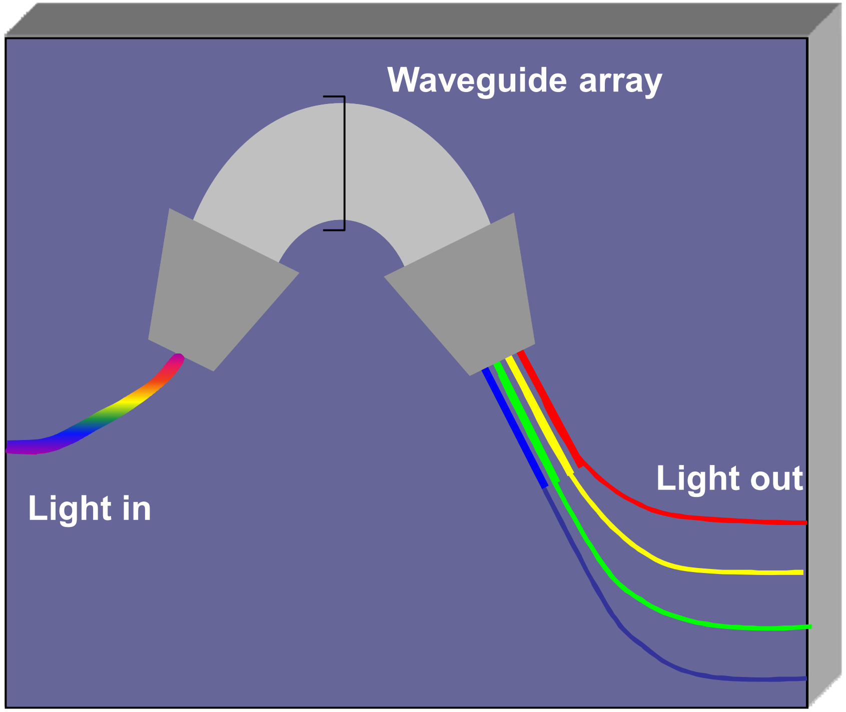

- Mux/dmux is a key device in WDM telecommunications
- Either an array of waveguides (AWG) or etched grating (EG) provide spectral dispersion
- Angle of the beam in the output slab waveguide steers with the wavelength
- Different wavelengths are separated into different output channels

From conventional gratings to arrayed waveguide gratings (AWGs)

Grating

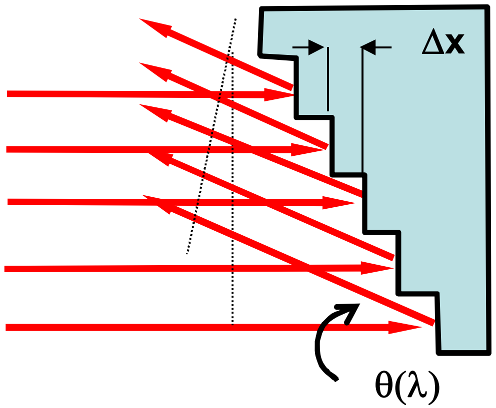

$$\Delta\phi_{retro} = k\Delta L = n(2\pi/\lambda)2\Delta x$$

A linear phase shift across the wavefront will bend the beam
If the phase shift is wavelength dependent, θ will change with wavelength

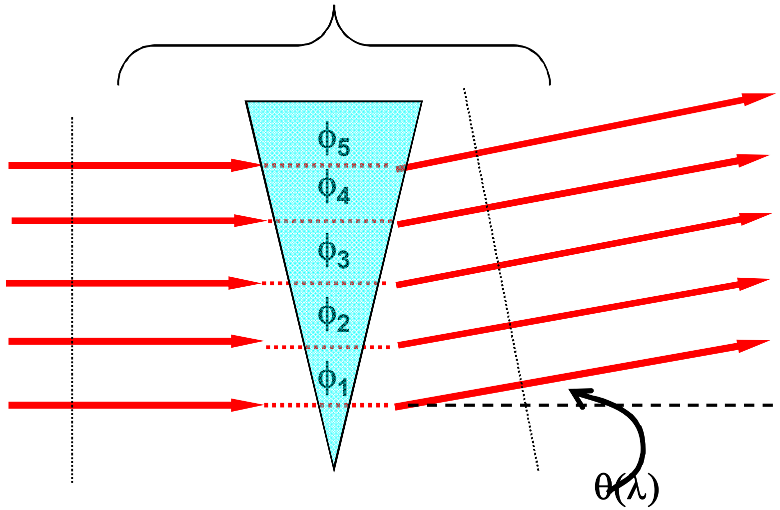

AWG

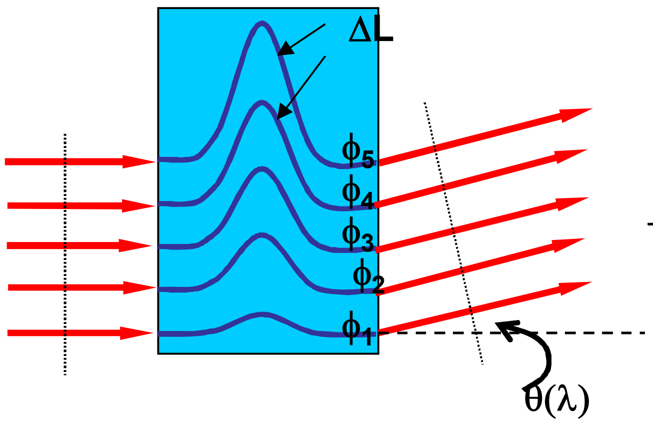

ΔL: length difference between adjacent waveguides in the waveguide array

$$\Delta\phi = \phi_i - \phi_{i-1} = k\Delta L = n(2\pi/\lambda)\Delta L$$

θ will change with wavelength exactly as in a diffraction grating

AWG demultiplexer

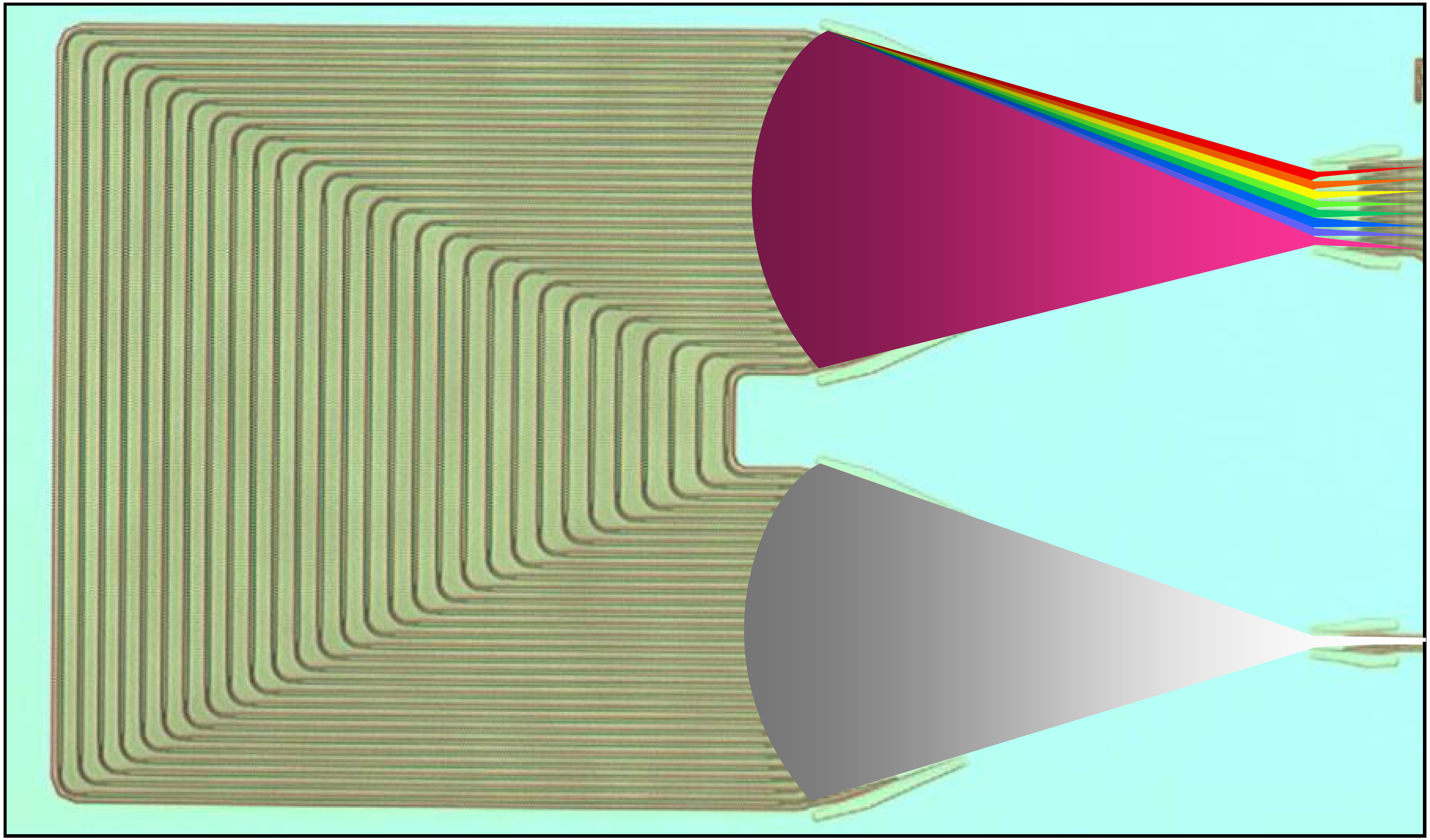

Courtesy, Prof. Roel Baets

AWG demultiplexer

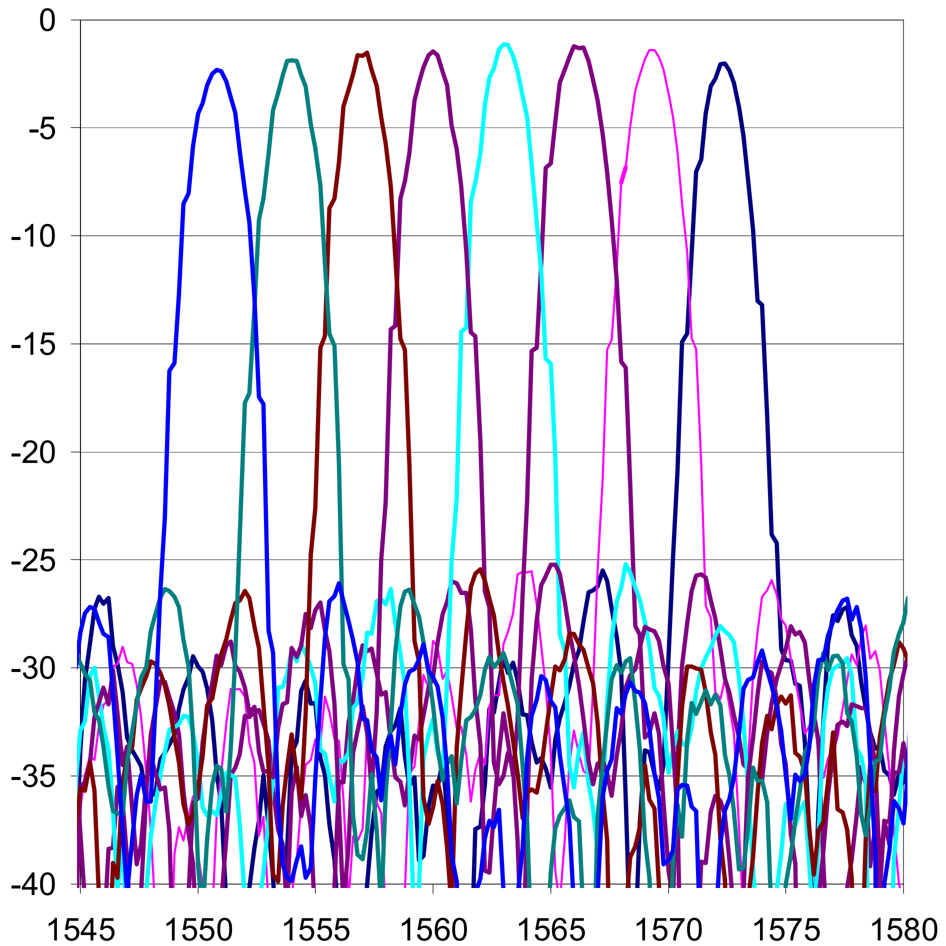

Courtesy, Prof. Roel Baets

AWG principle

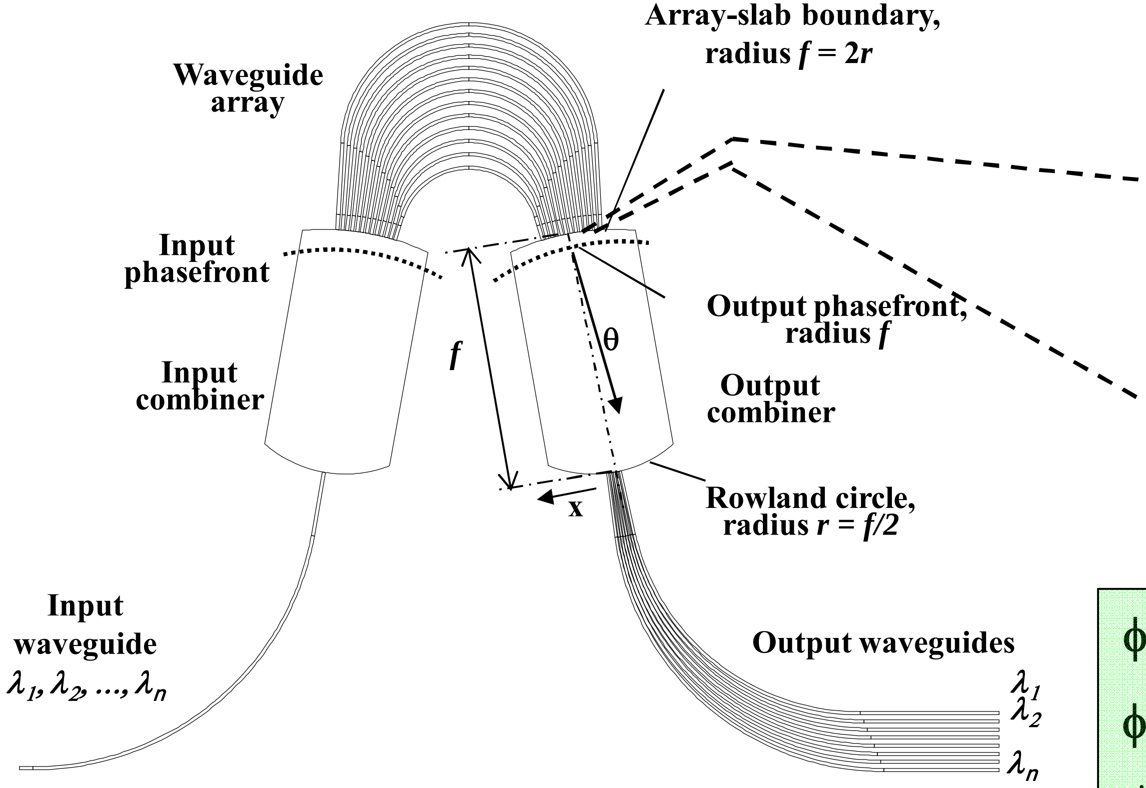

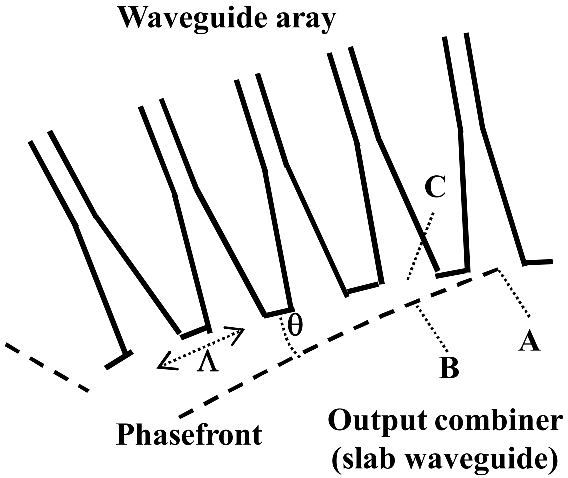

$$\phi_C - \phi_A = \beta_{array}\Delta L = 2\pi\Delta L n_{eff,array}/\lambda$$

$$\phi_C - \phi_B = \beta_{slab}|BC| = |BC| 2\pi n_{eff,slab}/\lambda$$

$$\phi_B - \phi_A = 2\pi m \quad \text{(phasefront)}$$

AWG equation: $n_{eff,s}\Lambda \sin\theta + n_{eff,a}\Delta L = m\lambda$

The light arrives to the end of the array with a phase difference between the adjacent waveguides of $\Delta\varphi_{AWG} = \beta_{array}\Delta L = 2\pi\Delta L n_{eff,array}/\lambda$.

This phase shift is $2\pi m$ for demultiplexer central wavelength $\lambda_c = n_{eff}\Delta L/m$

cusing Properties in 2nd Slab Region

Prof. K. Okamoto

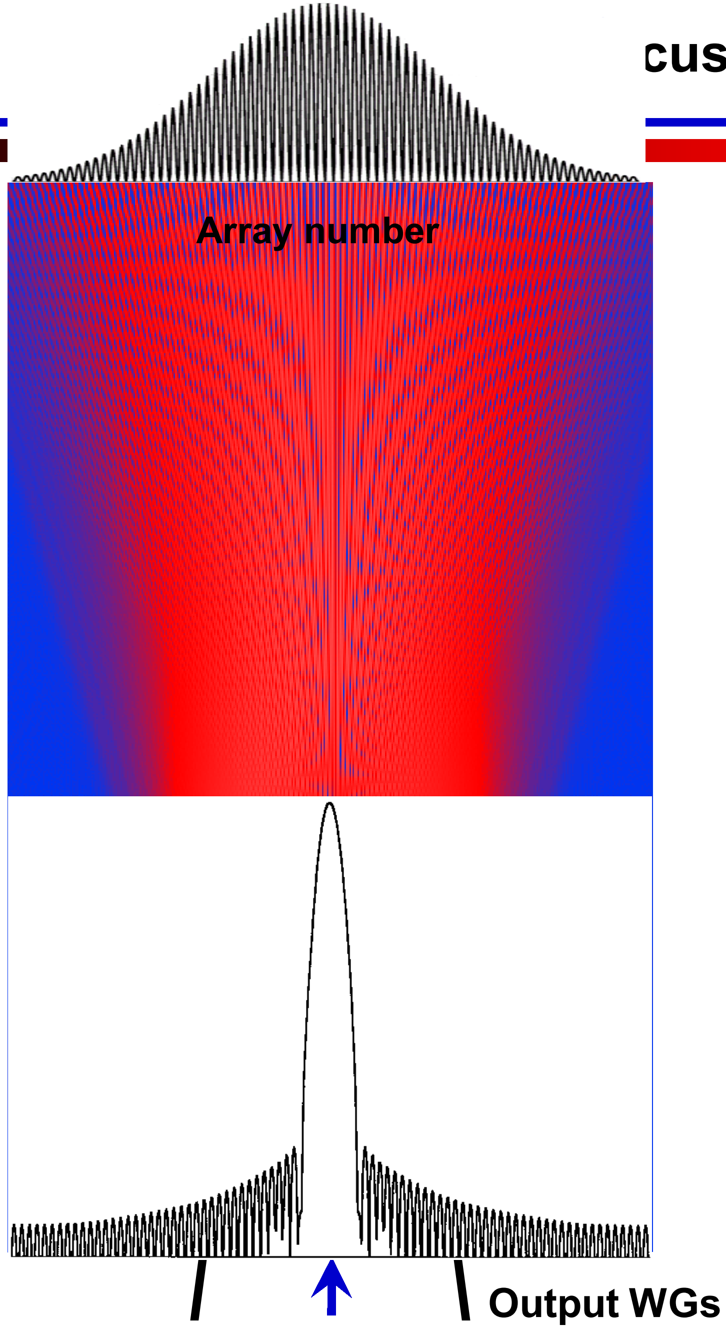

(a) Light focusing in 2nd slab region

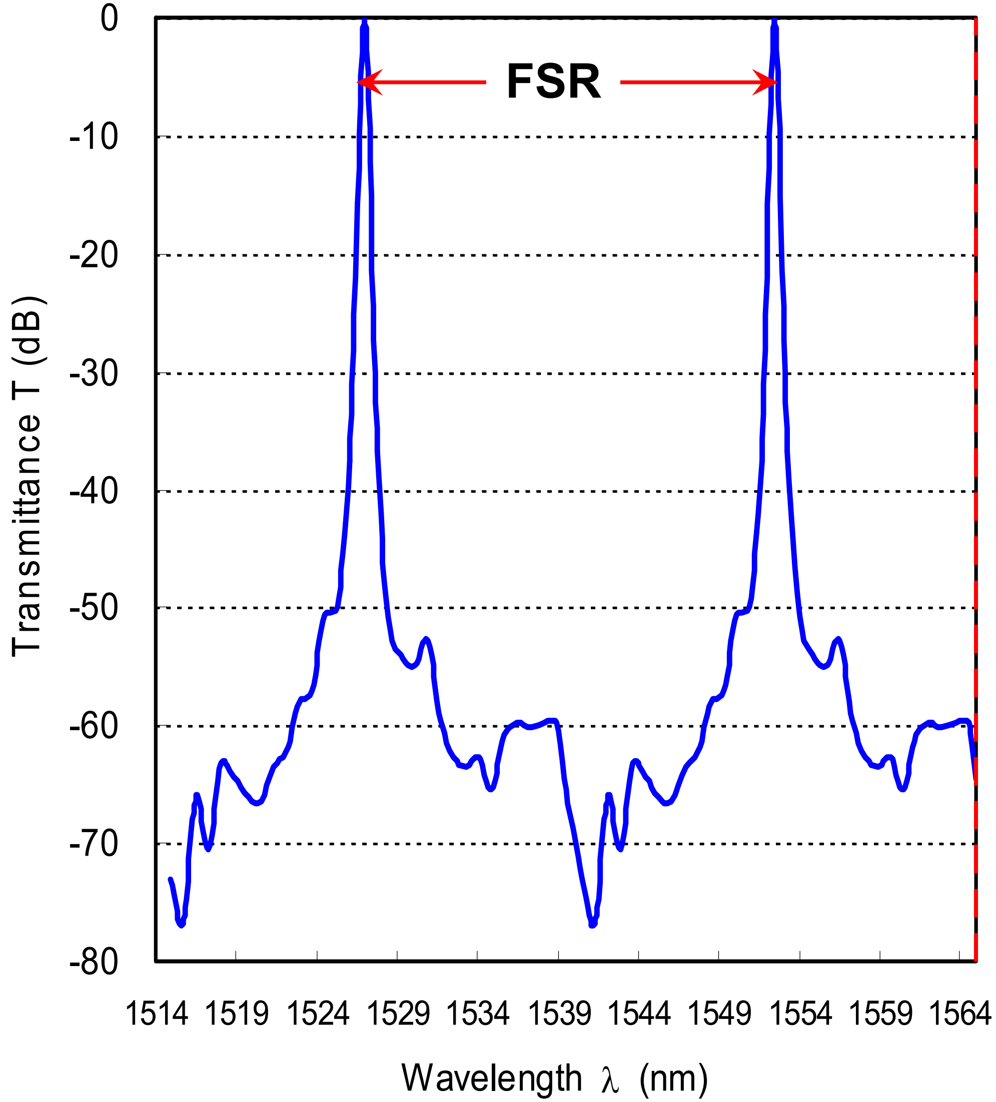

(b) Theoretical demultiplexing property at the center WG

Notes on AWG principle

- The AWG operates similar to a microwave phased array antenna often used in space communications or in satellite tracking. By controlling the phase relationship between the beams emitted by the individual elements of the array, antenna radiation direction is changed without mechanical movements.

- Though it may not look so at the first sight, AWG principle is identical to that of the waveguide echelle grating.

- In an echelle grating, the light interference producing a wavelength-varying propagation direction of diffracted light is due to the phase difference $\Delta\varphi_{EG} = 4\pi\Delta x n_{eff}/\lambda$ between the light reflected by the adjacent facets arranged in a staircase-like fashion with a step Δx.

- In an AWG, the required phase difference $\Delta\varphi$ is obtained by propagating the light in N waveguides of varying lengths with a constant length difference ΔL between the adjacent waveguides, so that $\Delta\varphi_{AWG} = 2\pi\Delta L n_{eff}/\lambda$, where n_{eff} is the effective index of a mode in an arrayed waveguide.

Notes on AWG principle

- Light comprising different wavelengths is coupled from an optical fiber to the input waveguide channel where it propagates towards the input combiner. The input combiner is a slab waveguide confining the light in direction normal to waveguide plane. In the in-plane direction light propagates as in free space, diverging to illuminate the waveguide array input aperture.

- The field profile at the junction between the input waveguide and the slab waveguide is typically Gaussian, so that the divergence half-angle α in the input slab waveguide can be estimated from the Gaussian diffraction formula as $\alpha = 2\lambda/(\pi w n_{eff})$ where w is the Gaussian beam waist (mode diameter) in the input channel waveguide.

- The light couples from the input combiner into the array of channel waveguides that start along an arc centered at the input waveguide/combiner junction, hence of a radius equal to the length of the combiner, also called focal length. This ensures that the light arrives at the beginning of each of the arrayed waveguides with the same phase. For a waveguide array with a constant length difference ΔL between the adjacent waveguides and effective index n_{eff}, the light arrives to the end of the array with a phase difference between the adjacent waveguides of $\Delta\varphi_{AWG} = 2\pi\Delta L n_{eff}/\lambda$.

Notes on AWG principle

- $\Delta\varphi_{AWG} = 2\pi m$ for demultiplexer central wavelength:

  $\lambda_c = n_{eff}\Delta L/m$,

- This results in constructive interference of order *m* between the waves emerging from the waveguide array output aperture. Because the latter is curved along an arc centered at the focal point where the central output channel waveguide joins the output combiner, the phasefront emerging from the waveguide array bears the same curvature hence converging towards the focal point, where it is collected by the central output waveguide. For a wavelength λ, interference maxima are produced in the output coupler in direction θ with respect to the coupler when:

  $$n_{eff,s}\Lambda\sin\theta + n_{eff,a}\Delta L = m\lambda$$

  as it is evident from phase conditions shown in inset of the AWG figure. This equation is equivalent to scalar grating equation, where Λ is the waveguide pitch at the interface of the waveguide array and the output coupler, and $n_{eff,s}$ and $n_{eff,a}$ are the effective indexes of the slab and array waveguides, respectively.

Notes on AWG principle

- Including the effect of varying mode index with wavelength by introducing a modified interference order $M = m(n_{g,a}/n_{eff,a})$, where $n_{g,a}$ is the group index of the arrayed waveguides, it is obtained for that angle θ of the diffracted beam in the output coupler:

$$\sin\theta = \frac{(\lambda - \lambda_c)M}{n_{eff,s}\Lambda} \qquad\qquad n_g = n_{eff} - \lambda\frac{dn_{eff}}{d\lambda}$$

- By differentiating this equation, AWG linear dispersion along the focal curve is: $dx/d\lambda = f\, d\theta/d\lambda = f\, n_{g,a}\Delta L/(\lambda_c n_{eff,s}\Lambda) = f\, M/(n_{eff,s}\Lambda)$, for a coupler of length *f*. This dispersion results in a constant channel spacing if the receiver waveguides are equidistantly spaced along the focal curve that is the Rowland circle of radius *f/2* tangent to the arc contouring the array output aperture of radius *f*.

- Free spectral range is $FSR = \lambda_c/M$, similar to an ordinary diffraction grating.

- Similar equivalence also applies to other AWG parameters. For example, as in a conventional grating, the far field pattern is given the slit function *SF* arising from diffraction from a single arrayed waveguide with mode width *w* at slab-array interface. Hence, changing the waveguide width by tapering the waveguides near the slab-array interface has the same effect as varying grating facet width, namely the loss penalty (roll-off) when approaching the peripheral output channels increases with the slit width.

Waveguide echelle gratings

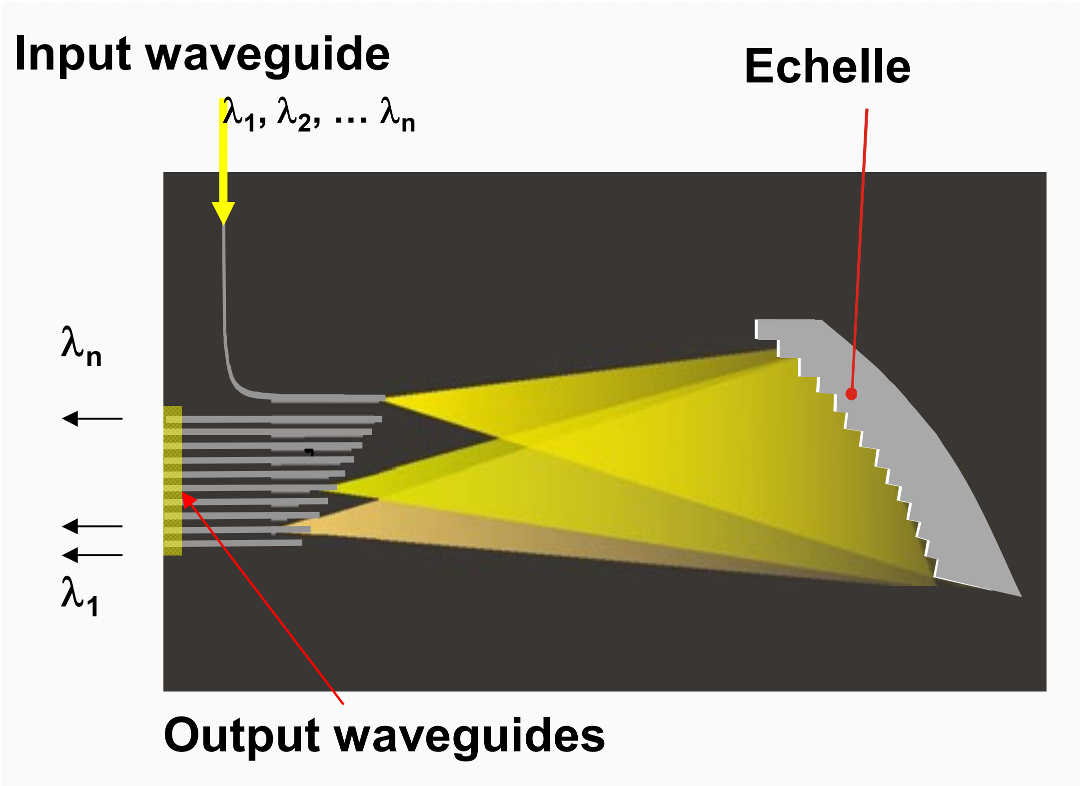

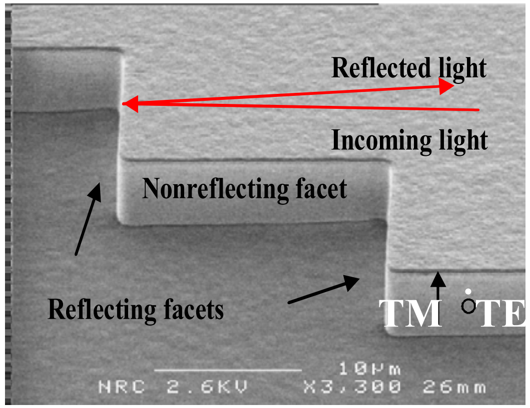

40 and 256 channel waveguide echelle grating mux/dmux

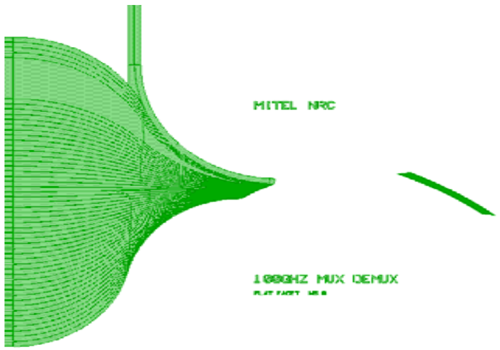

40 Channel DMUX
100 GHz

1.7 x 1.8 cm,
40 dies / 6"wafer

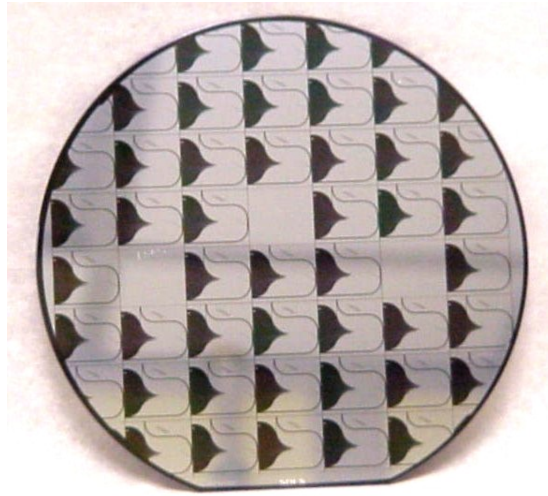

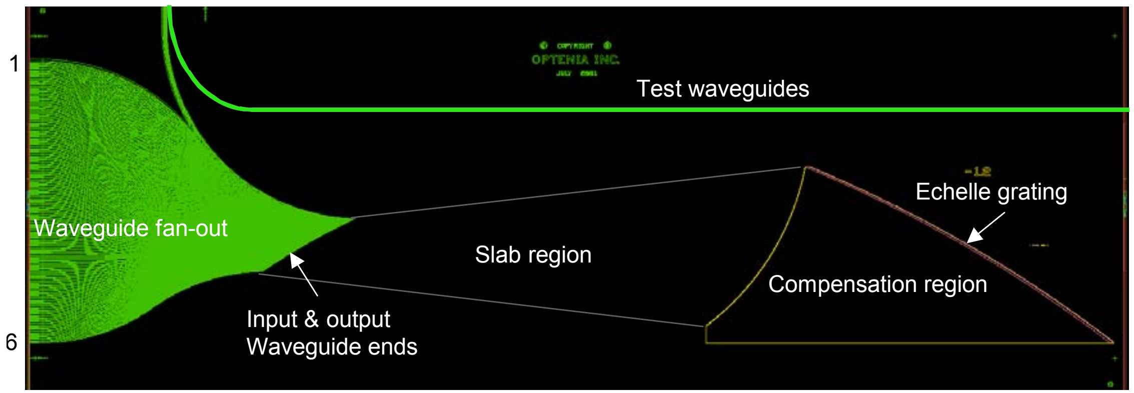

256 Channel DMUX
25 GHz

2 x 4 cm

All process steps
are identical

S. Janz et al., Photon. Technol. Lett. **6,** 503-505 (2004).

40 and 256 channel EG dmux, measured spectra

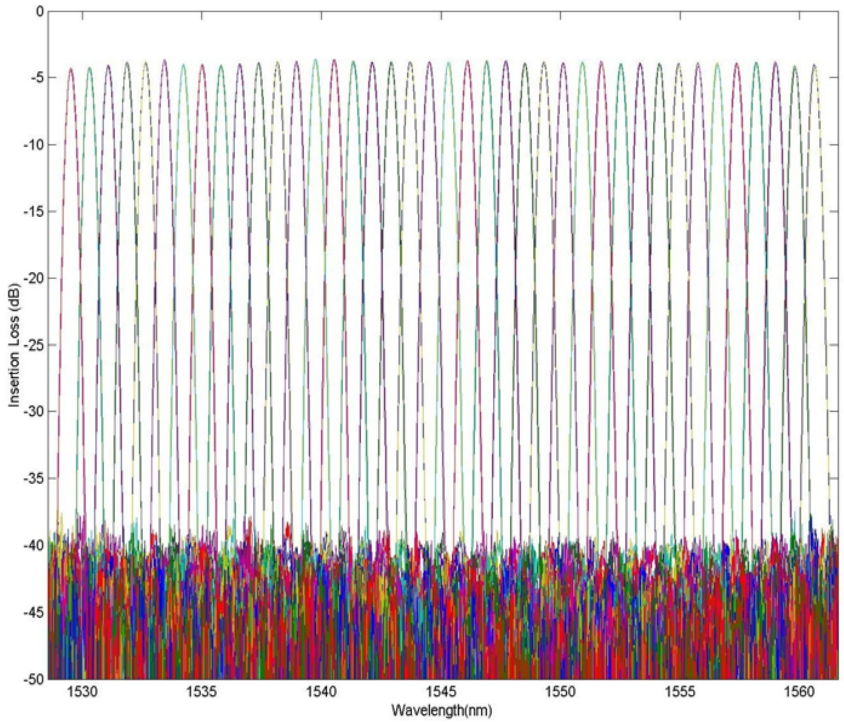

40 channel echelle grating DMUX

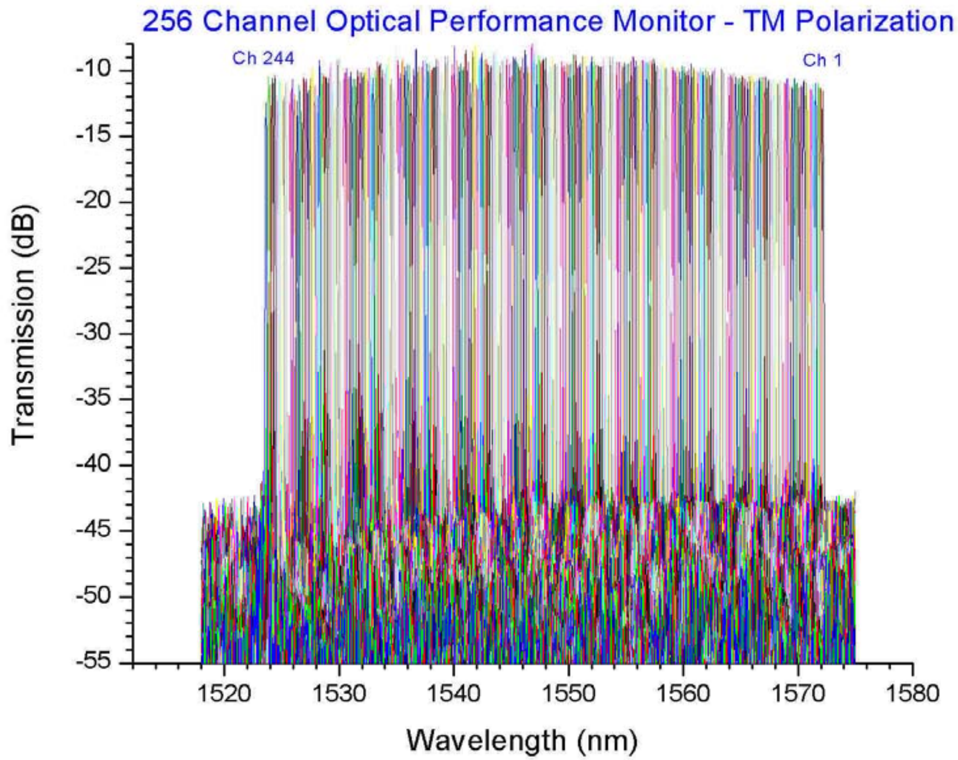

256 channel echelle grating DMUX

Loss - 4.4 dB (packaged)

Loss uniformity < 0.8 dB

PDL < 0.3 dB

PD-λ < 10 pm

Crosstalk < - 35 dB

S. Janz et al., Photon. Technol. Lett. **6,** 503-505 (2004)

Size advantage of SOI waveguides

Packaged 256 channel AWG WDM demultiplexer
glass waveguides, NTT

~ 30 cm

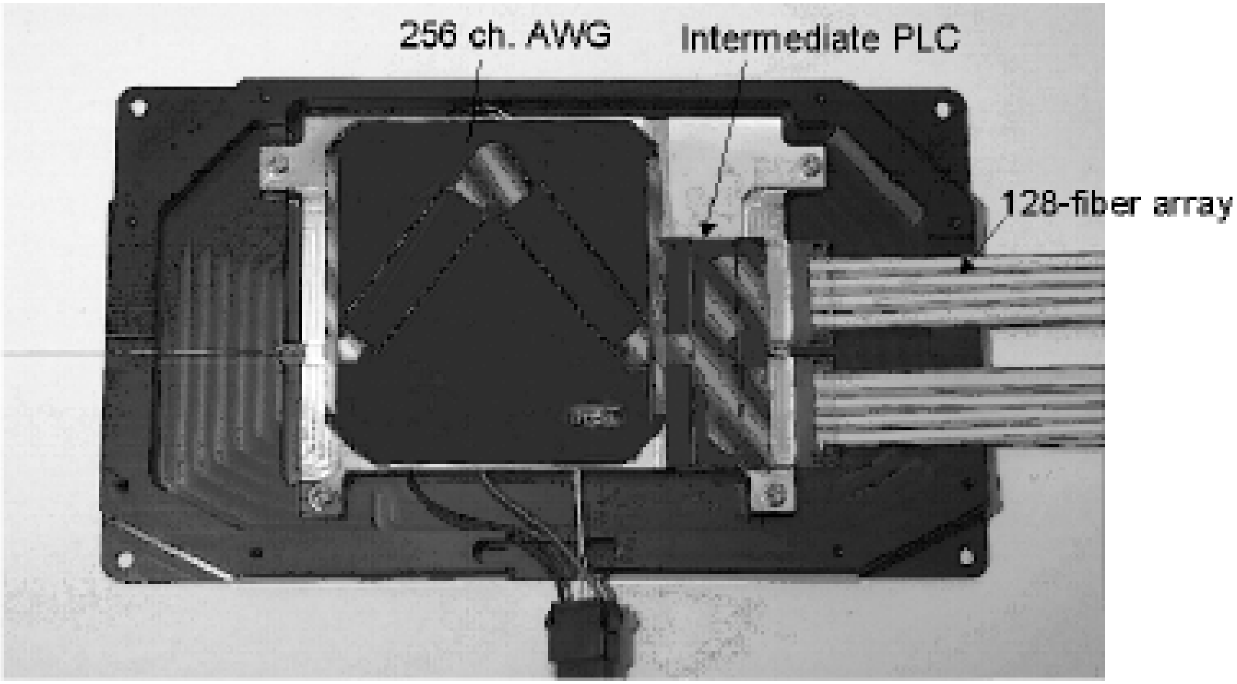

Silicon AWG microspectrometer,
NRC Canada, 1999
~0.5 cm²

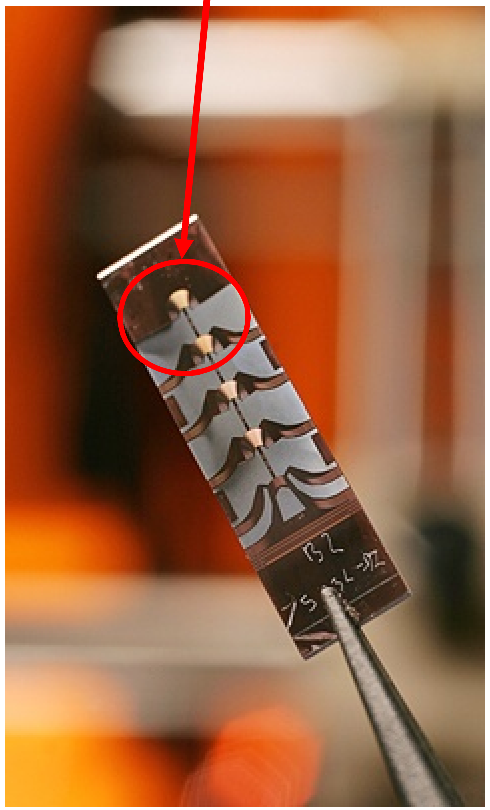

P. Cheben et al., SPIE Proc. **4293**, pp. 15-22 (2001)
P. Cheben et al., SPIE Proc. **4997**, pp. 181-189 (2003)

AWG high resolution spectrometers in SOI

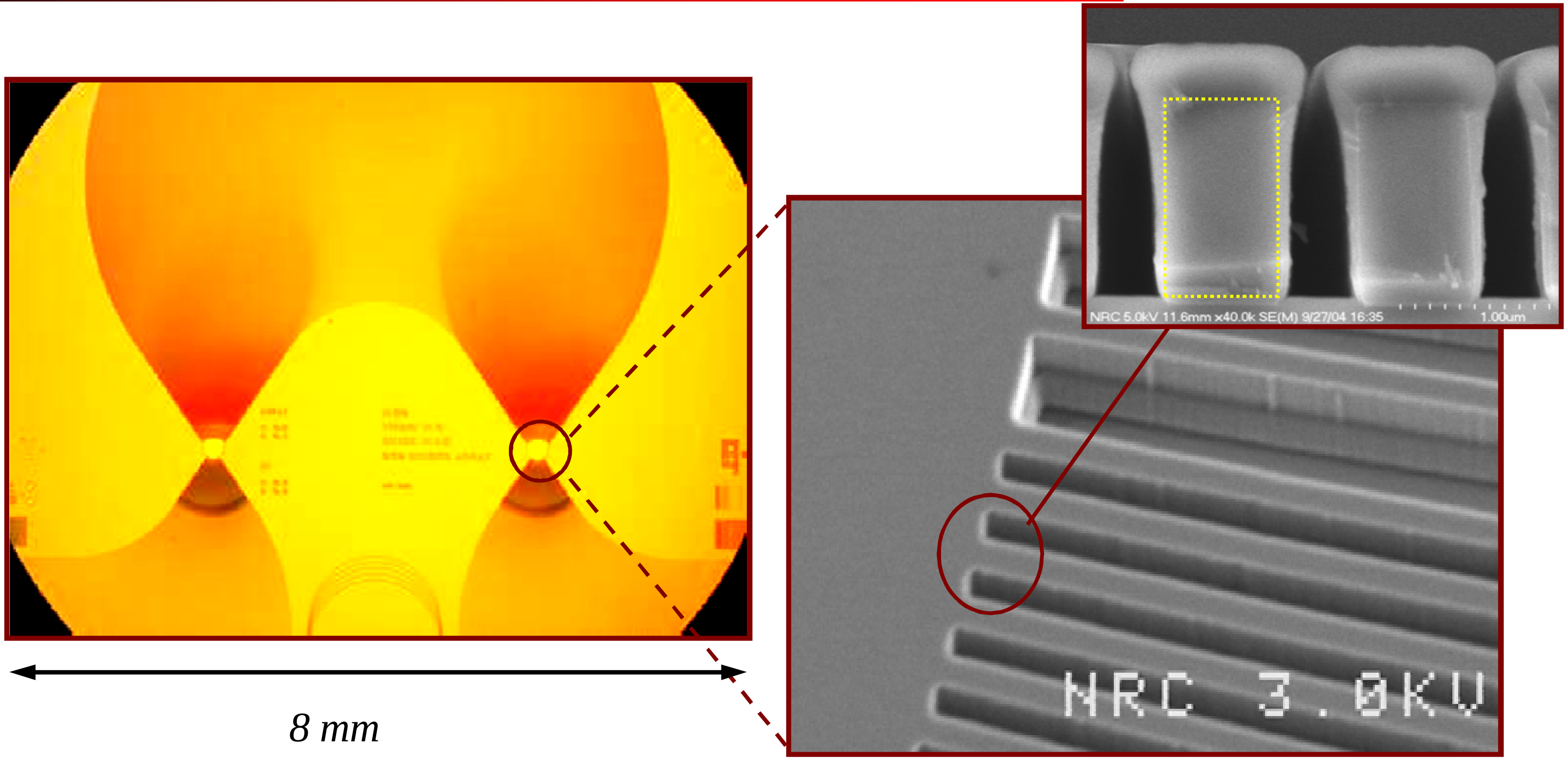

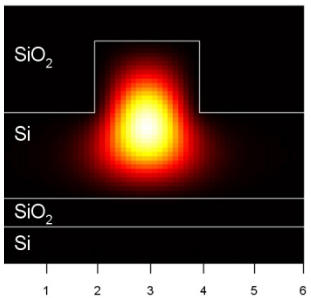

- The waveguide array consists of 125 waveguides in a ~ 5×5 mm^2 area, that is only possible in high index contrast platforms such as SOI.
- Spectrometer aperture is reduced to a 1.5 x 0.6 μm slit
- Channel spacing is **0.2 nm** (**25 GHz**), with 50 output channels.

P. Cheben et al., Optics Express, vol. 15, p. 2299, 2007

Measured microspectrometer response

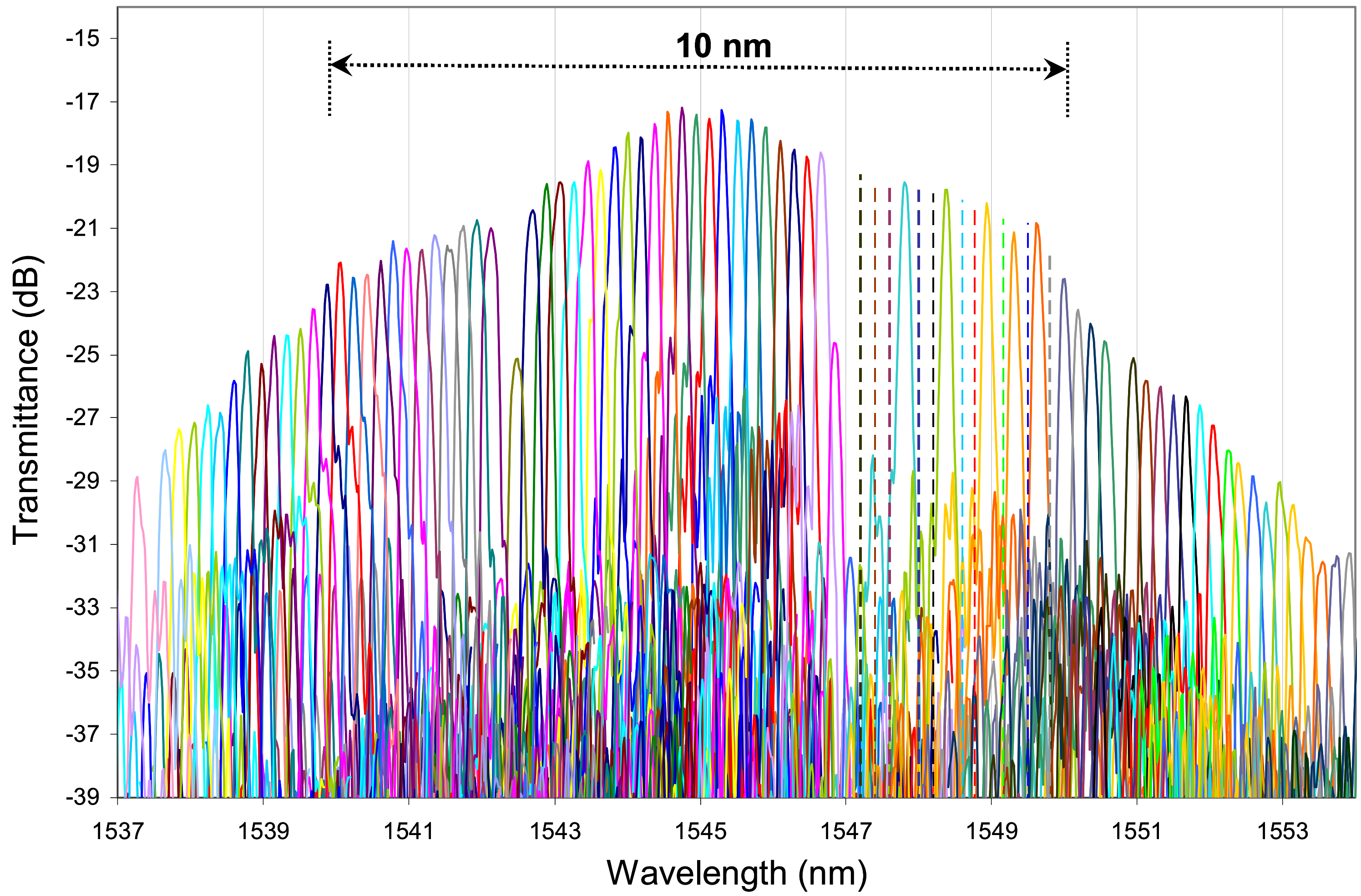

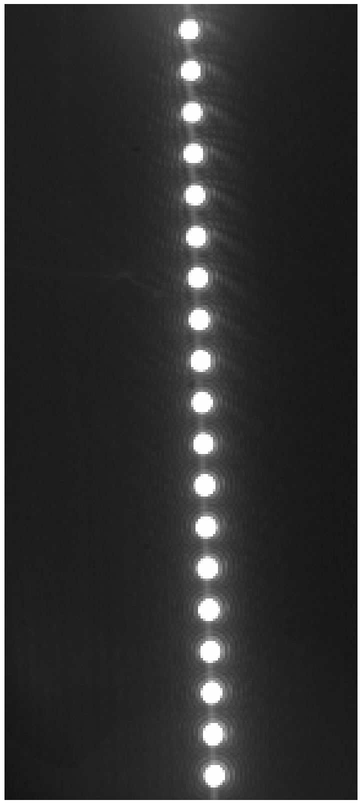

Output waveguide array IR image

P. Cheben et al., Optics Express, Vol. 15, p. 2299, March 5, 2007

Microspectrometer interrogation of FBG sensors

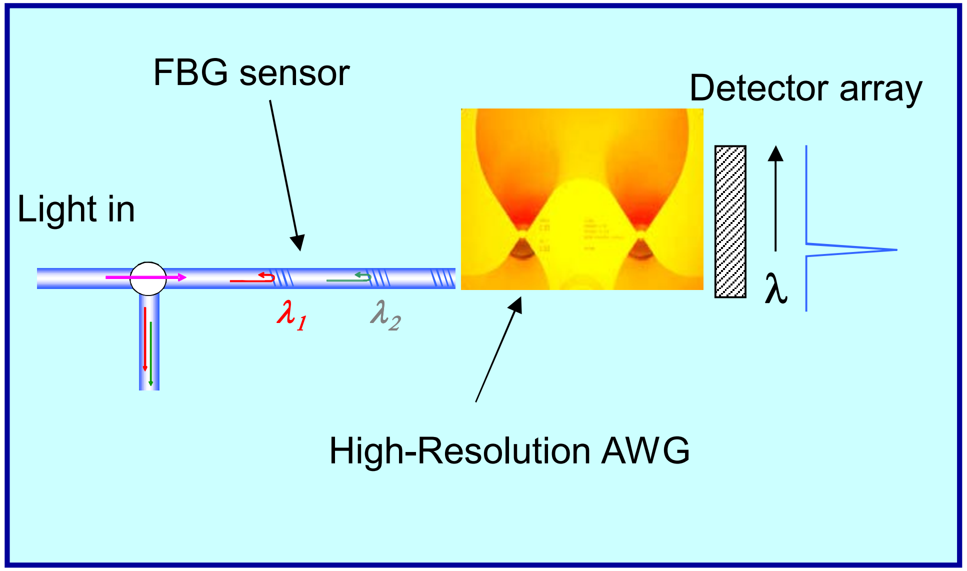

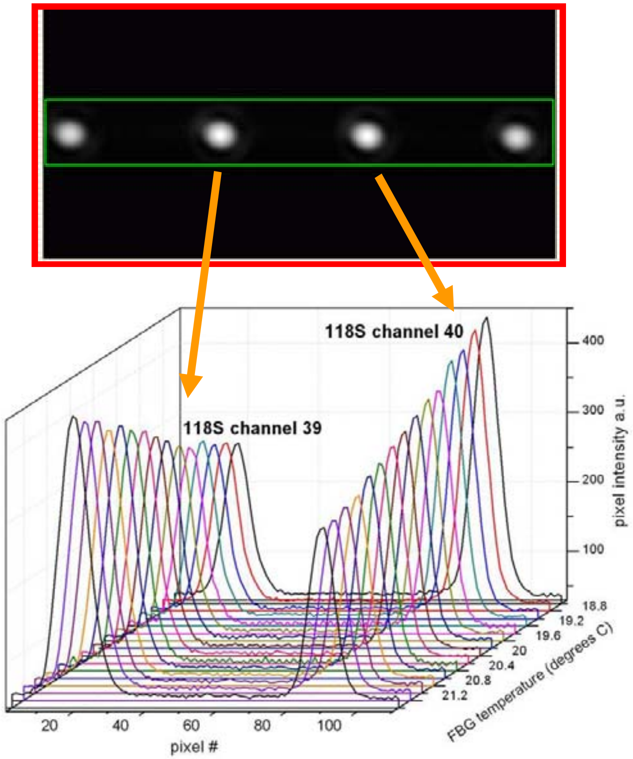

- Fiber Bragg Grating (FBG) sensors are extensively used as strain and temperature sensors.
- Using SOI high resolution microspectrometer, FBG resonance wavelength is determined to an accuracy of ± *0.8 pm* from the intensity ratio of adjacent AWG channels, achieving similar resolution as an optical spectrum analyzer.
- Multiple FBG gratings can be simultaneously monitored.

P. Cheben et al., Optics Letters, Vol. 33, pp. 2647-2649, 2008

Interrogating a fibre Bragg grating sensor using SOI AWG

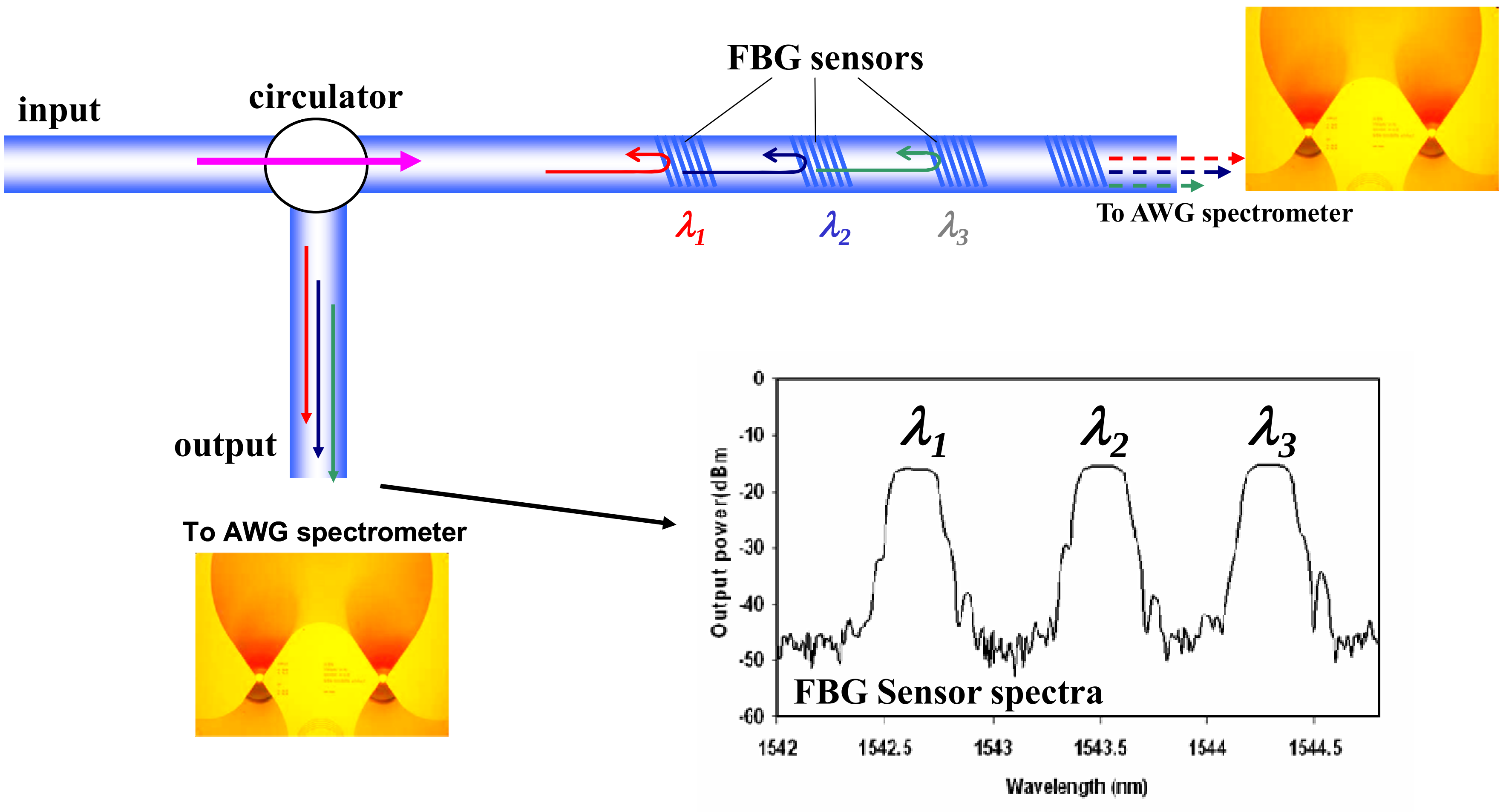

Monitoring AWG adjacent output channels

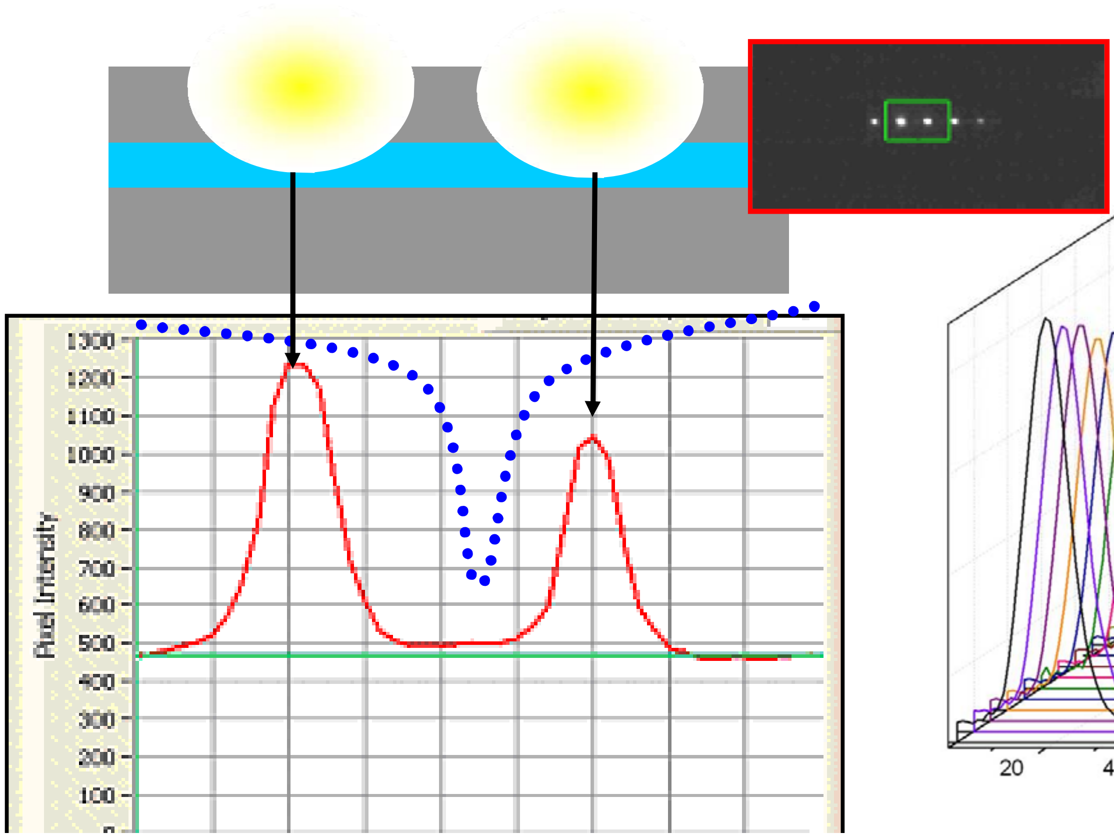

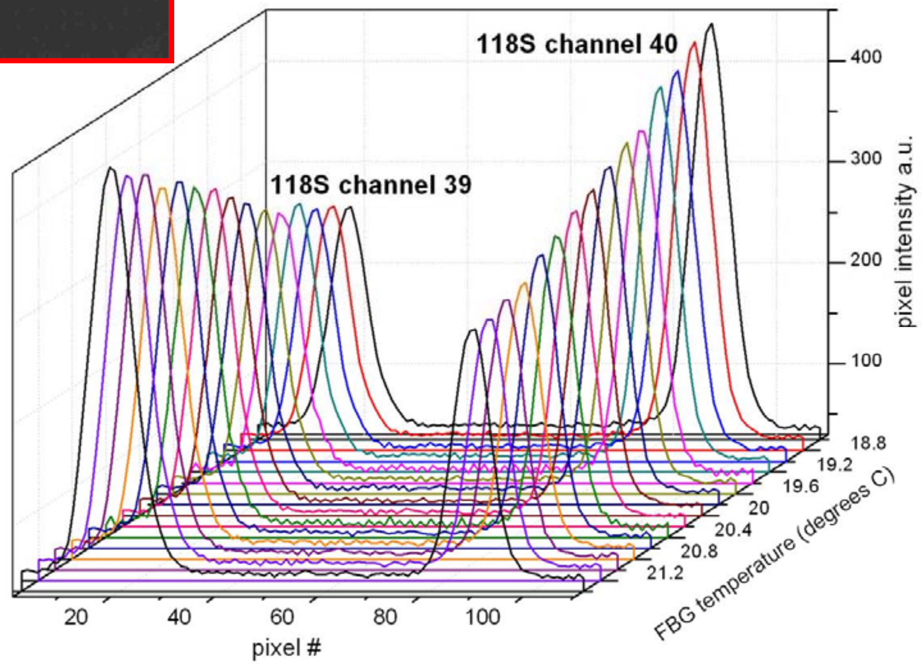

- *FBG resonance wavelength is determined from the intensity ratio of nearby AWG channels*
- *Multiple FBG gratings can be simultaneously monitored*
- *Suppressed temperature sensitivity to 0.3 pm/℃ by monitoring a differential wavelength shift between the Bragg and cladding resonances*

Using micro-spectrometer to determine surrounding refractive index of TFBG

- Cladding modes are sensitive to surrounding refractive index, but the core (Bragg) mode is not
- Cladding modes and the core mode are (nearly) equally temperature sensitive
- Separation between the core and cladding modes changes due to surrounding refractive index change

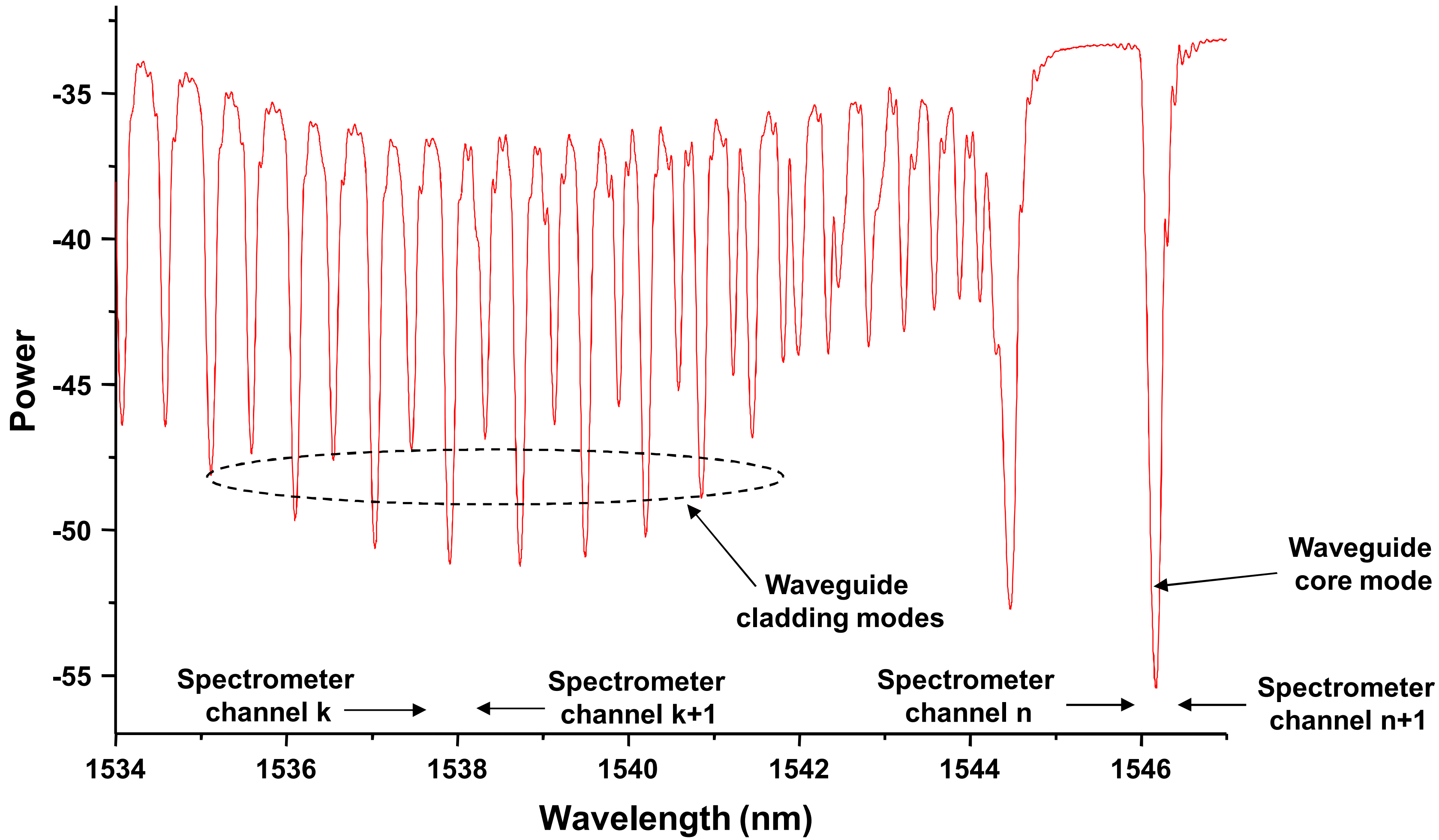

Using micro-spectrometer to determine surrounding refractive index of TFBG

- Cladding modes are sensitive to surrounding refractive index, but the core (Bragg) mode is not
- Cladding modes and the core mode are (nearly) equally temperature sensitive
- Separation between the core and cladding modes changes due to surrounding refractive index change

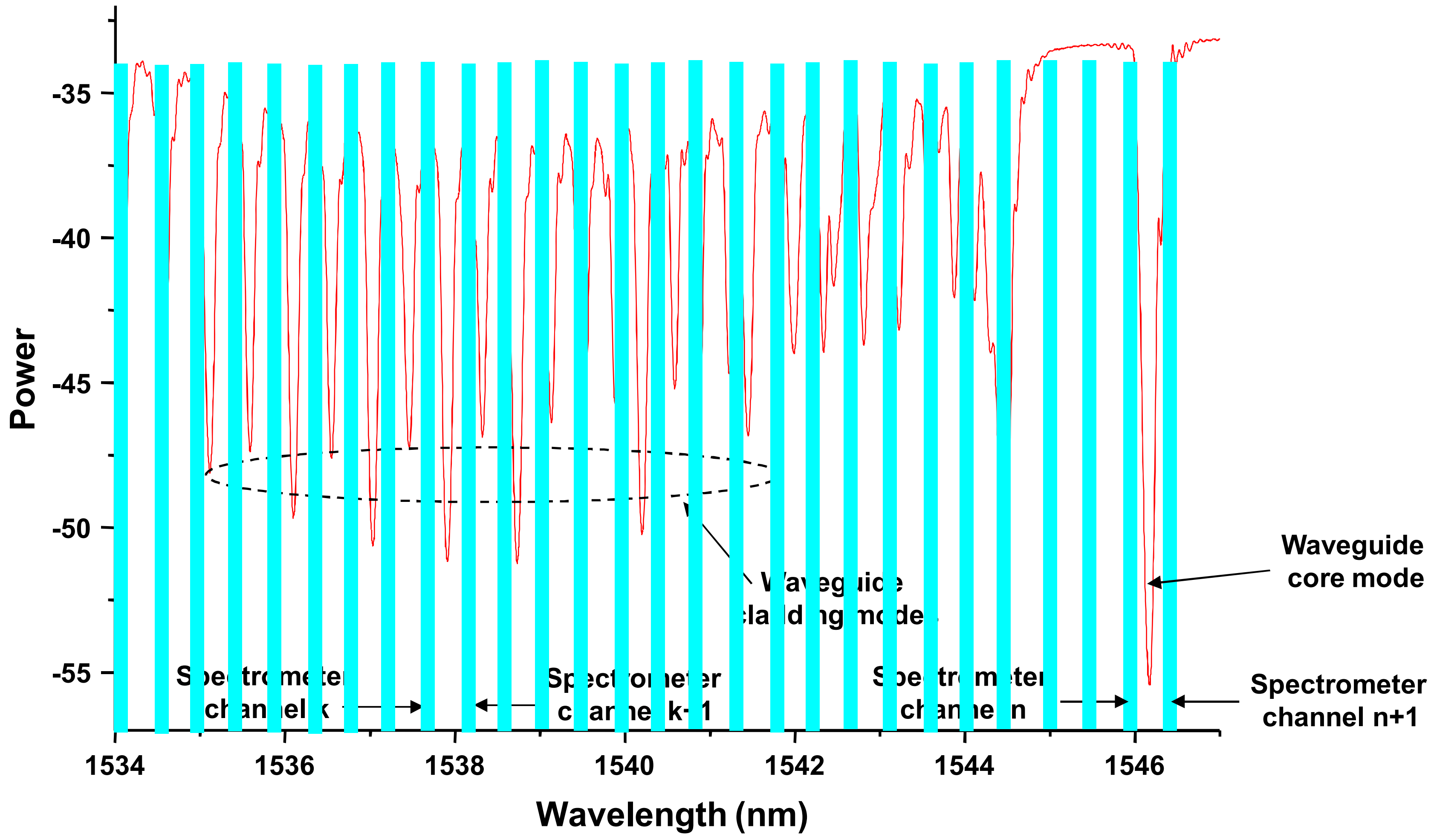

Using micro-spectrometer to determine surrounding refractive index of TFBG

- Cladding modes are sensitive to surrounding refractive index, but the core (Bragg) mode is not
- Cladding modes and the core mode are (nearly) equally temperature sensitive
- Separation between the core and cladding modes changes due to surrounding refractive index change

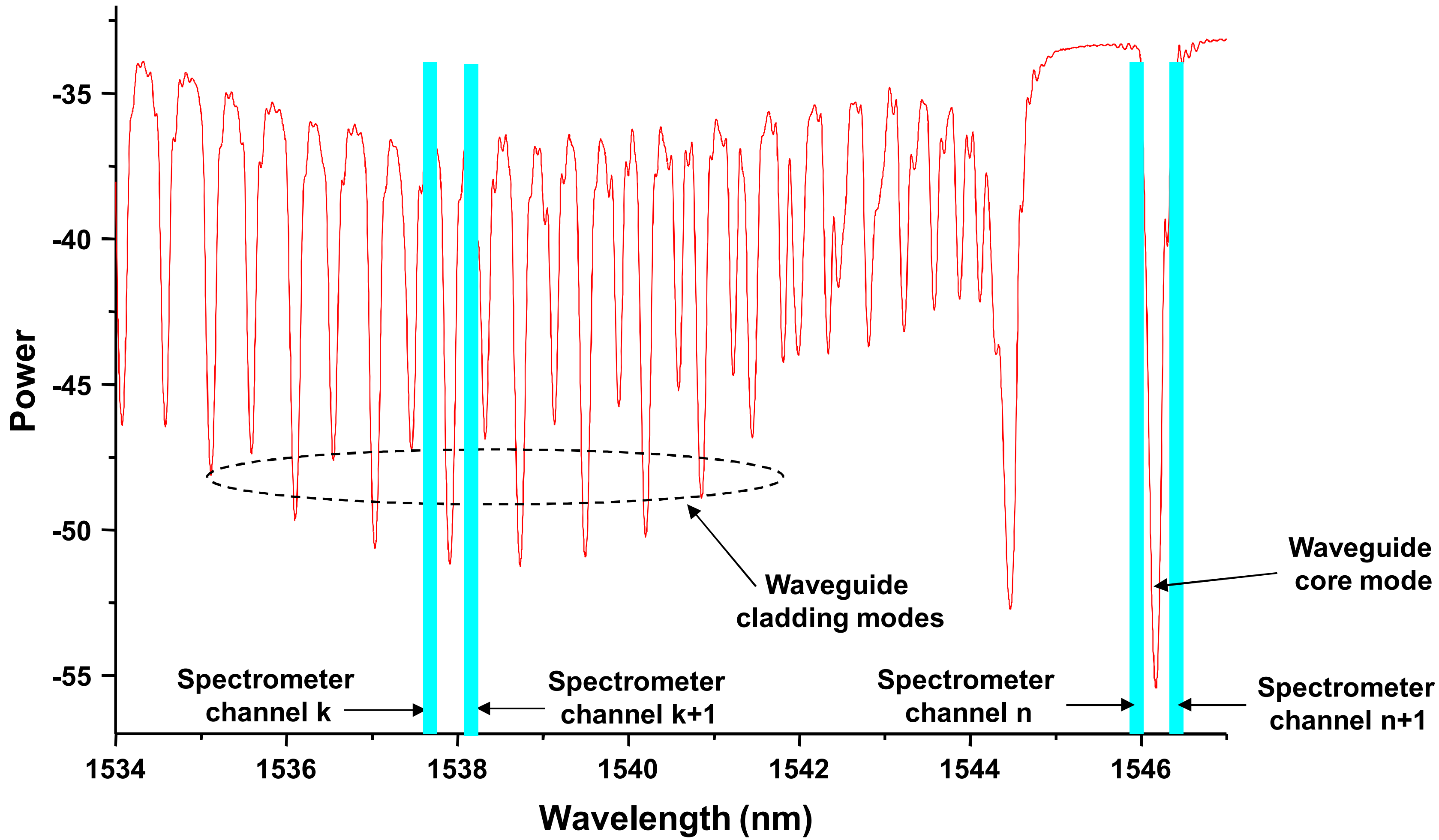

Sensor interrogation experimental set-up

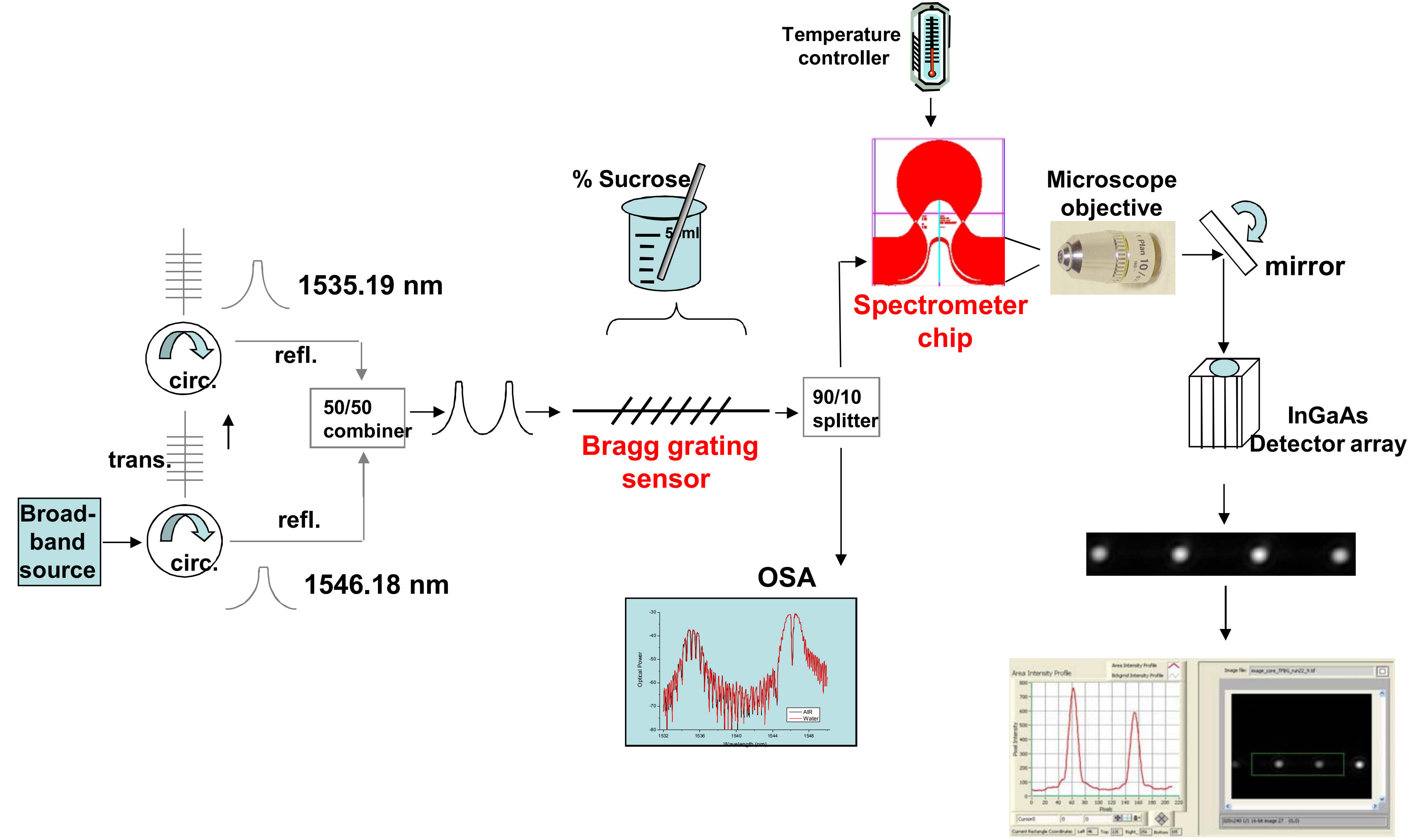

Experimental results

Comparing measured wavelength shifts: micro-spectrometer versus optical spectrum analyzer

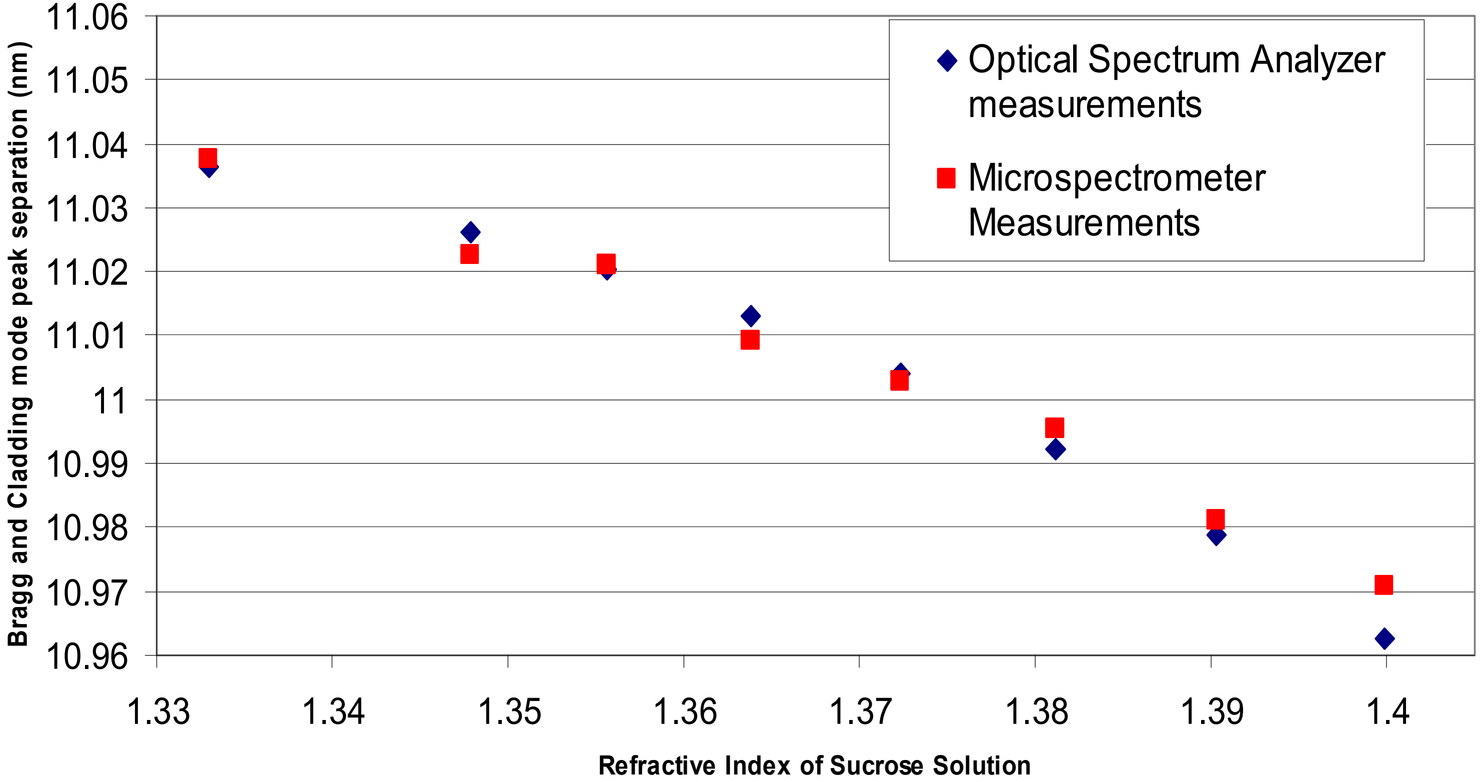

Wavelength accuracy 0.8 pm

P. Cheben et al., Optics Letters, Vol. 33, No. 22, pp. 2647-2649, 2008

Slow light AWG spectrometer

Modified group index

$n_g' = n_g + \Delta n_g$

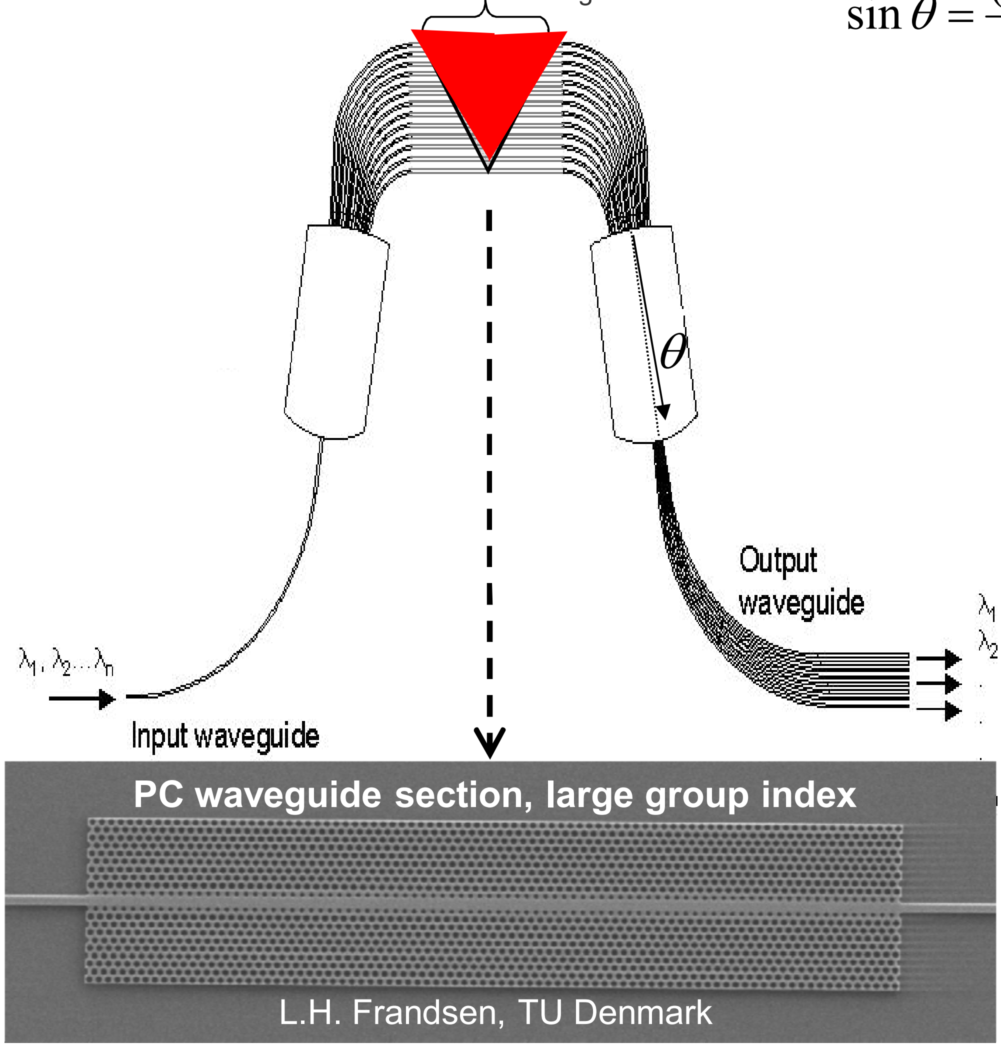

Dispersion:

$$\sin\theta = \frac{(\lambda-\lambda_c)(M+M')}{n_{eff,s}\Lambda} = \frac{(\lambda-\lambda_c)(n_g\Delta L + \Delta n_g \Delta L_g)}{\lambda_c n_{eff,s}\Lambda}$$

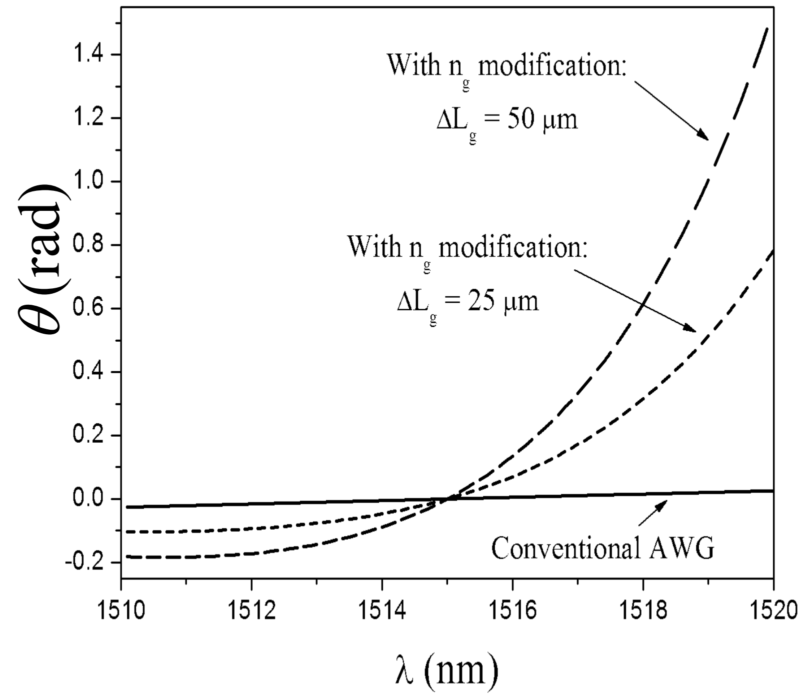

O. Martinez et al., J. Lightwave Technol. **24,** p. 1551, 2006

S. Murugkar et al., SPIE Proc. Vol. 8264 , art. no. 82640T, 2012

Curved waveguide sidewall grating demultiplexer

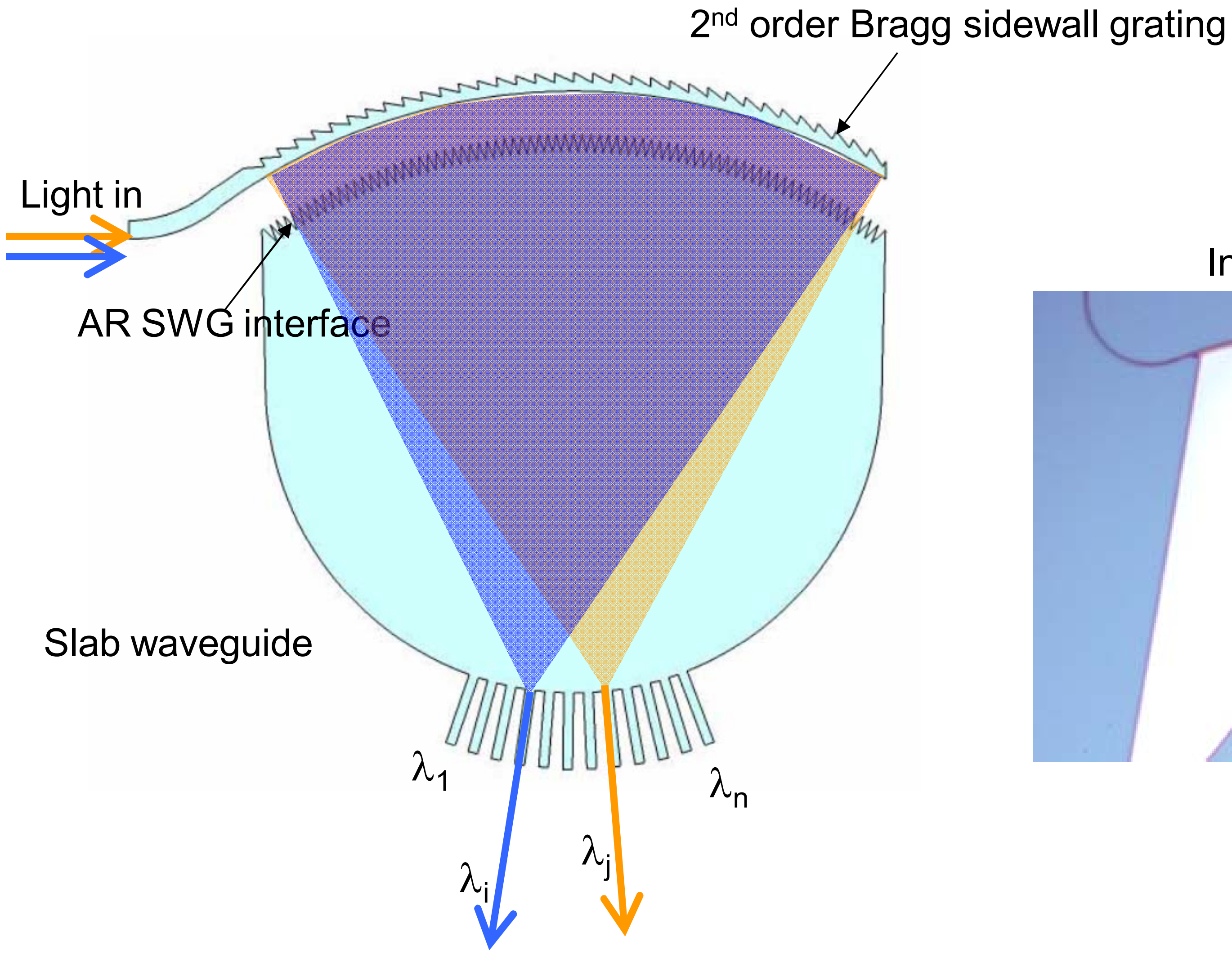

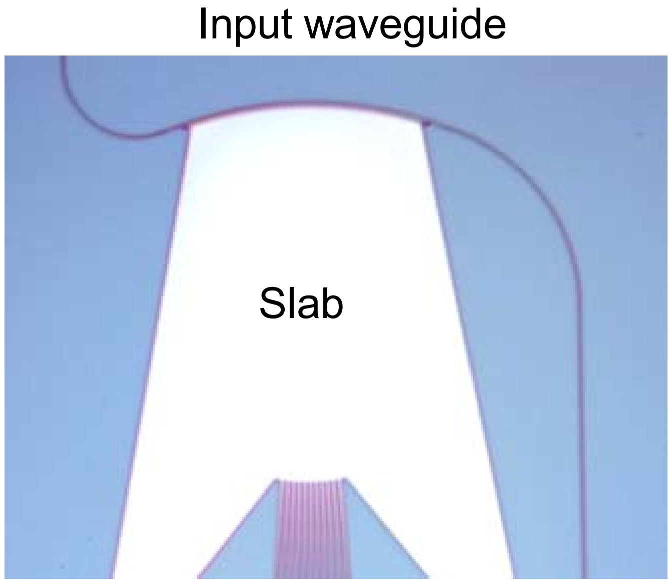

P. J. Bock , P. Cheben et al., Optics Express **16**(22) 17616-17625 (2008)

Subwavelength grating demultiplexer

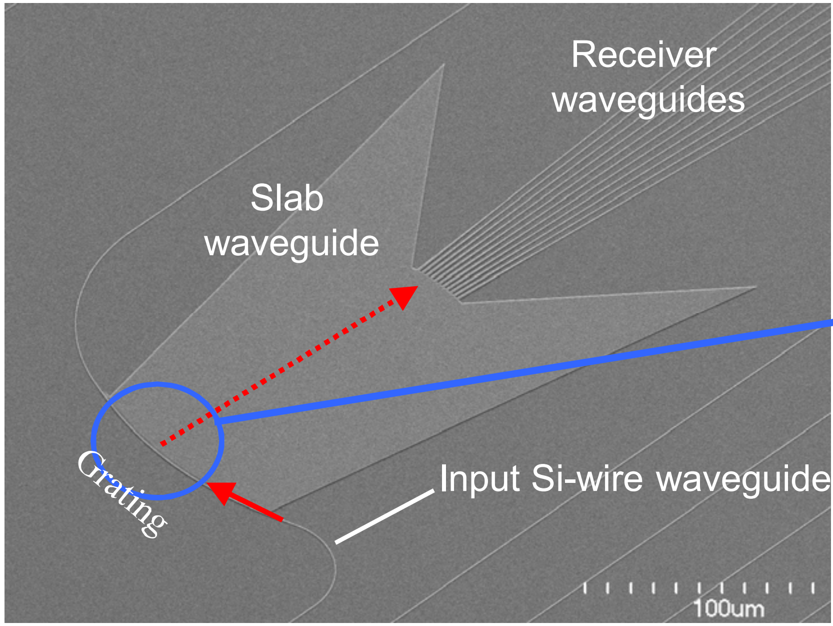

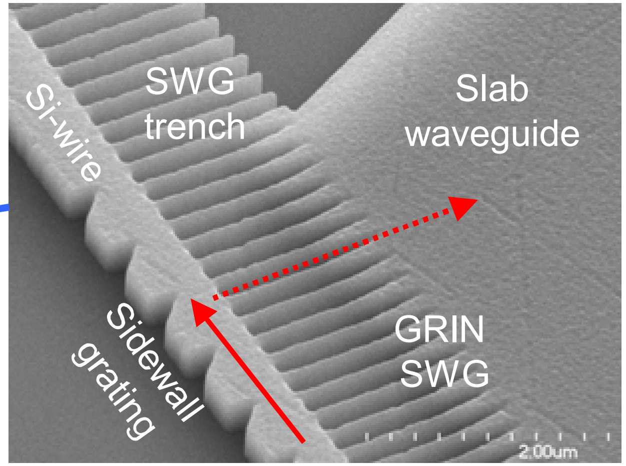

SWG acts as:

1) Lateral cladding for the strip waveguide
2) Slab waveguide for light diffracted by the grating
3) GRIN anti-reflective interface

P. J. Bock et al., Opt. Express 16, 2008
P. Cheben et al., Opt. Lett. 35, p. 2526, August 2010
P. J. Bock et al., Optics Express 20, 19882, 2012

Measured demultiplexer spectrum

CWDM
11 channels spaced at 18 nm
200 nm bandwidth

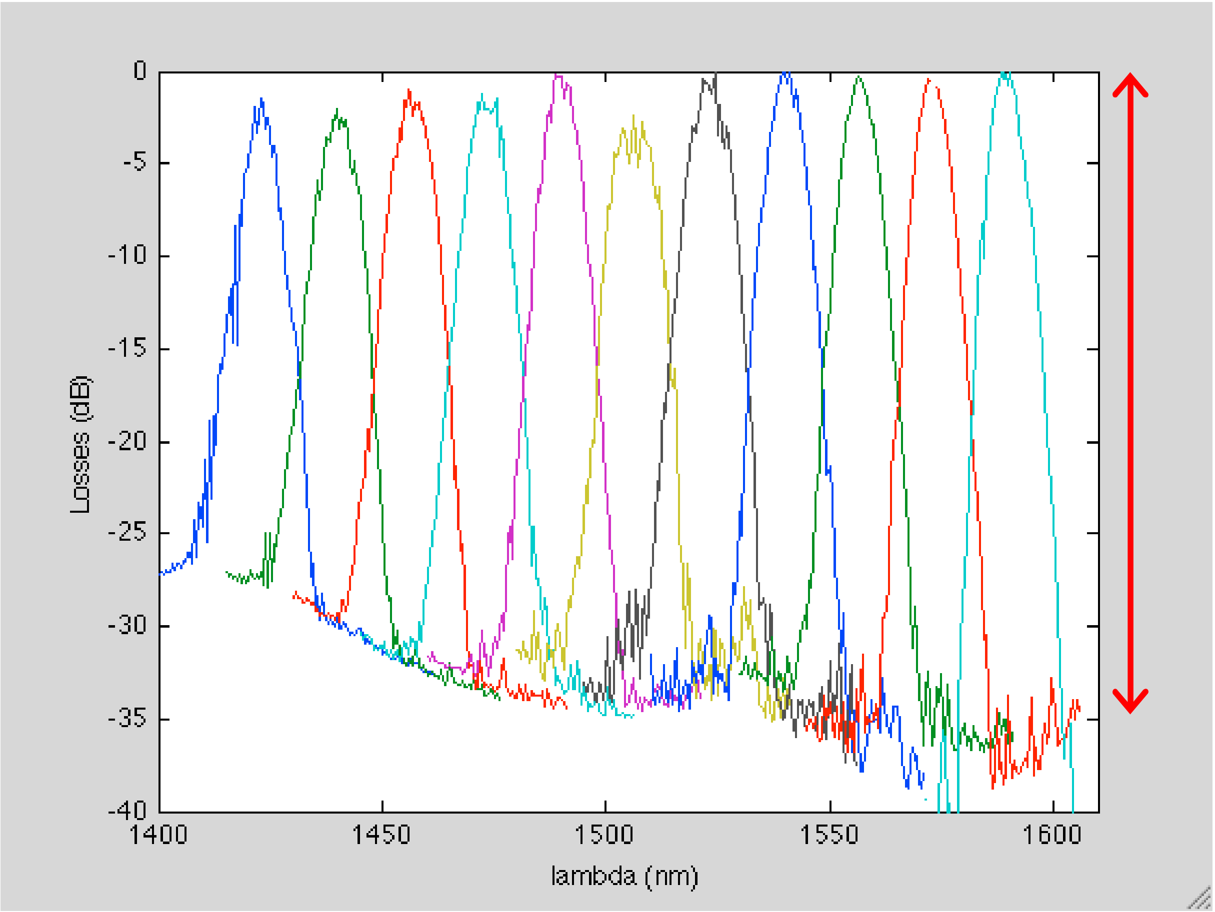

Crosstalk -35dB (double pass)

Size: 160μm×100μm

P. J. Bock et al., Optics Express 20, 19882, 2012

An integrated spectrometer

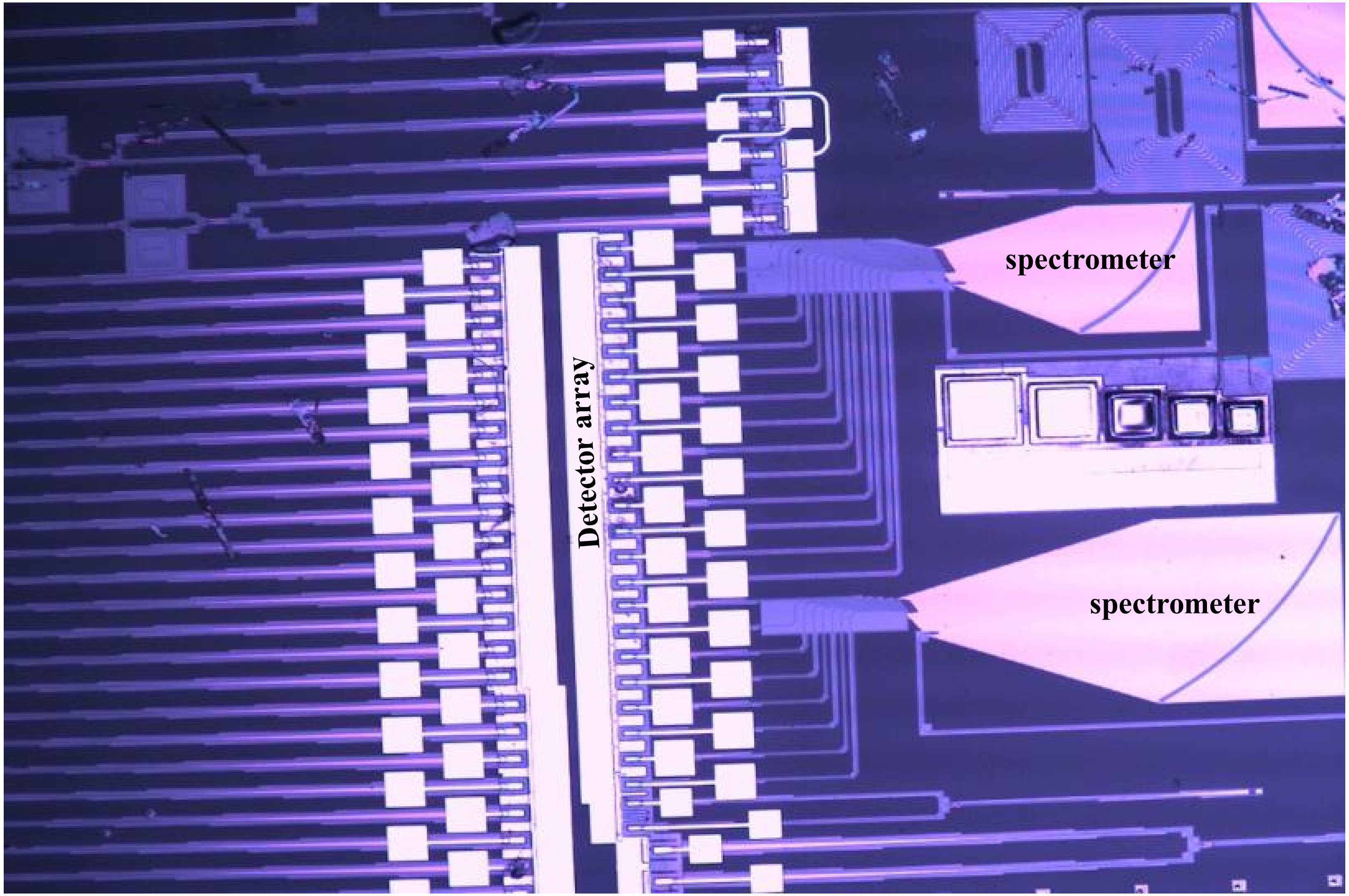

Ghent University

E. Ryckeboer et al., Opt Express 2013

Phased array beam scanners

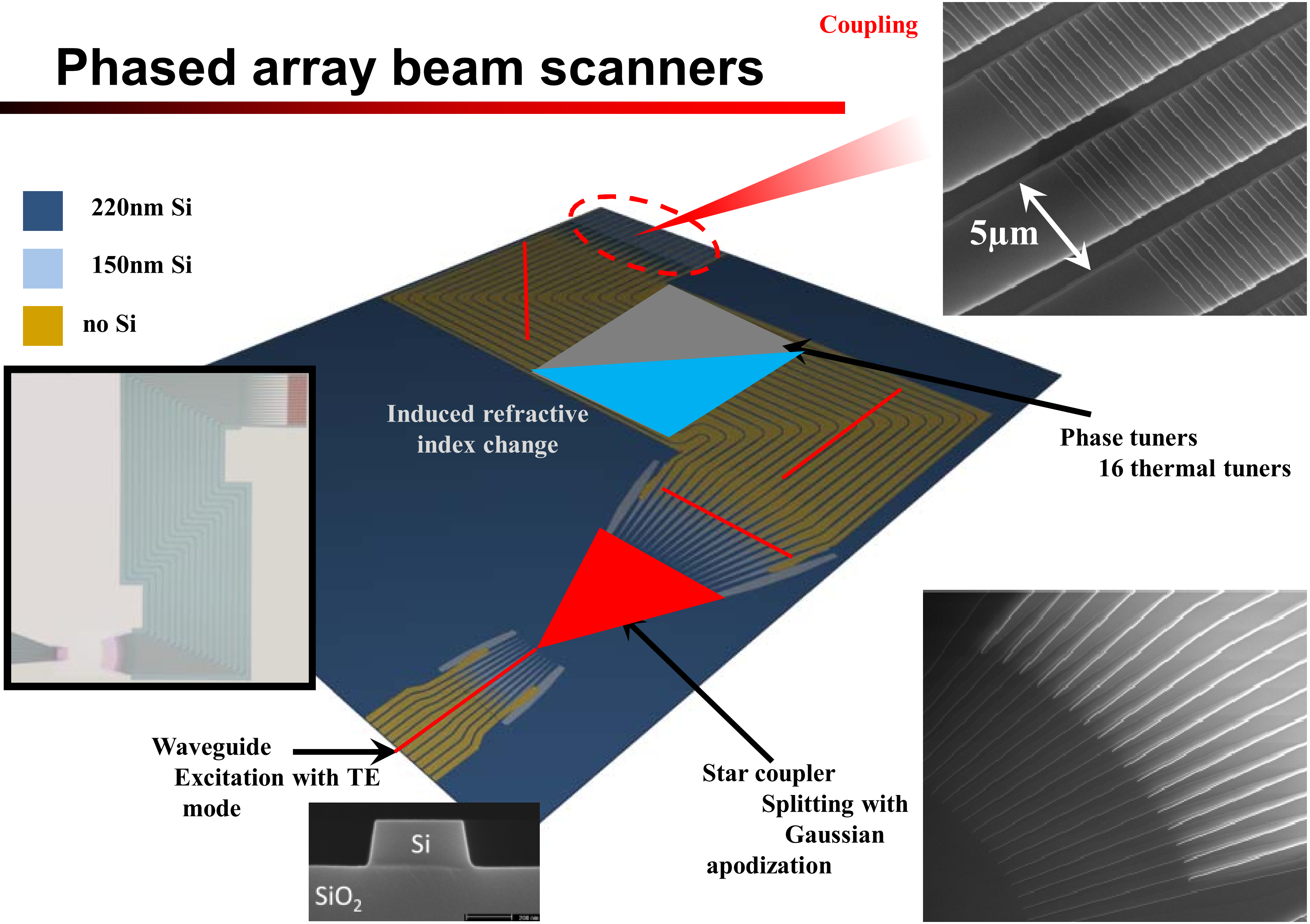

Courtesy: Prof. Roel Baets

Efficient light collection

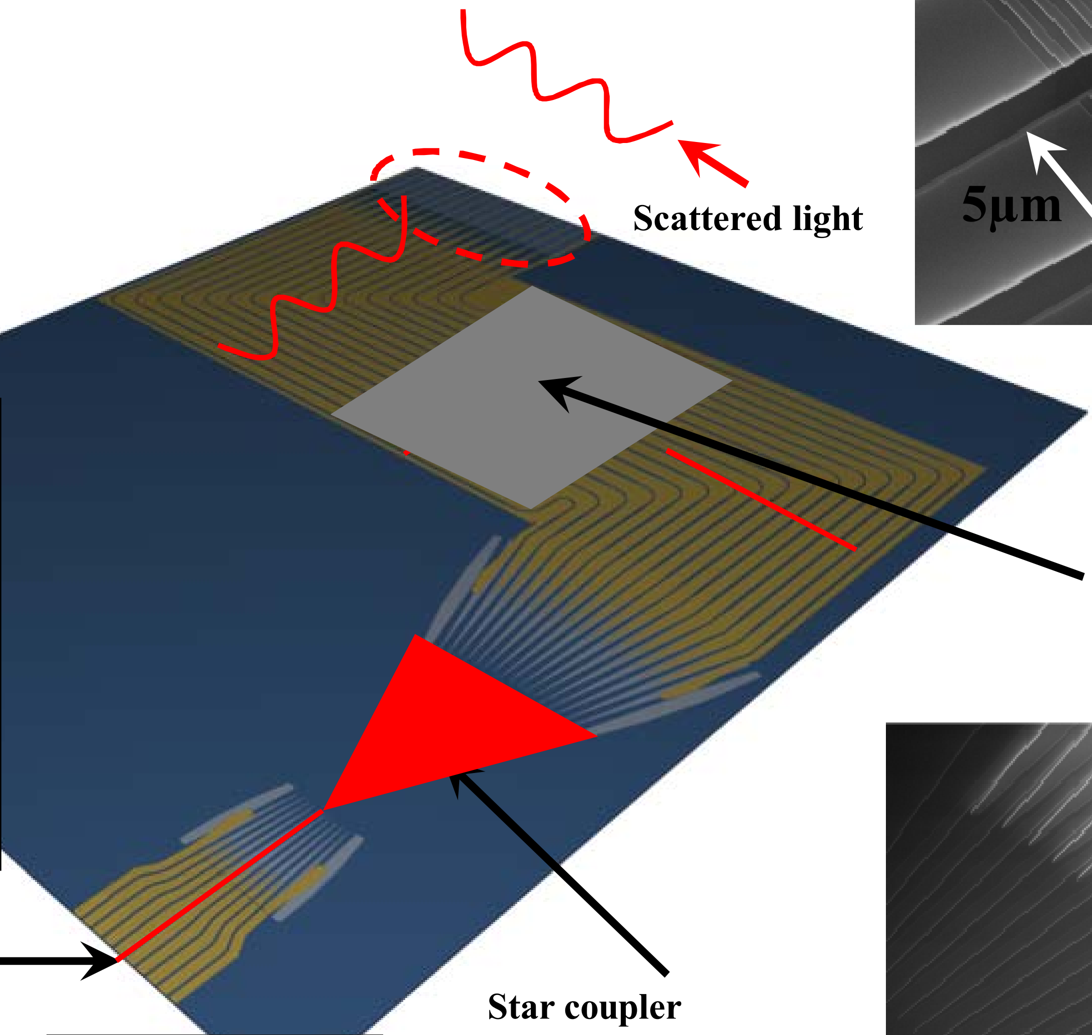

Coupling
16 grating couplers

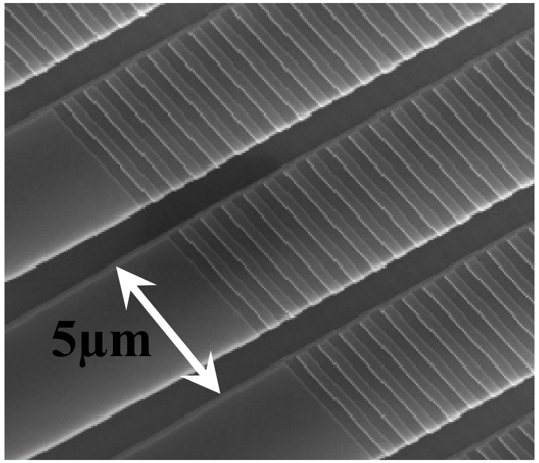

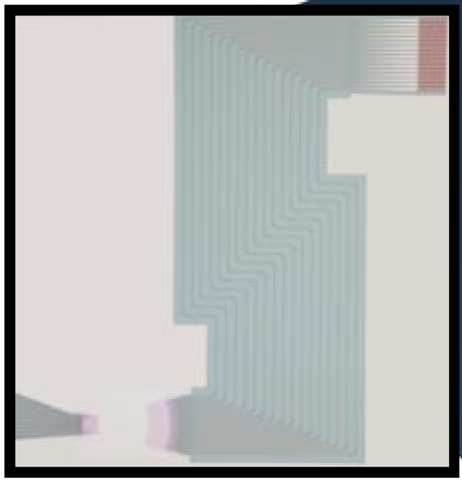

Waveguide
Collected light for further processing

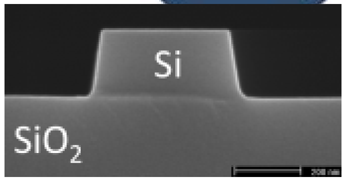

Star coupler
Combining in phase light contributions

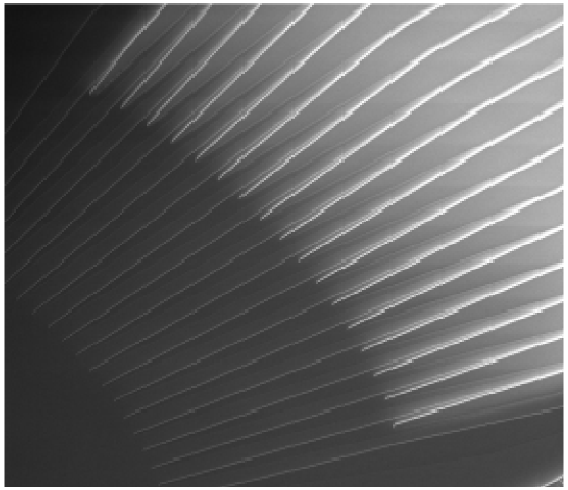

Courtesy: Prof. Roel Baets

How to increase light throughput? Fourier-transform spectrometer

$10^2 – 10^4 \times$ increase in light gathering capability (*étendue*) compared to grating spectrometers (P. Jacquinot, JOSA, vol. 44, p. 761, 1954)

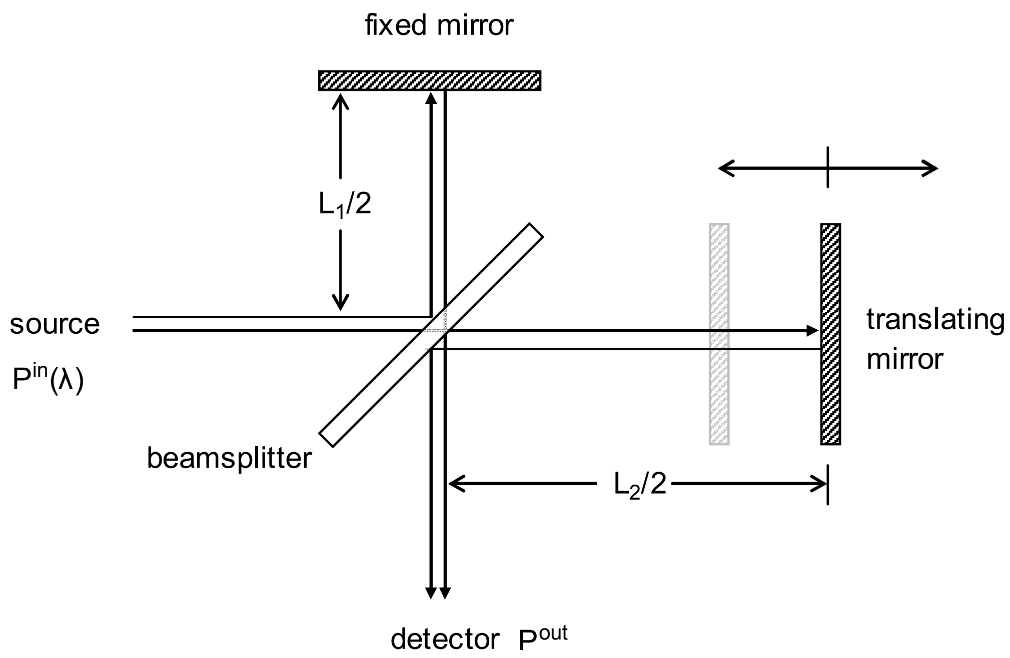

Translating mirror produces an interference pattern from which the spectrum of the source is calculated by Fourier transformation

Spectrum = *FT* (Interferogram)

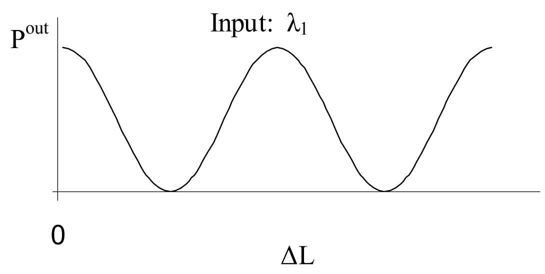

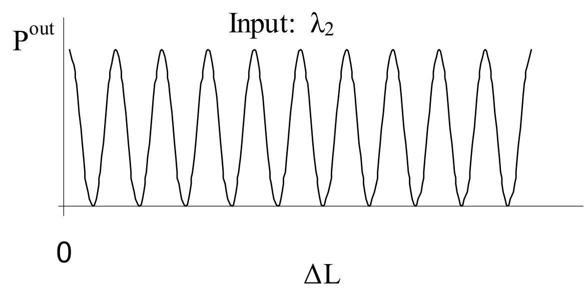

State of the art Fourier-transform spectrometers

FT interferometers (spectrometers) presently dominate the field of IR spectroscopy
Large optical throughput, low noise, high sensitivity …

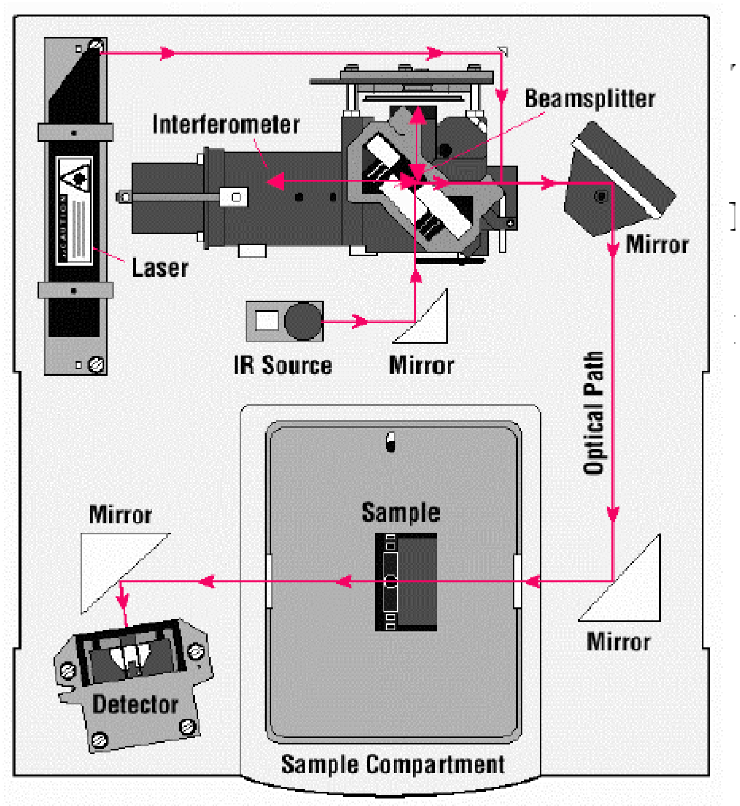

These are large, complex and expensive instruments

Miniature FTIR spectrometer: 2003 Mars Exploration Rover

Miniature Thermal Emission Spectrometer (Mini-TES)

Detecting the composition of rocks from a distance

Mars Rover

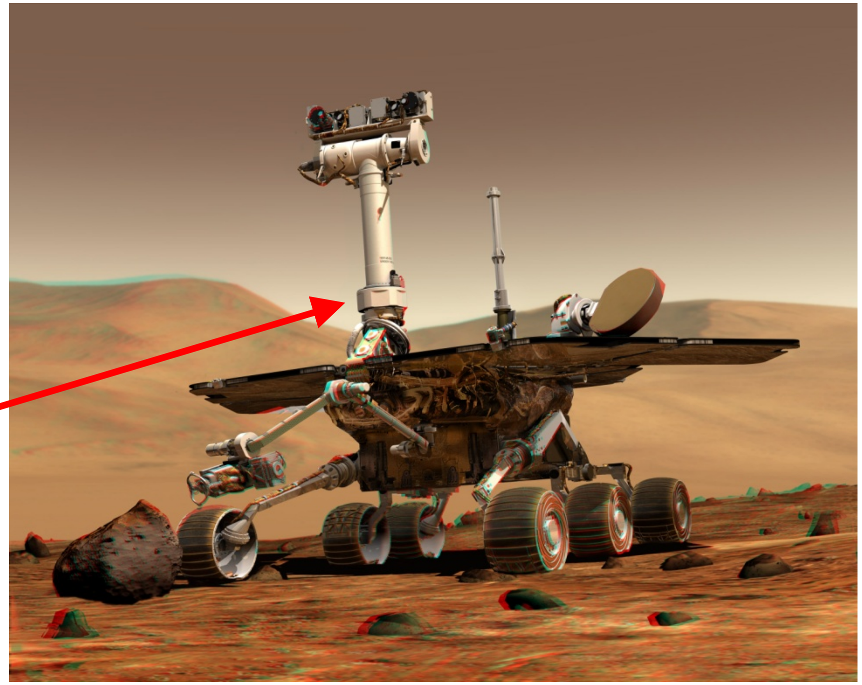

Thermal IR image of Mars landscape (5 – 29 μm)

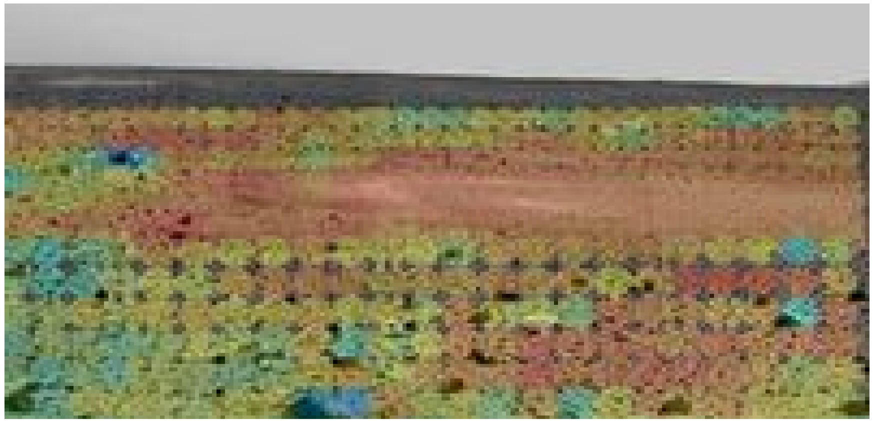

Spatial heterodyne spectrometer (SHS)

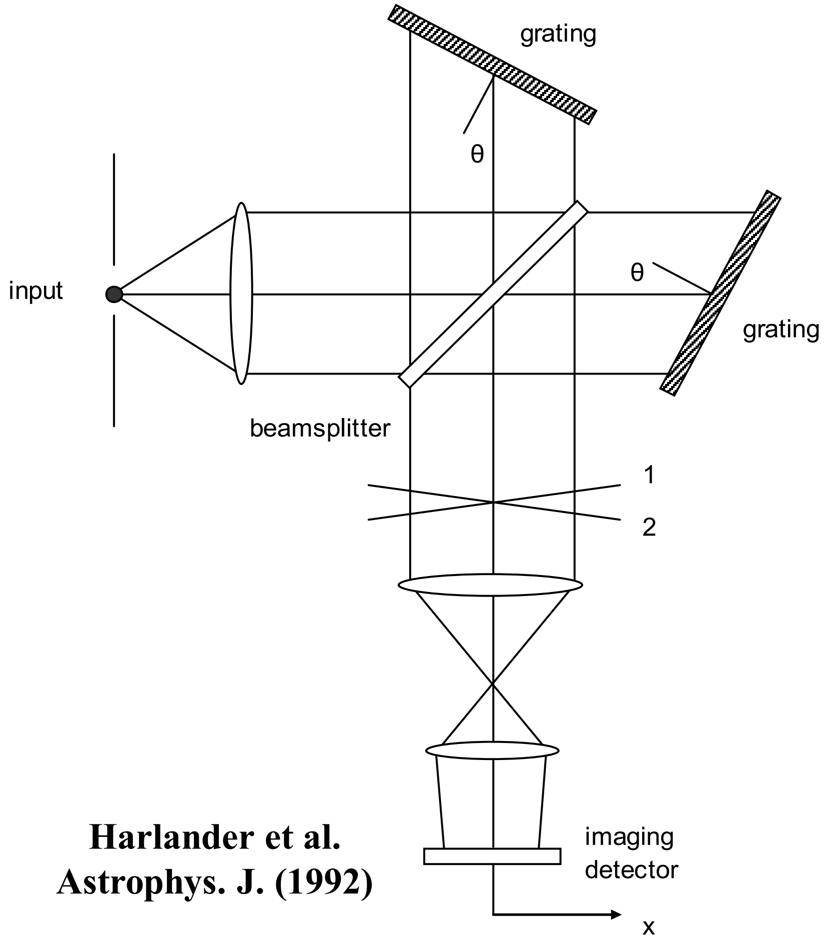

Harlander et al.
Astrophys. J. (1992)

Angle between wavefronts in recombined beam is wavelength-dependent

Angle-dependent interference (Fizeau) fringes

Spectrum = *FT*(Spatial Interferogram)

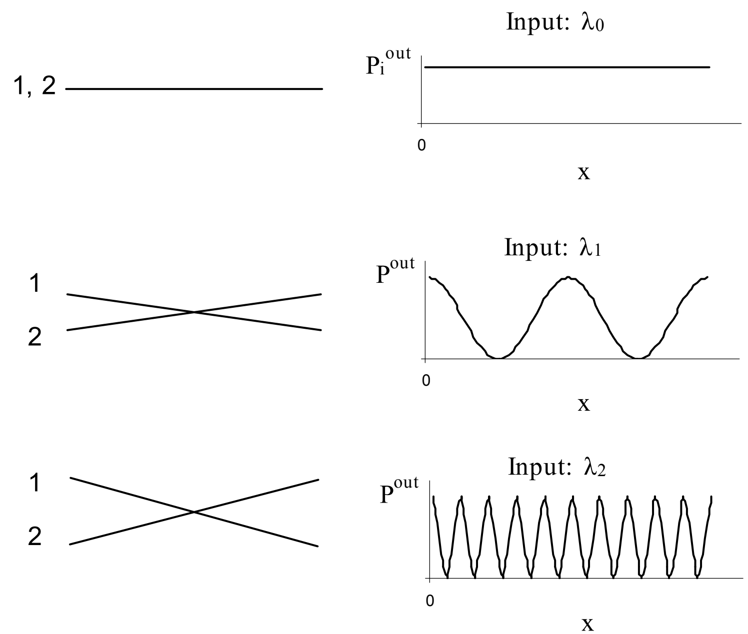

No need for moving parts (scanning mirror)

FT Mach-Zehnder interferometer array

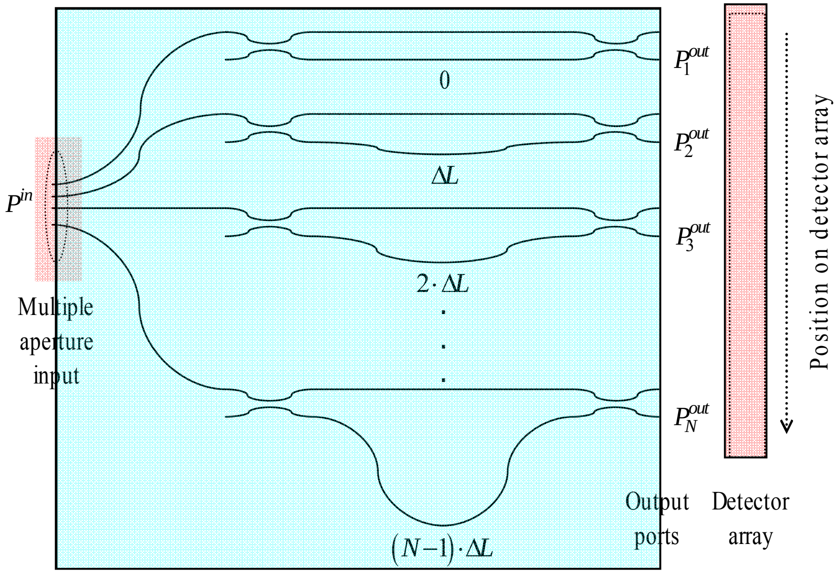

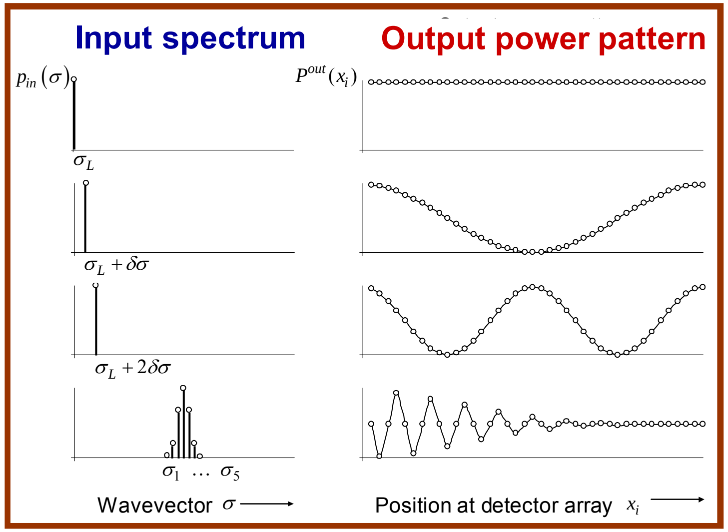

Input spectrum = FT {Output power pattern}

- **SHFT spectrometer can be advantageously implemented as an array of waveguide Mach-Zehnder interferometers (MZI)**
- **Each MZI samples a linearly increasing optical path difference**
- **This configuration allows a multiple aperture input; *étendue* is increased N-times compared to devices with a single input aperture (e.g., AWG)**

P. Cheben et al., US patent

M. Florjańczyk et al., Optics Express **15,** 18176, 2007

Mathematical model of MZI array

Monochromatic light, modal power: $P = \frac{1}{2}|a|^2 \iint \mathbf{e} \times \mathbf{h}^* \cdot \hat{\mathbf{z}}\, dx\, dy$

Transfer matrix model:

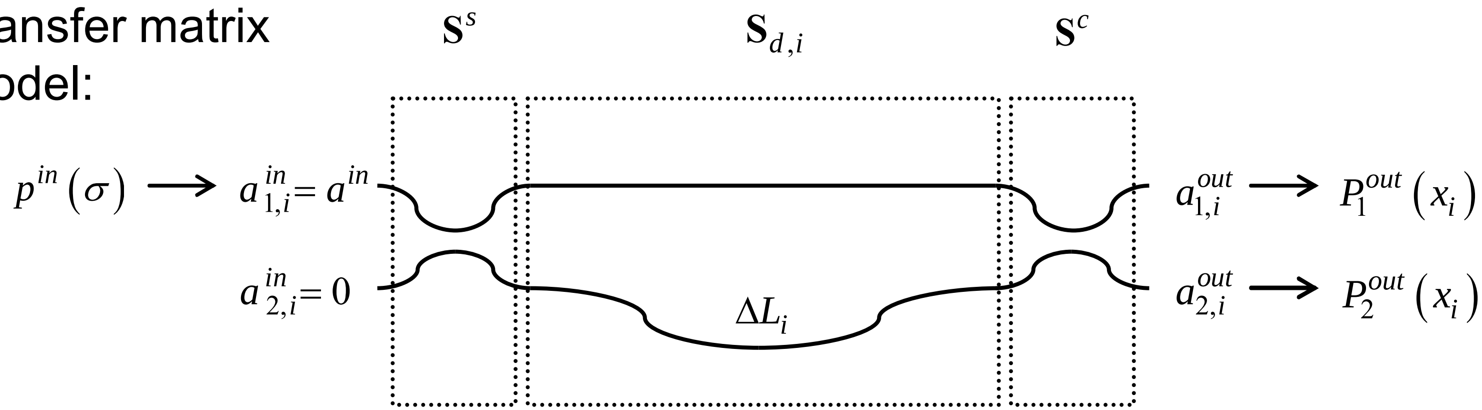

$$\begin{bmatrix} a_{1,i}^{out} \\ a_{2,i}^{out} \end{bmatrix} = \mathbf{S}_i \cdot \begin{bmatrix} a_{1,i}^{in} \\ a_{2,i}^{in} \end{bmatrix} = \mathbf{S}_c \cdot \mathbf{S}_{d,i} \cdot \mathbf{S}_s \cdot \begin{bmatrix} a_{1,i}^{in} \\ a_{2,i}^{in} \end{bmatrix}$$

Transfer matrices:

$$\mathbf{S}_s = \gamma_s \begin{bmatrix} \sqrt{1-\kappa_s} & -i\sqrt{\kappa_s} \\ -i\sqrt{\kappa_s} & \sqrt{1-\kappa_s} \end{bmatrix} \quad \mathbf{S}_c = \gamma_c \begin{bmatrix} \sqrt{1-\kappa_c} & -i\sqrt{\kappa_c} \\ -i\sqrt{\kappa_c} & \sqrt{1-\kappa_c} \end{bmatrix} \quad \mathbf{S}_{d,i} = \gamma_{d,i} e^{-i\beta L_{2,i}} \begin{bmatrix} e^{-\alpha \Delta L_i} e^{-i\beta \Delta L_i} & 0 \\ 0 & 1 \end{bmatrix}$$

Mathematical model of MZI array

Max delay in array

Input power

$$p^{in}(\bar{\sigma}) = \frac{\Delta x}{N} P^{in} + 2\frac{\Delta x}{N}\sum_{i=1}^{N} W(x_i) F(x_i) \cos 2\pi\bar{\sigma} x_i$$

Input spectrum

Number of MZIs

Apodization function

Output fringe pattern

Device particulars (materials, design, fabrication) are known:

$$A_{1,i} = 2\gamma_s^2 \gamma_{d,i}^2 \gamma_c^2 \left[\kappa_s \kappa_c + (1-\kappa_s)(1-\kappa_c) e^{-2\alpha\Delta L_i}\right]$$

$$A_{2,i} = 2\gamma_s^2 \gamma_{d,i}^2 \gamma_c^2 \left[\kappa_s (1-\kappa_c) + \kappa_c (1-\kappa_s) e^{-2\alpha\Delta L_i}\right]$$

$$B_i = 4\gamma_s^2 \gamma_{d,i}^2 \gamma_c^2 \left[\kappa_s \kappa_c (1-\kappa_s)(1-\kappa_c)\right]^{\frac{1}{2}} e^{-\alpha\Delta L_i}$$

$$F_i = -\frac{1}{B_i}\left(2P_{1,i}^{out} - A_{1,i} P^{in}\right) = \frac{1}{B_i}\left(2P_{2,i}^{out} - A_{2,i} P^{in}\right)$$

M. Florjańczyk et al., Optics Express **15,** 18176, 2007

Basic design rules

Spectral resolution is defined by the most unbalanced interferometer:

$$\delta\lambda = \frac{\lambda_0^2}{\Delta L_{\max} n_g}$$

Free Spectral Range (operational bandwidth) is defined by the number of interferometers:

$$FSR = \delta\lambda \frac{N}{2}$$

HCN spectrum measurement

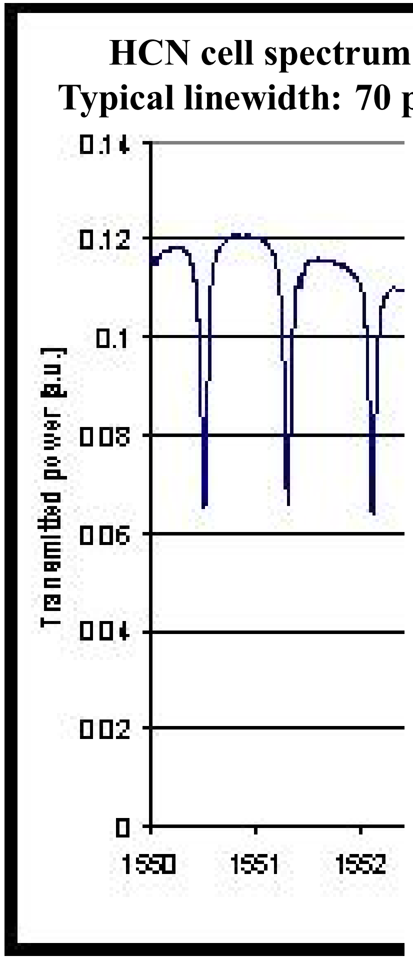

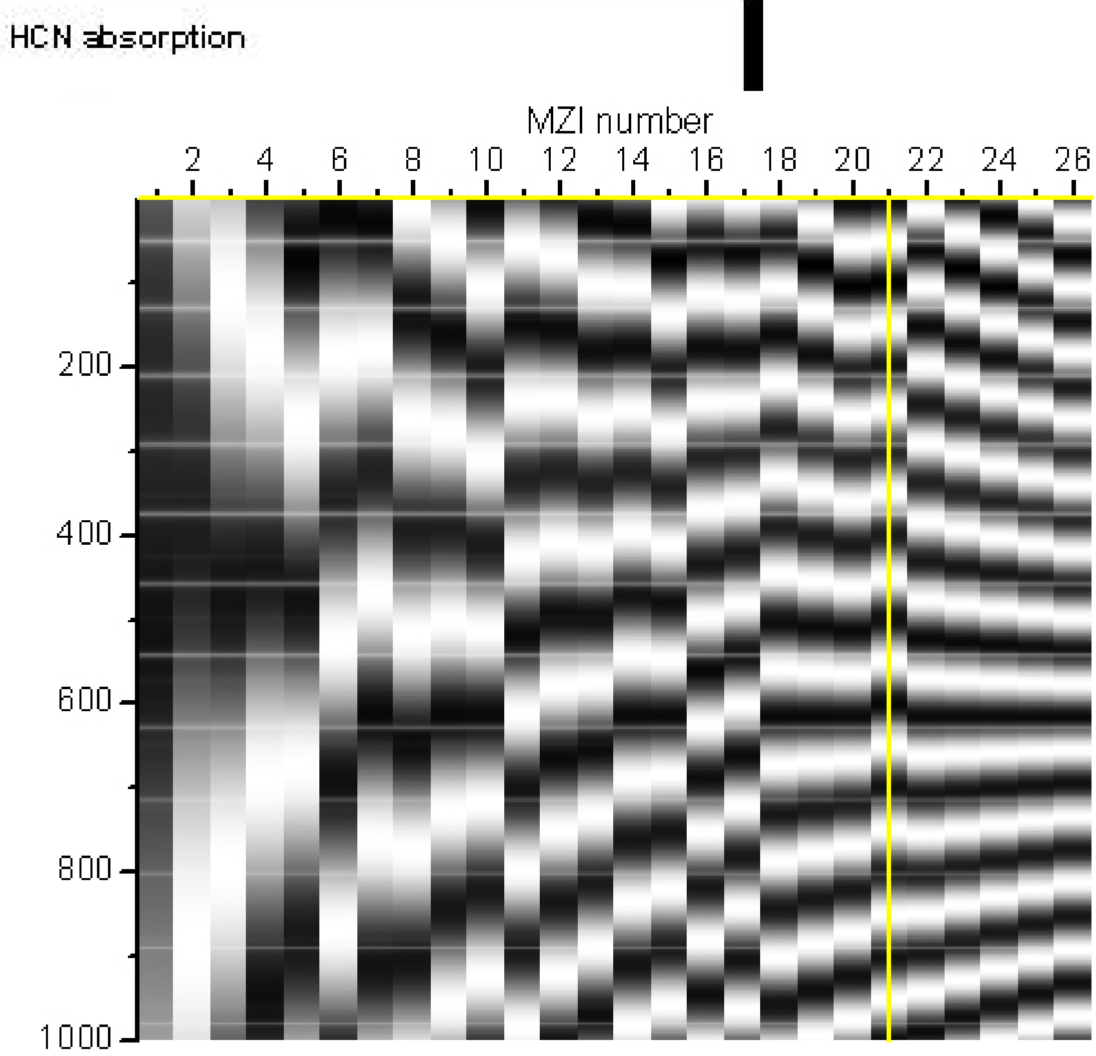

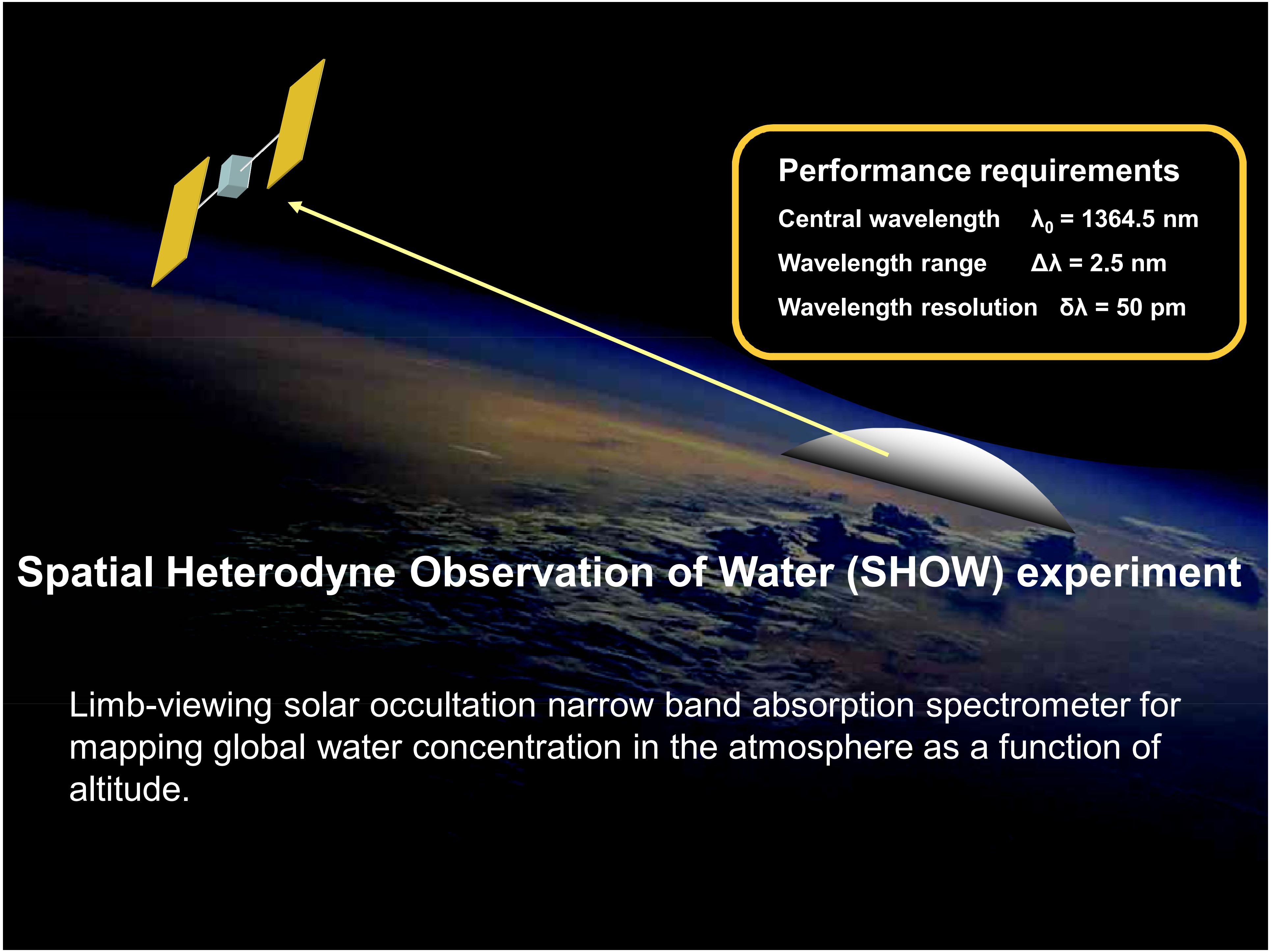
Performance requirements
Central wavelength λ_0 = 1364.5 nm
Wavelength range $\Delta\lambda$ = 2.5 nm
Wavelength resolution $\delta\lambda$ = 50 pm
Spatial Heterodyne Observation of Water (SHOW) experiment
Limb-viewing solar occultation narrow band absorption spectrometer for mapping global water concentration in the atmosphere as a function of altitude.

Formation of spatial fringes – water spectrum

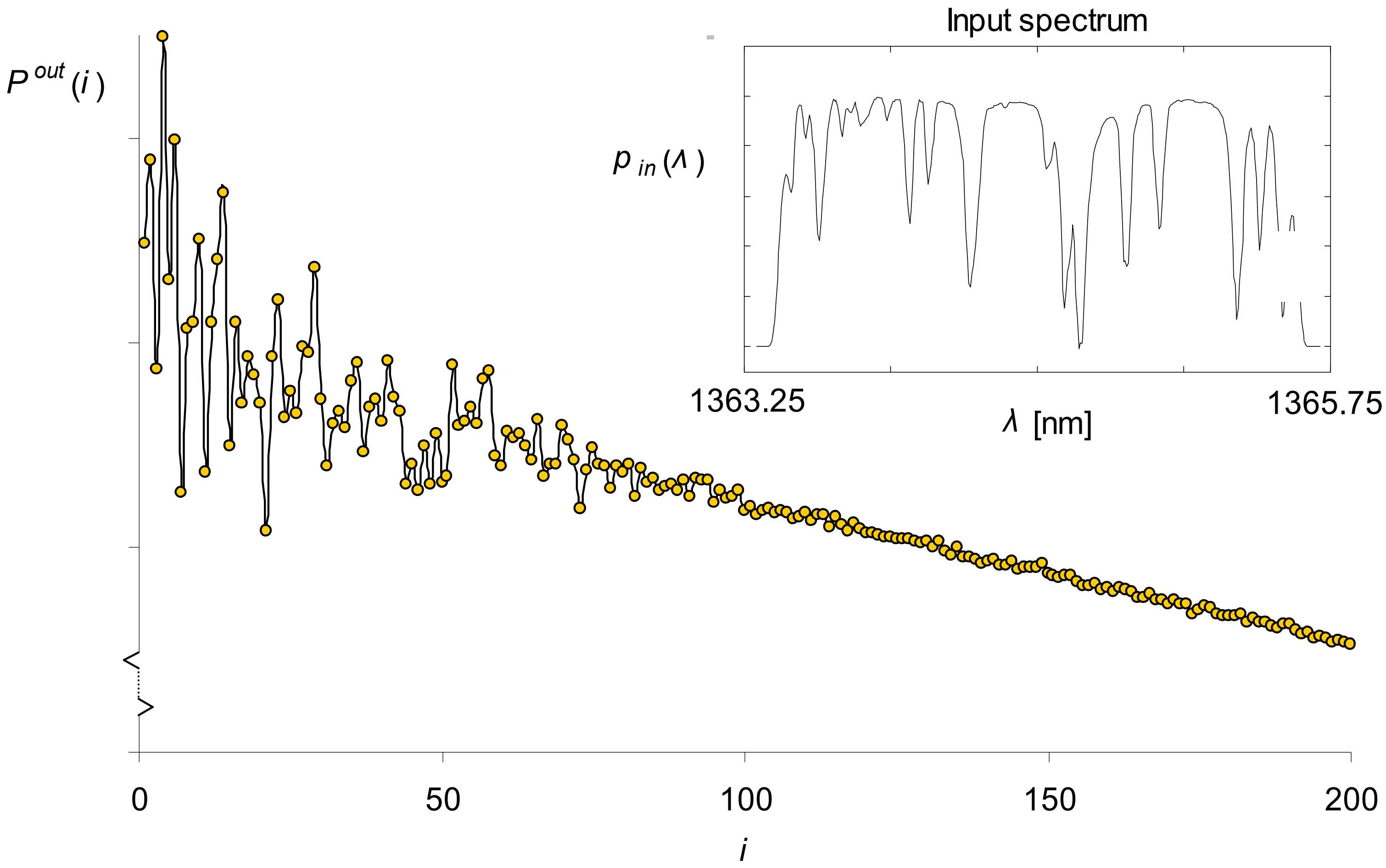

2.5 nm bandwidth
50 pm spectral resolution

First Fourier-transform spectrometer chip

- Developed at the NRC with the Canadian Space Agency and ComDev Ltd.
for microsatellite sensing application
- http://www.nrc-cnrc.gc.ca/eng/achievements/highlights/2009/spectrometer.html

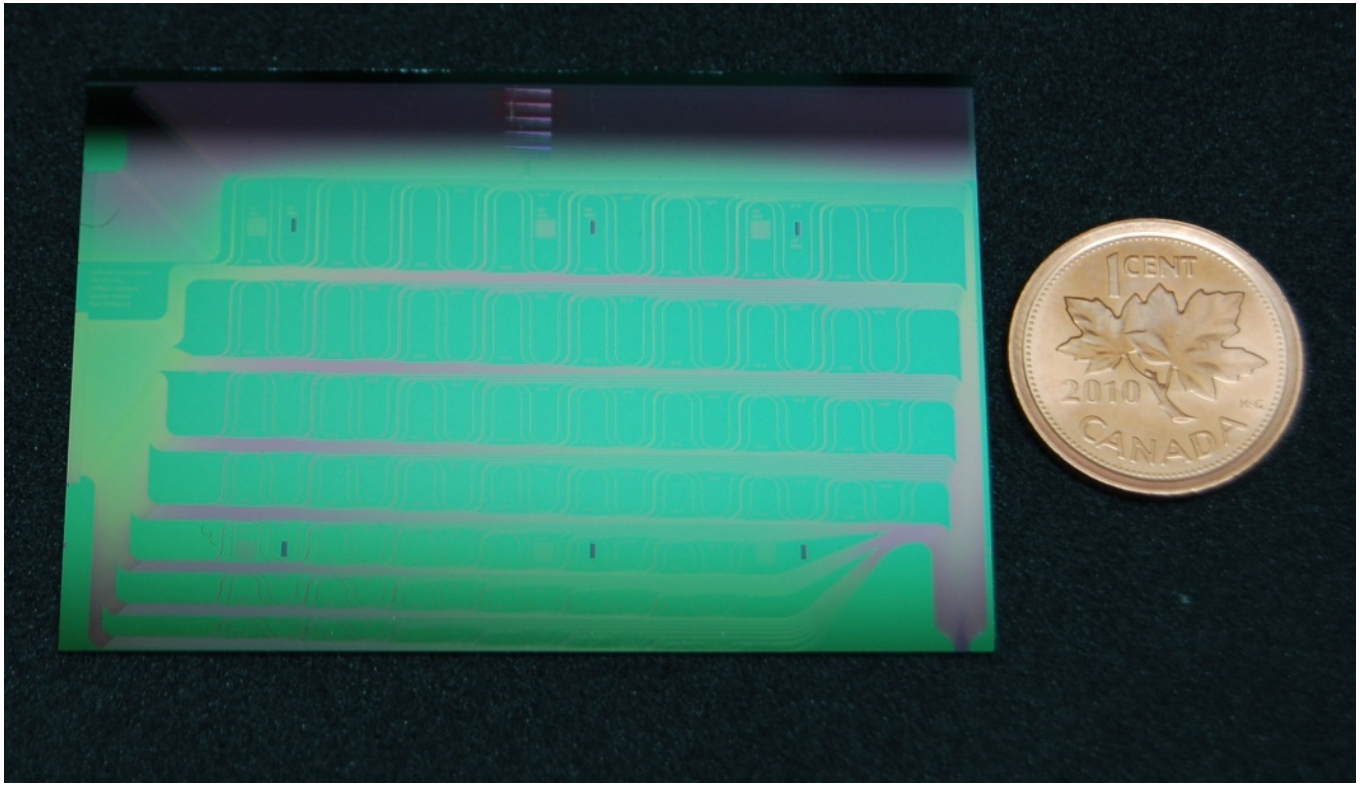

- 100 MZIs, Si ridge waveguides
- 10.8 mm long delays
- 50 pm spectral resolution

Fourier-transform spectrometer chip (NASA)

The concept has been adopted by NASA and Aidi Corporation

NASA: "The potentially revolutionary miniaturized waveguide Fourier-transform spectrometer"

http://www.nasa.gov/topics/technology/features/chip-spectrometer.html

Surface grating coupler in thick SOI

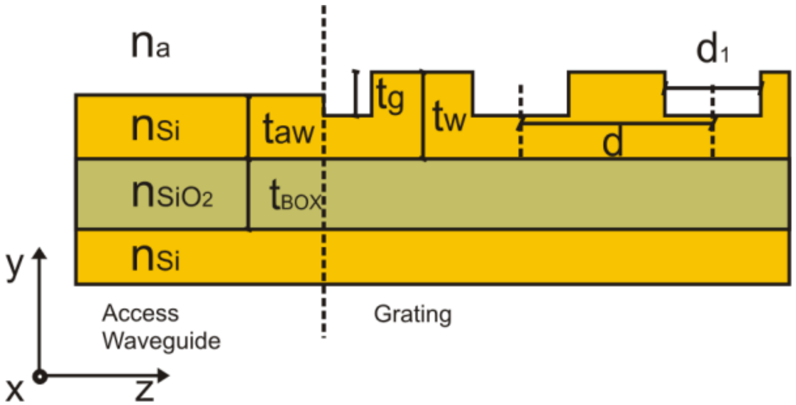

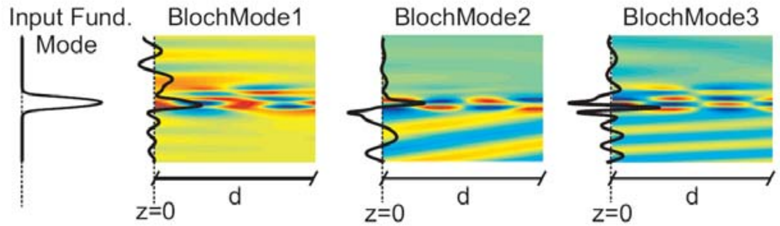

Single-mode excitation

$$t_{aw}^{opt} \approx t_w - t_g$$

Single-mode excitation

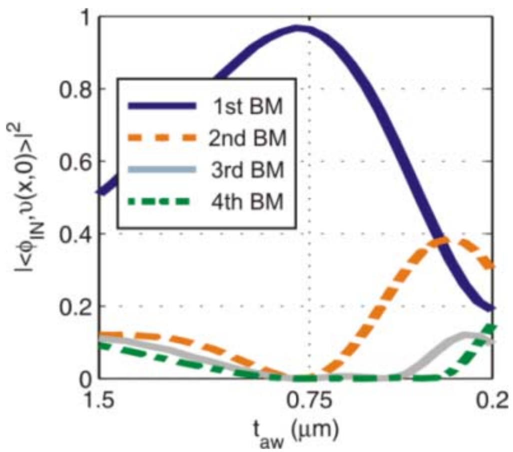

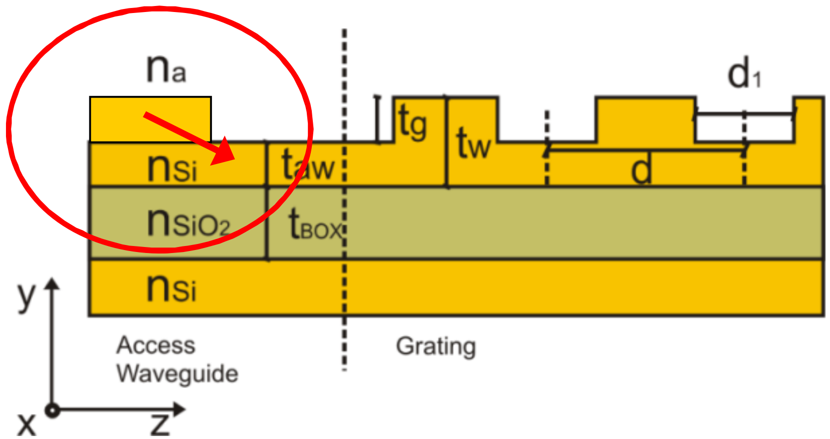

Carlos A. Ramos et al., Optics Express, vol. 18, p. 15189 (2010)

Single etch step

Coupler schematics

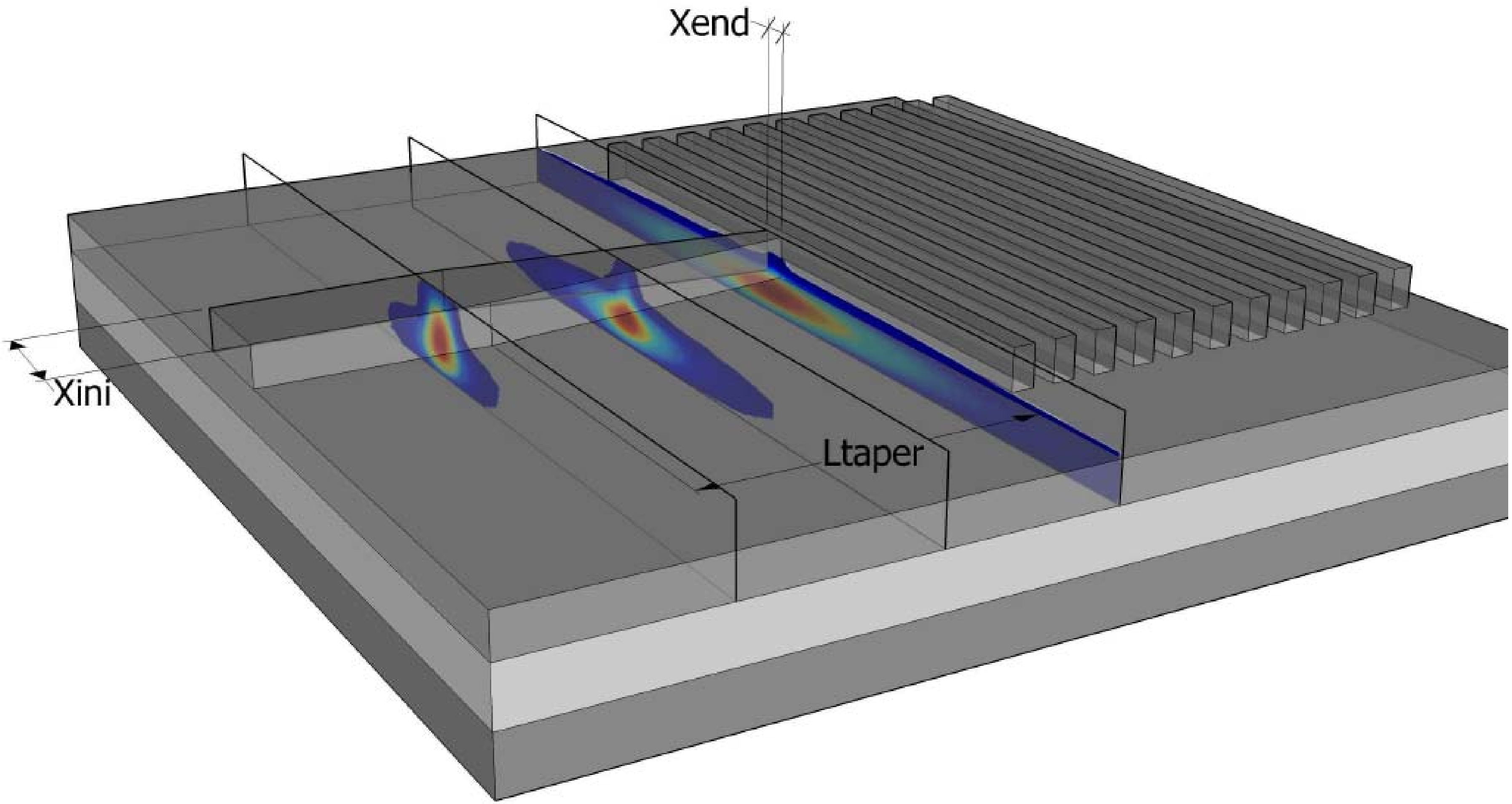

Our grating coupler concept is followed by Intel

Grating Coupler design

- **Grating doesn't radiate efficiently in first order (k=-1).**
- **Exhaustive search: Floquet mode analysis (no FDTD).**

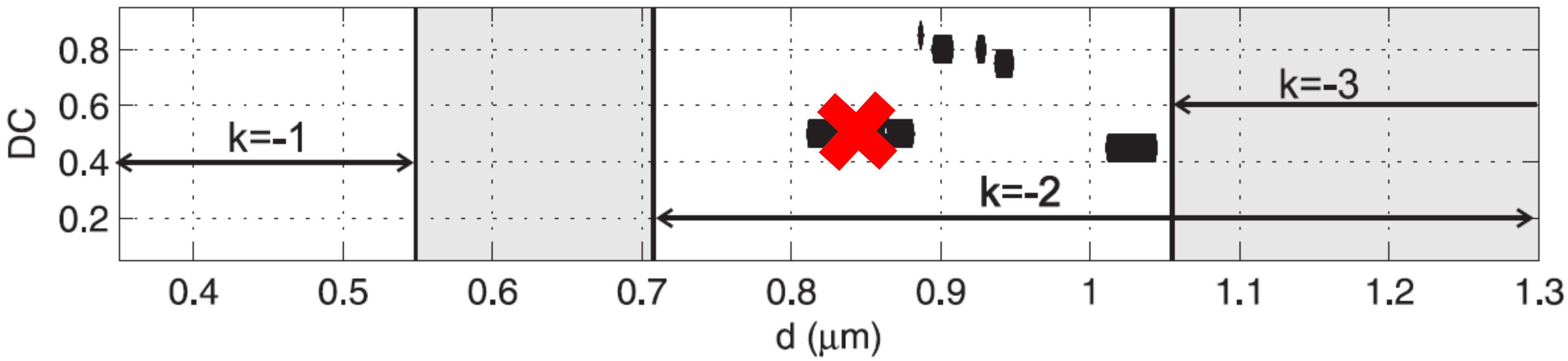

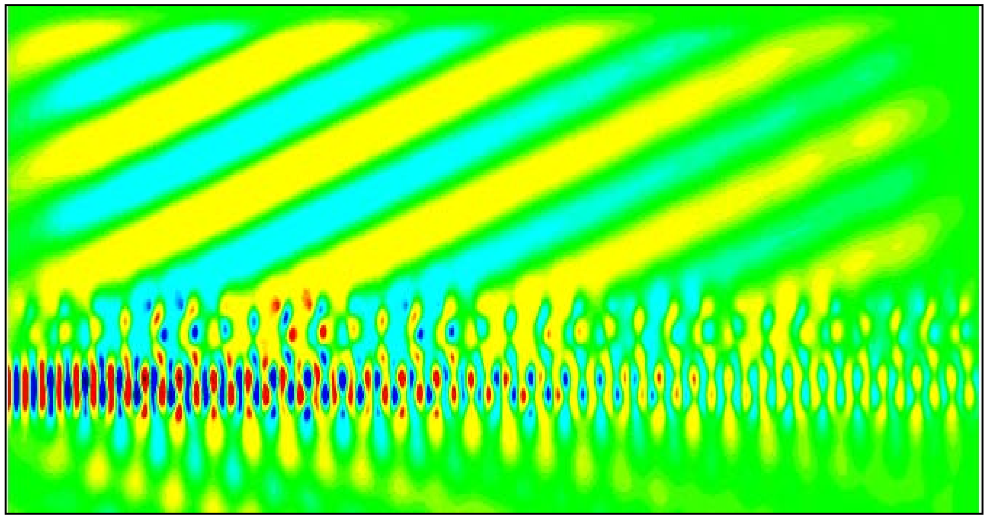

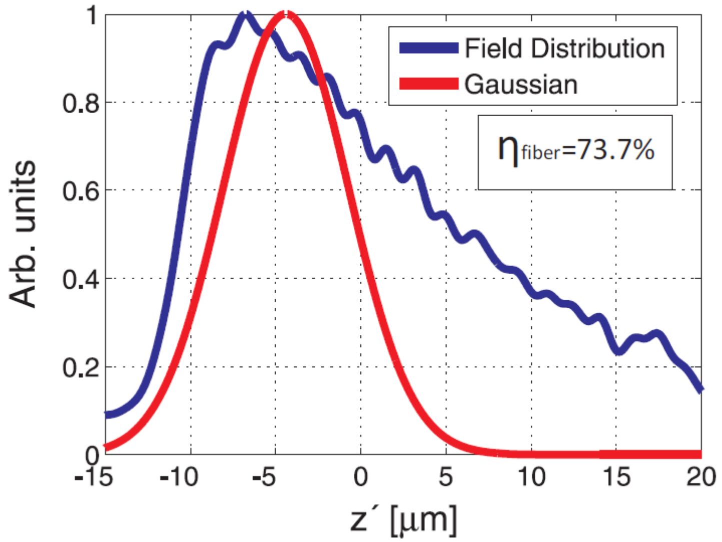

This coupler concept is followed by INTEL

Fabricated grating couplers

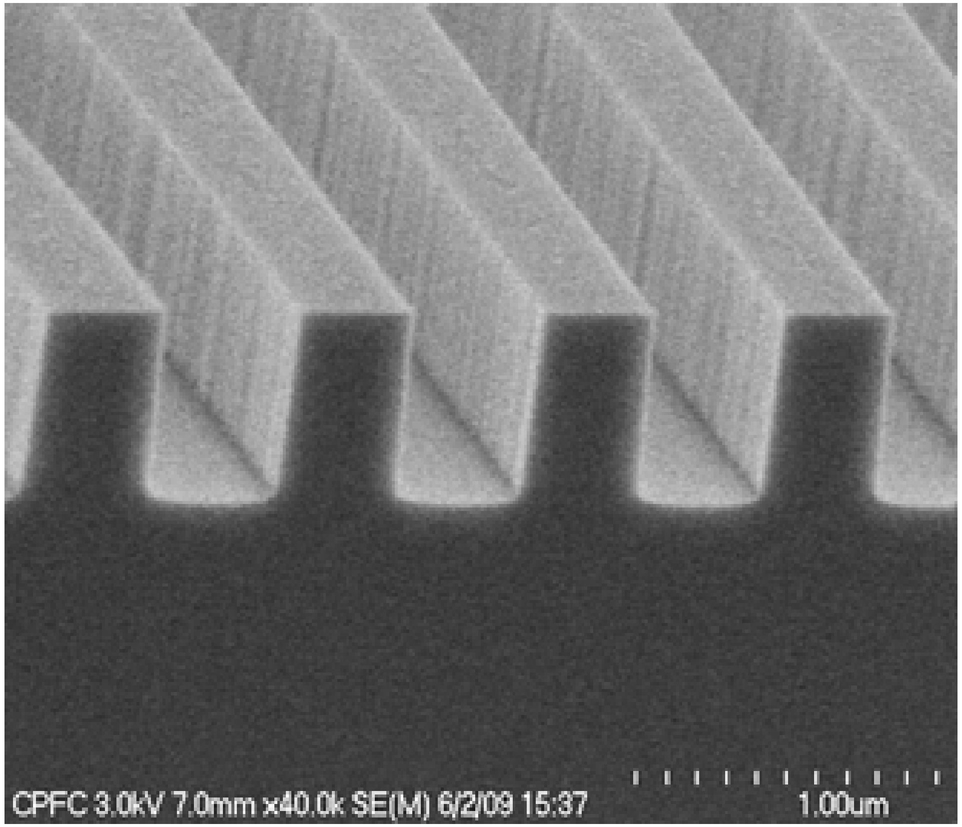

Second order grating, pitch 740 nm

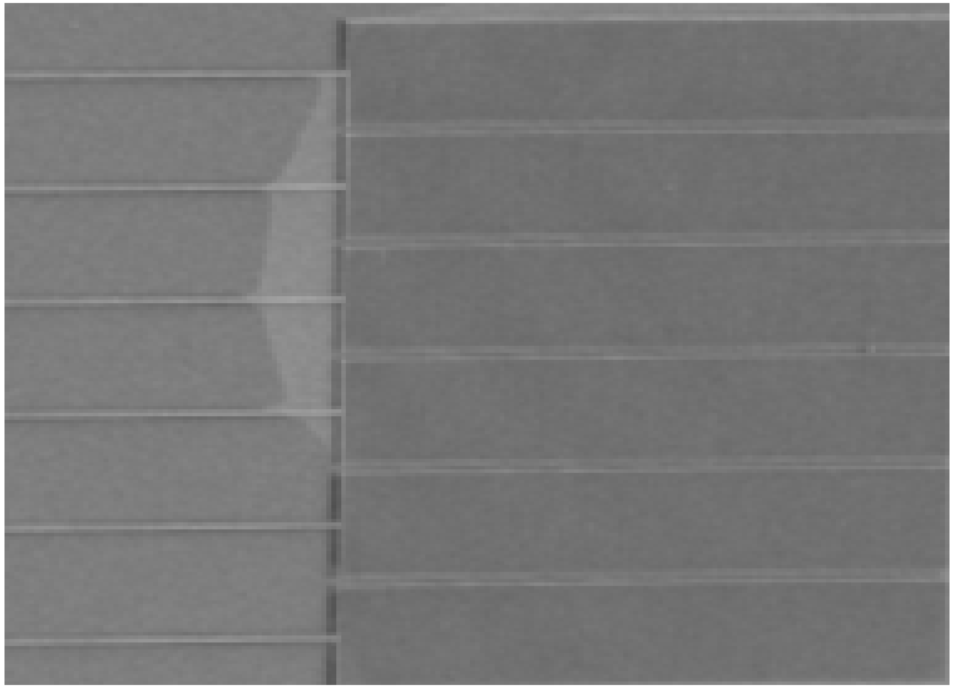

Grating coupler array
90 µm × 90 µm

Fabricated at the Canadian Photonics Fabrication Center
using i-line stepper lithography and reactive ion etching

Grating coupler measurement

Gratings are measured in back-to-back configuration

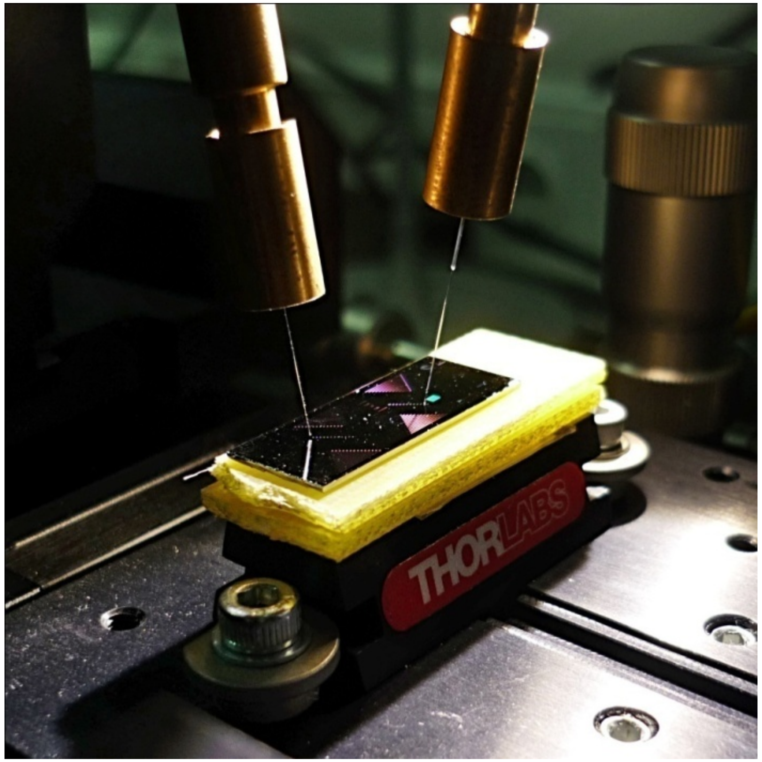

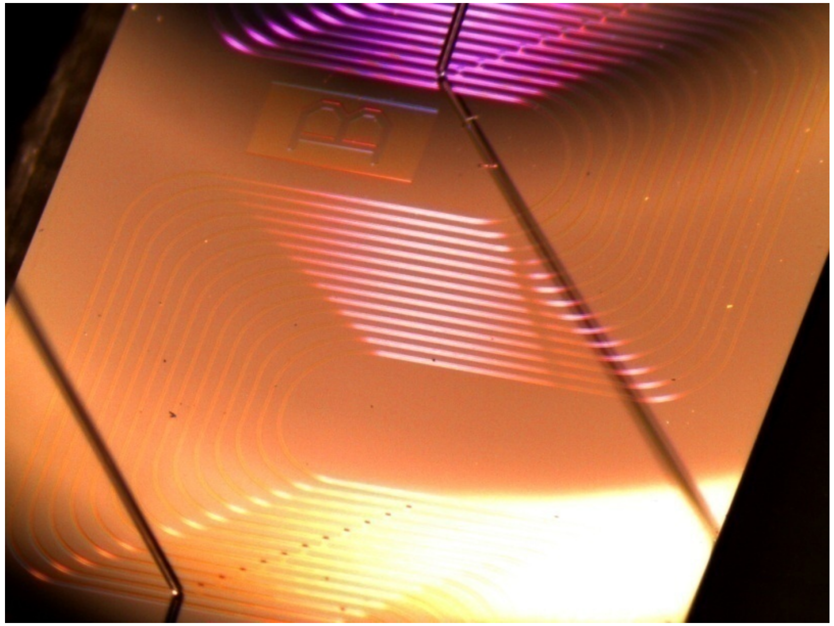

Grating coupler measurement

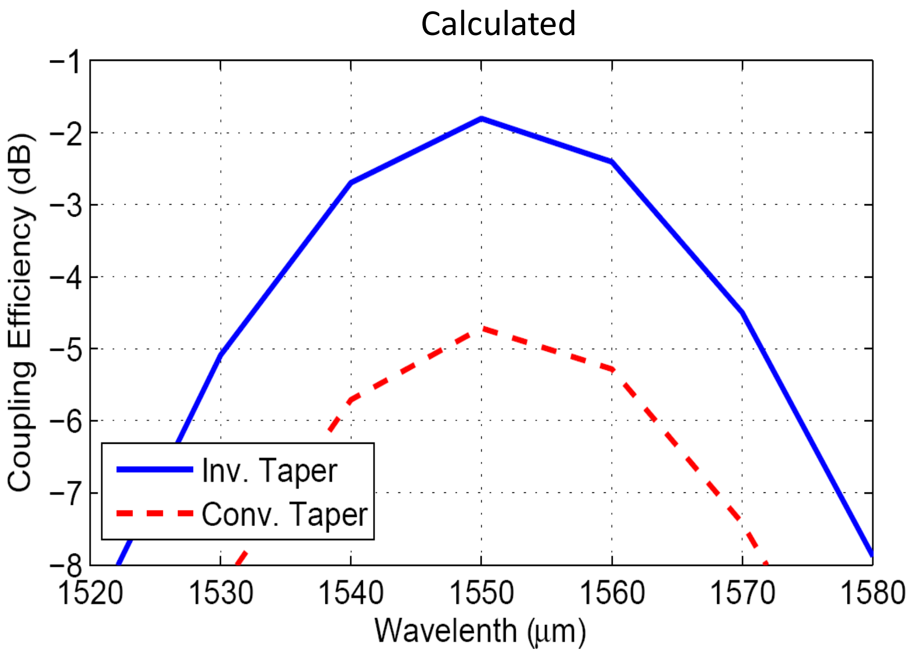

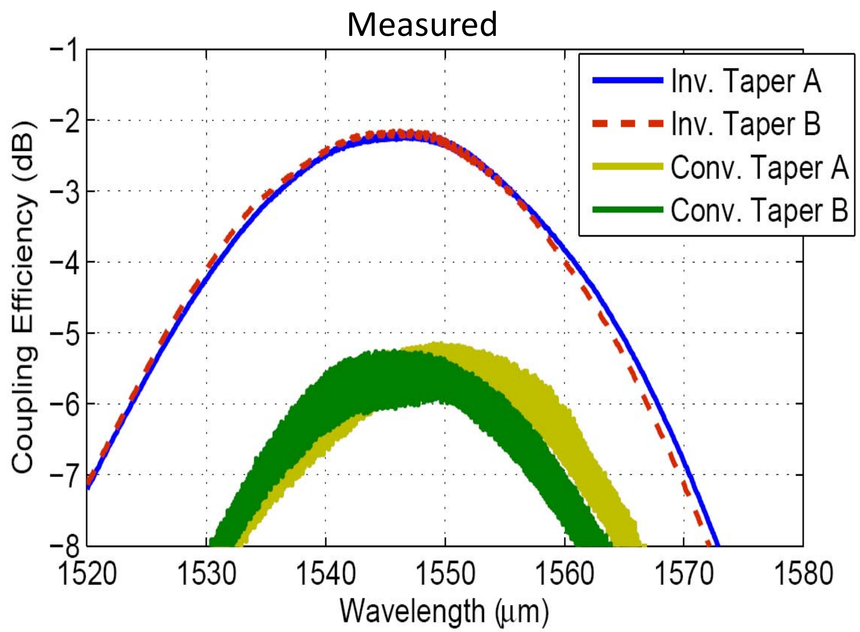

2.2dB coupling efficiency, 40nm 3dB BW

3.3dB coupling efficiency improvement and 10x back reflections reduction compared to conventional taper

C. A. Ramos et al., Opt. Lett. 36, p. 2647 (2011)

MZ interferometer array with microphotonic spiral waveguide delays

- **MZI optical path delays implemented using silicon wire-waveguides with microphotonic spirals**

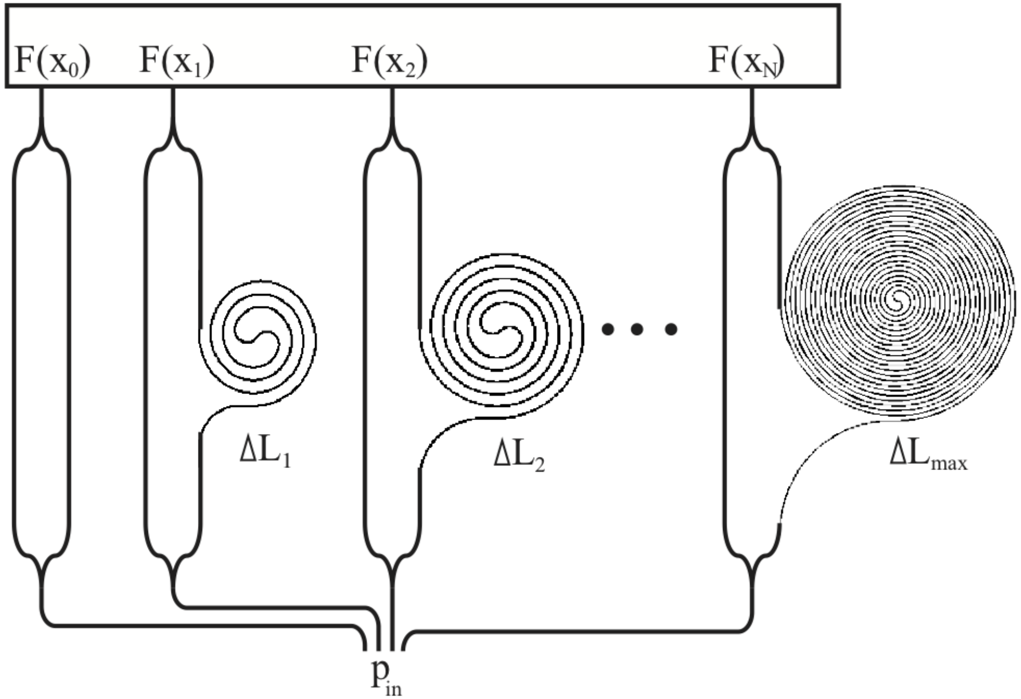

- The high index contrast of SOI allows high confinement of the mode and small bend radii (2-5 microns).
- Spirals can be easily coiled very tightly and densely arrayed.
- Path-lengths of several centimeters can be implemented with a diameter of only a few hundred micrometers.

A. Velasco, P. Cheben, et al., Optic Letters 38, 706 (2013)

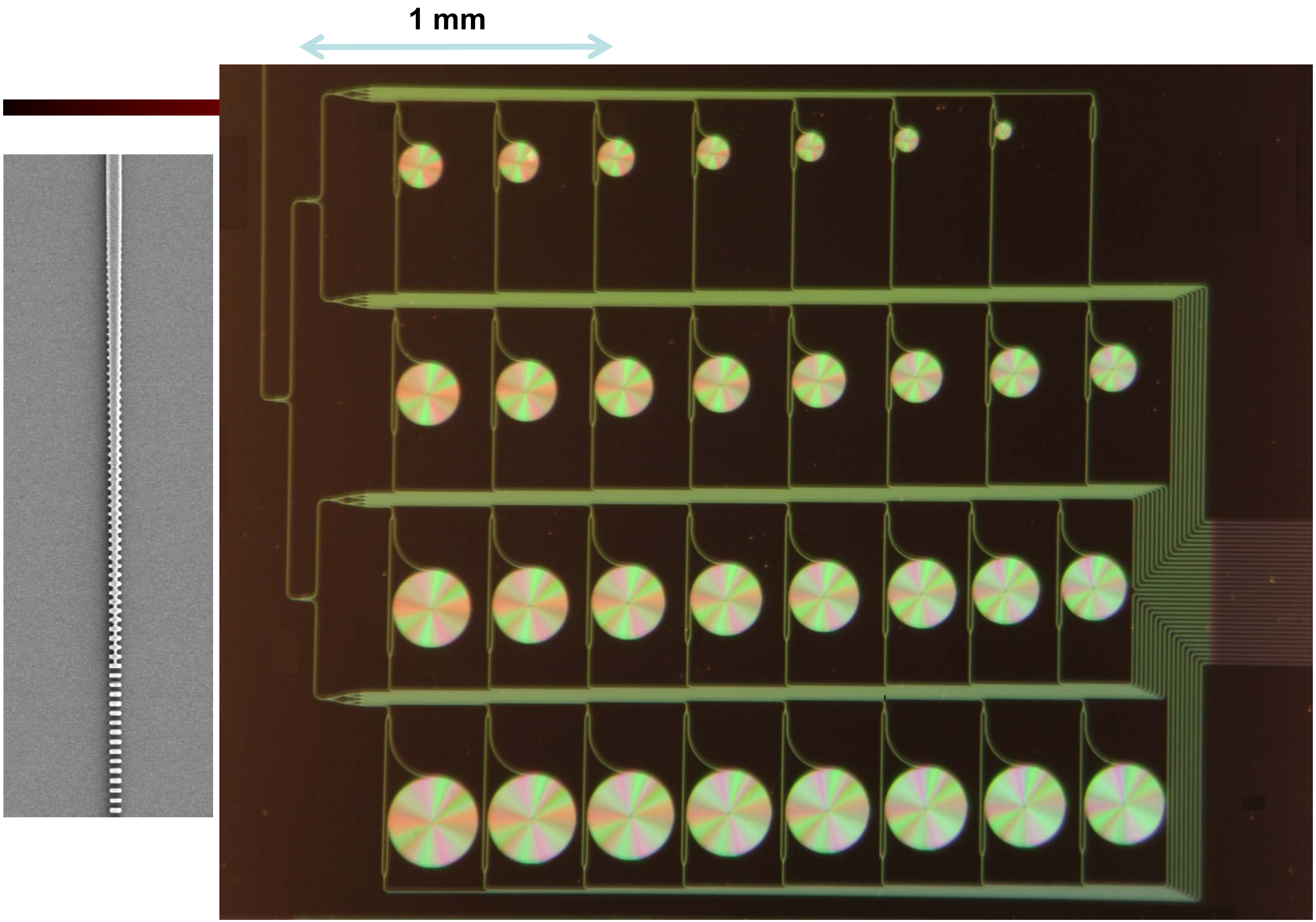

A. Velasco, P. Cheben, et al., Optic Letters 38, 706 (2013)

Design parameters

- **Maximum path delay ΔL_{max} = 1.13 cm**
- 32 MZ interferometers
- n_{eff} = 2.12 @ 1550 nm

→

- **Resolution = 50 pm**
- **Free Spectral Range= 0.8 nm**
- **Footprint = 12 mm^2**

ΔL = 365 µm

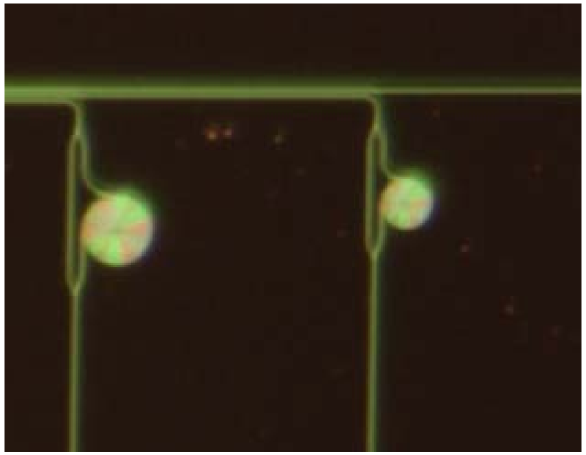

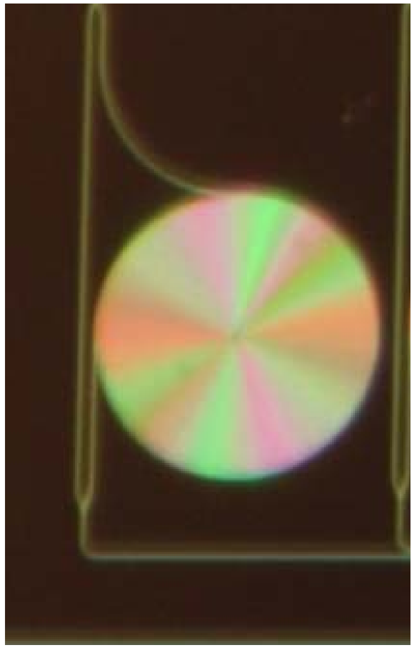

ΔL_{max} = 1.13 cm

A. Velasco, P. Cheben, et al., Optic Letters 38, 706 (2013)

Spectral retrieval example

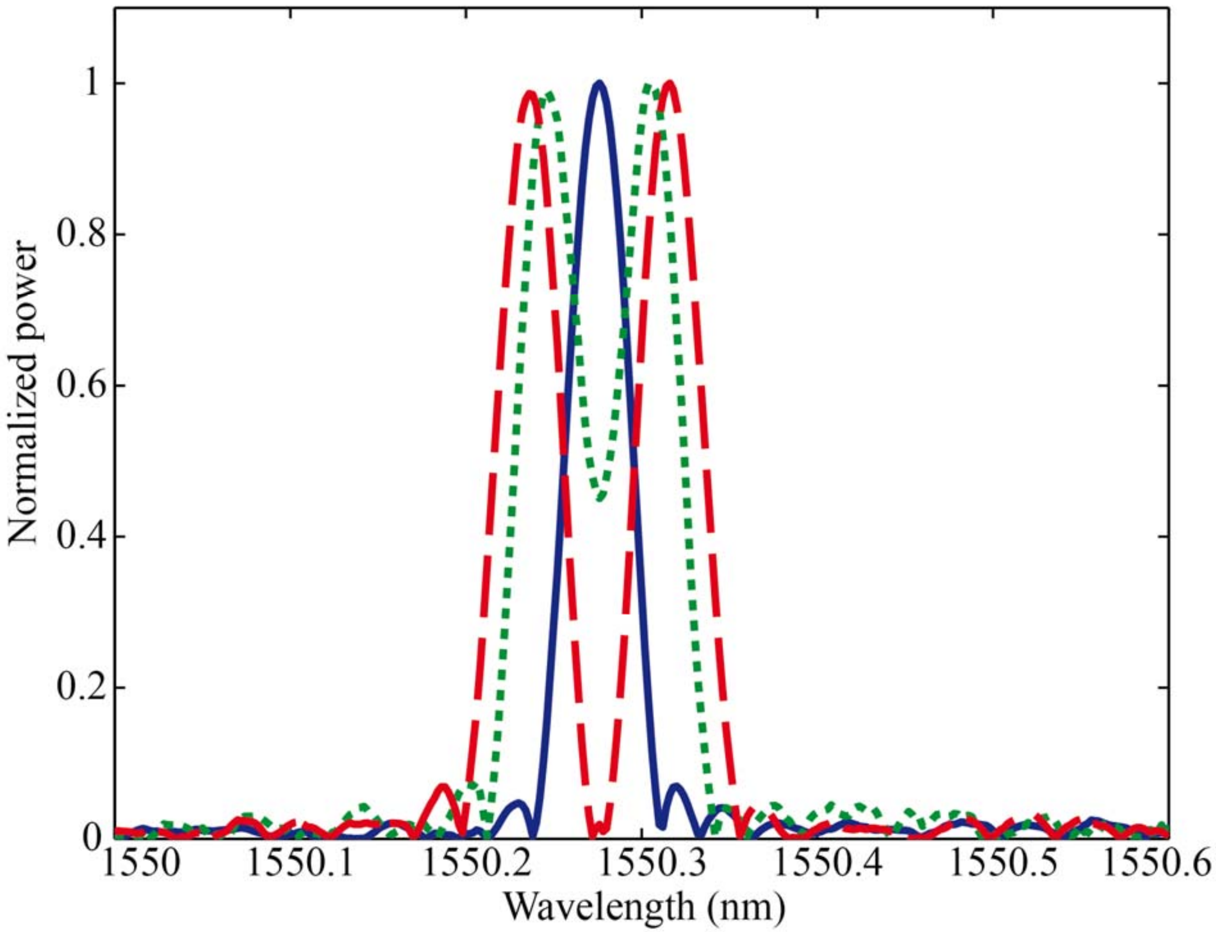

- **Experimental measurements**
  - **Single narrowband laser(blue)**
  - **Doublet separated 56 pm (green)**
  - **Doublet separated 80 pm (red)**
- **Resolution: 42 pm**
- **FSR = 0.75 nm**

A. Velasco, P. Cheben, et al., Optic Letters 38, 706 (2013)

FT spectrometer with SWG waveguides

- **Very compact design by implementing the optical delays with subwavelength grating waveguide sections**

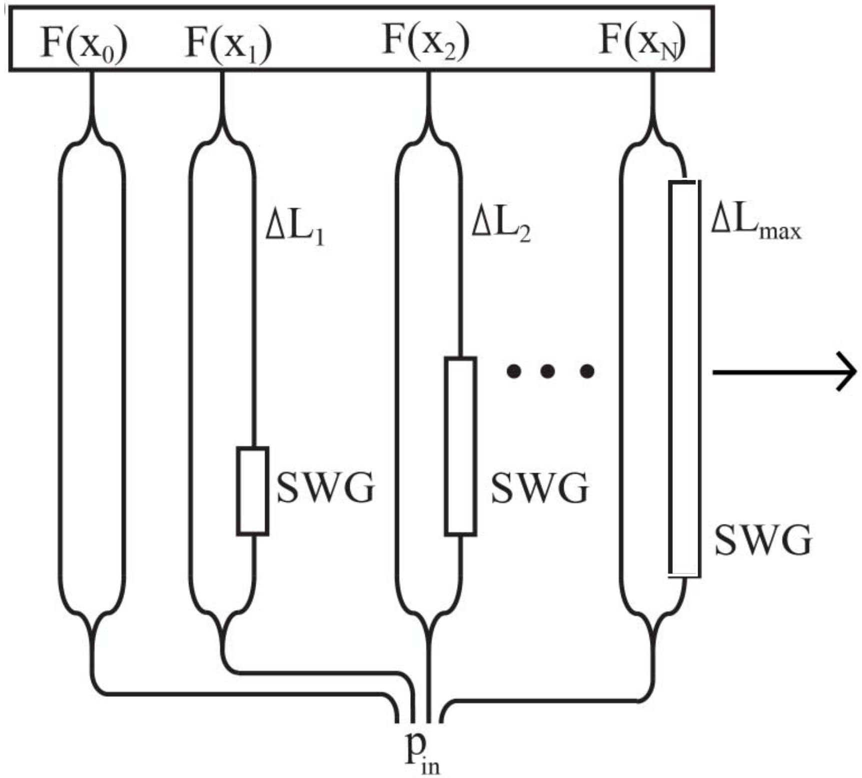

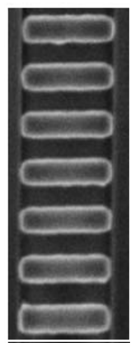

- A refractive index difference is introduced between the interferometer arms without changing their physical length
- The length of the subwavelength section varies linearly along the array
- Parallel orientation with no waveguide bends allows high-density interferometer arrays
- High fringe visibility (exctinction ratio 25-30 dB) because SWG and strip waveguides have similar loss.

P. Bock, P. Cheben et al., Lasers and Photonics Reviews, Vol. 7, pp. L67 - L70 (2013)

MZI array with subwavelength grating waveguides

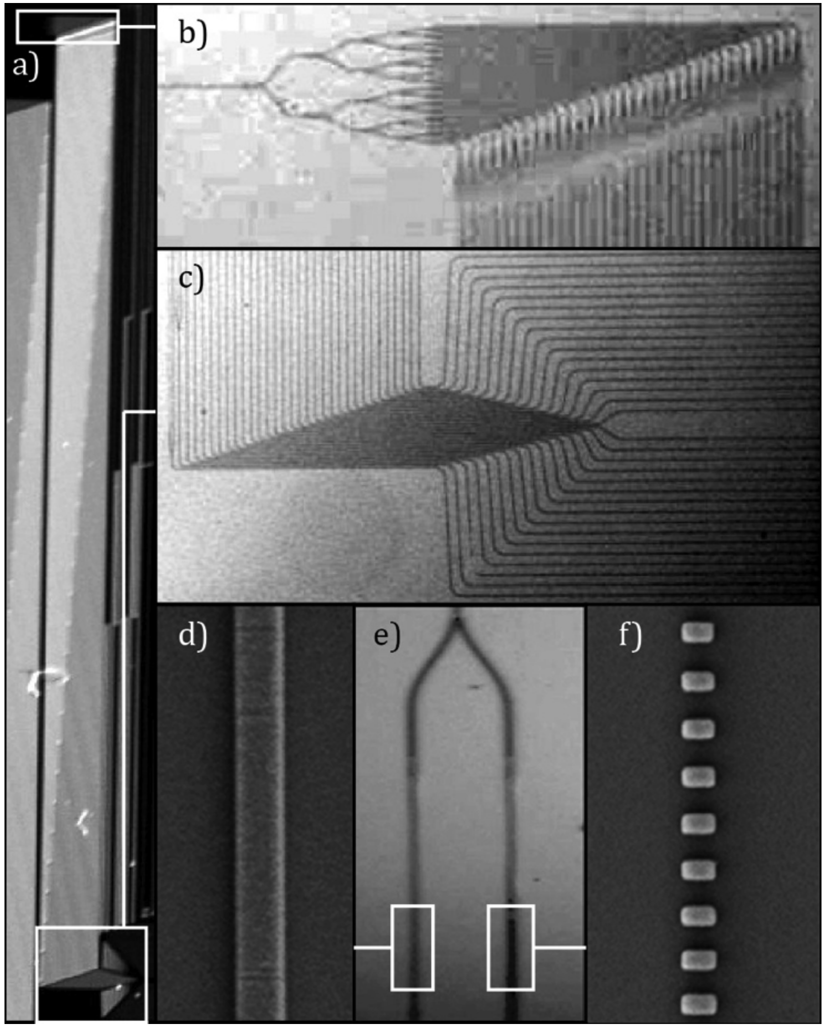

Input

Output

50% Duty cycle

L_{max} = 1.5 cm

n_{SWG} (TM)= 1.51

n_w (TM)= 4.38

P. Bock, P. Cheben, Lasers and Photonics Reviews, 2013

Spectral retrieval experiment

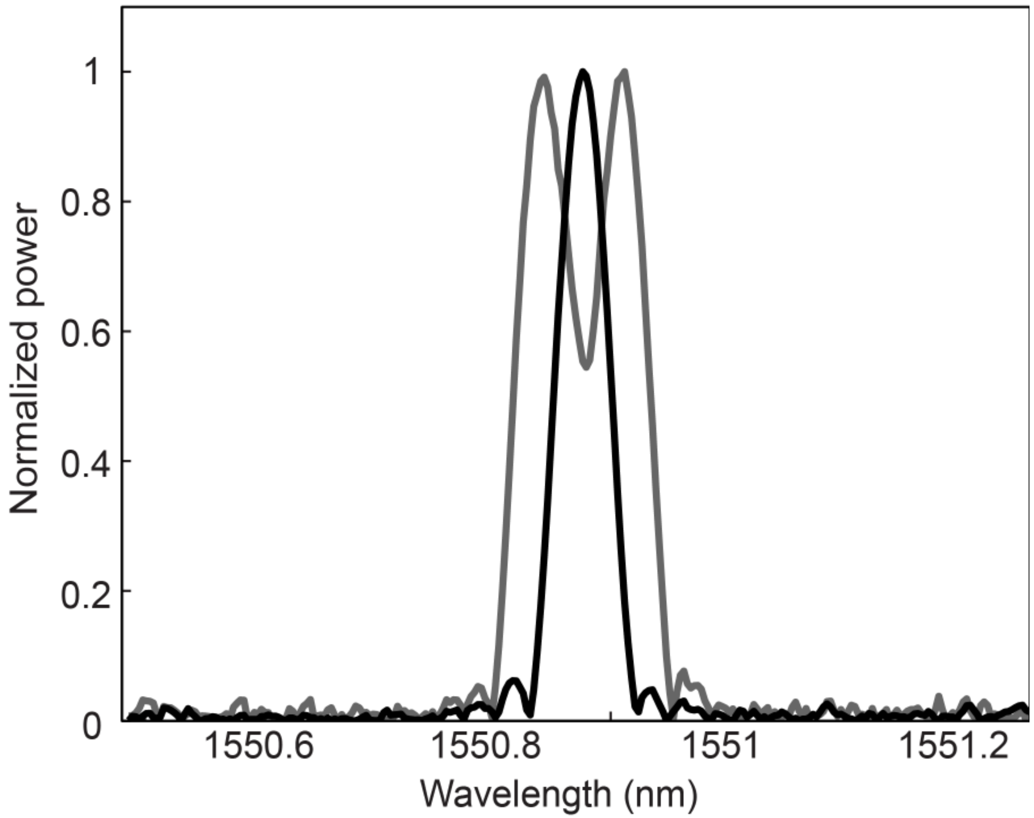

- **Experimental measurement:**
  - **Single narrowband laser(black)**
  - **Doublet separated 65 pm (grey)**
- **32 MZI**
- **Resolution: 50 pm**
- **FSR = 0.78 nm**
- **Interferometer length: 1.5 cm**
- **Total footprint: 18 mm^2**

Extending the SHFT concept to fiber optics: a path towards extreme resolution spectroscopy

The SHFT concept implemented with fiber optics interferometers.

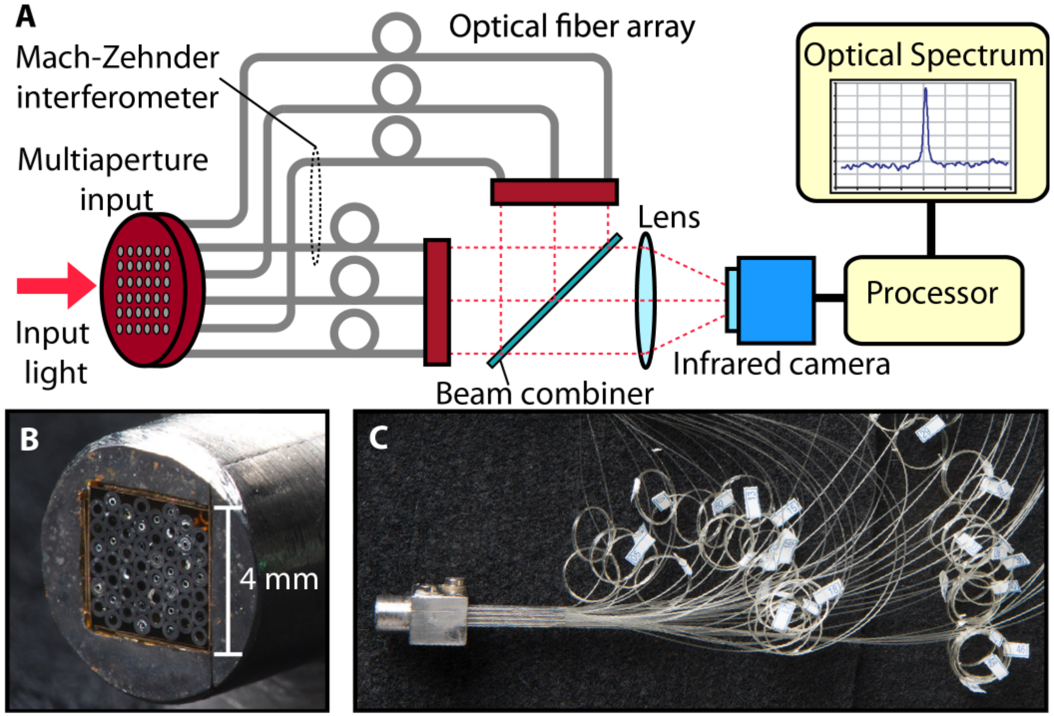

- The extremely low losses of optical fiber enable to implement very long optical path delays.
- This results in a device with a very high resolution
- Fabricated device:
  - 24 interferometers
  - Maximum optical path difference: 24 cm
  - Resolution: 3 pm

A. Villafranca, P. Cheben, et al., Optics Letters, 2013

Experimental demonstration

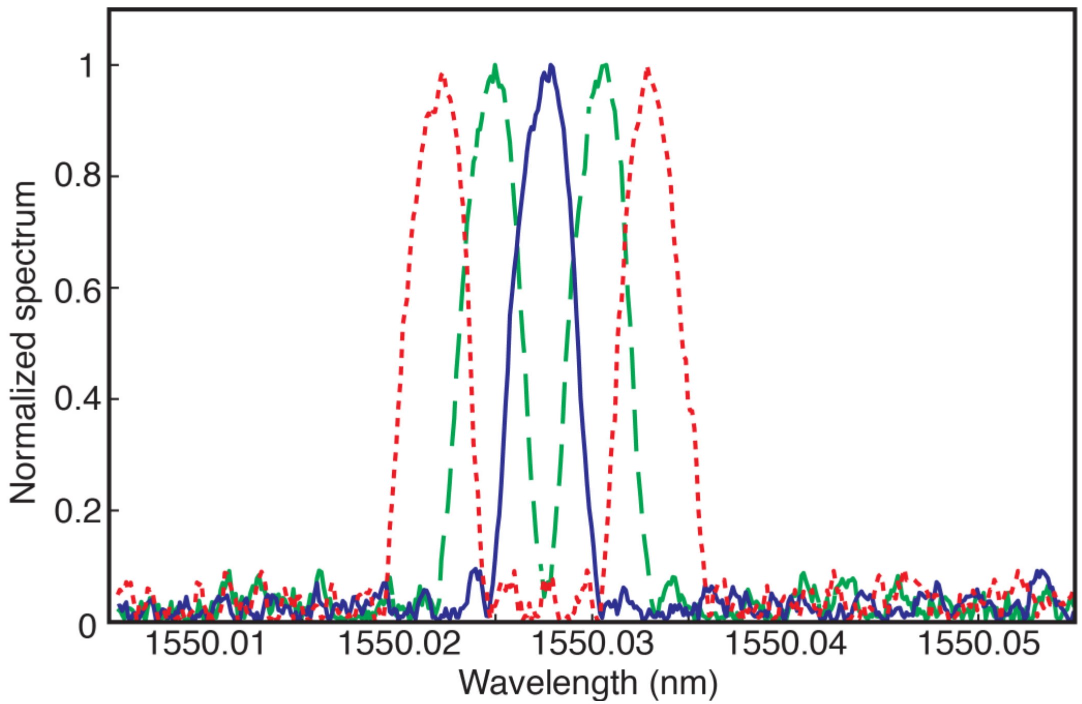

- **Experimental measurement:**
  - **Single narrowband laser (blue)**
  - **Doublet separated 5.5 pm (green)**
  - **Doublet separated 11 pm (red)**
- **24 MZIs**
- **Resolution: 3 pm**
- **FSR = 50 pm**

A perspective to think about

- Optical fibre FT spectrometer implementation allows very long optical delays and possibly unprecedented spectral resolutions.

- As an example, an optical fibre interferometer array with a path difference of 1 km, working with the demonstrated spectral retrieval technique, would enable measuring spectral lines with a 700 attometer FWHM broadening, that is, an unprecedented spectroscopic resolution of 3×10^{-6} cm^{-1}.